TWENTIETH ANNUAL HIGHWAY GEOLOGY SYMPOSIUM

Proceedings of a Symposium
held at the
University of Illinois, Urbana-Champaign
April 17–19, 1969

FOUNDATION SECTION

TWENTIETH ANNUAL
HIGHWAY GEOLOGY SYMPOSIUM

Proceedings of a Symposium
held at the
University of Illinois, Urbana-Champaign
April 17–19, 1969

Local Chairman:
  Don U. Deere
1969 Program Committee:
  Gordon R. Benson
  Kenneth R. Keene
  W. Calhoun Smith

CONTENTS

I. SOILS OF ILLINOIS AND THEIR ENGINEERING CHARACTERISTICS

T. H. Thornburn* and T. K. Liu**

Highway engineering design and construction problems in the state of Illinois are almost all related either directly or indirectly to deposits of the Pleistocene. Although the extent of deposits of the Nebraskan stage is not well delineated, Kansan drift has been identified over a large portion of the state. The Illinoian drift covered earlier deposits throughout most of the state, with the exception of extreme southern, western, and northwestern portions. Consequently, except in these areas and along some of the major river valleys, foundation or construction problems dealing with the underlying bedrock are relatively rare. The Illinoian drift is locally thin in the southern and western part of the state, but even here the topography is usually constructional on the drift.

Ice of the Wisconsinan stage covered only about the northeastern one-quarter of the state. Because of the relatively short time of weathering of its deposits compared with those of the

Illinoian stage, there is much more variability in the surficial soils of this region. Even in areas of southern Illinois which the Wisconsinan ice did not reach, most of the surface deposits in the valleys were affected by it. Some of these are lacustrine in nature and appear to be the result of the damming of the Mississippi, Ohio, and Wabash drainageways by outwash or ice blocks from the Wisconsinan glaciers.

Outside of the most recently glaciated area where the older drifts are thin or nonexistent, the surficial soils have been influenced to varying degrees by the thickness of overlying loessial material, again associated primarily with Wisconsinan time. On the field trip some of the problems associated with deep cuts in loess or the underlying bedrock were noted.

This discussion will not attempt to cover the engineering characteristics of all the soils in the state. It is related primarily to the northeastern portions of the state where the research work on highway soils has been concentrated.

Figure 1 is a map prepared more than ten years ago by a compilation of several maps of the Illinois State Geo-

---

*Professor of Civil Engineering, University of Illinois, Urbana.
**Senior Associate, Haley & Aldrich, Cambridge, Massachusetts.

2

logical Survey and the University of Illinois Agricultural Experiment Station.[1]* It needs a few corrections in the light of present knowledge, particularly with respect to the correlation of some of the morainic ridges and the position of the glacial boundaries in western Illinois. It is, however, sufficiently accurate to show the variability in the character and topography of the surface deposits. The contours of loess thickness show the relationship between the loessial deposits and their principal sources, which were the alluviated valleys of the Illinois, Mississippi, and Green Rivers. The loess is thickest immediately adjacent to the source areas and thins toward the south and east. In much of the northeastern part of the state the loess influence is minor. Those areas which apparently were never covered by glacial ice or at least do not contain any significant deposits of till are also indicated. While there are a few morainic systems which can be distinguished within the Illinoian drift region, it is evident that the majority of the moraines are located in the northeastern part of the state, forming more or less concentric rings around the lower end of Lake Michigan. There is an indication, however, that some of the earliest Wisconsinan ridges may have been built by a lobe which originated in the Lake Erie basin and extended across Indiana.

Figure 2, a cross section through

the drift which begins near the southwestern corner of the Wisconsinan glaciated area and proceeds about half-way to the Lake Michigan basin, is typical of northeastern Illinois.[2] It shows that the drift thickness throughout most of this area is a minimum of 50 ft and is more than 400 ft over a major bedrock valley. There are some locations in northeastern Illinois where the drift is less than 50 ft thick, but these represent a small fraction of the total area glaciated in Wisconsinan time. In these locations, however, the shallow depth to rock presents special highway engineering problems. It may also be noted that the Wisconsinan drift is often only a thin veneer on the earlier deposits. An indication of the character of the upper drift may be obtained from Figure 3, prepared from a series of borings taken close to Farmer City (see Figure 2). Figure 3 shows 10-12 ft of topsoil and loess over about 10 ft of Wisconsinan till over 4-5 ft of Farmdalian (?) silt over the greenish-gray weathered surface of the Illinoian till. The correspondence to the profile of Figure 2 is quite good. In general, the unconfined compressive strength of the upper till sheet ranges from 2 to 8 tons/sq ft. At the location of Figure 3, the average value was found to be 4.5 tons/sq ft. In many respects the characteristics of the Illinoian till are similar. At the reported location its unconfined compressive strength ranged from 2 to 10 tons/sq ft with an average value of 4.5 tons/sq ft.

Figure 4 is a recently-published generalized map of the soils of Illinois prepared by the University of Illinois

---

*Superscript numbers in parentheses refer to the References at the end of this paper.

th-
la-
-way
cal
ows
most
and
l-
ns
rift

tal
ln
w
ay
e.

er
c-
d

ft

..
ln
le
,

l-
h

s
l

Agricultural Experiment Station.[3] It
will be noted that the major subdivi-
sions are "dark colored soils," "light
colored soils," and "dark and light
colored soils." The dark colored soils
are those developed under prairie vege-
tation; the light are those developed
under forests. The mixed forest and
prairie are designated as "dark and
light." The "L" and "O" areas corre-
spond to the very thick loessial depos-
its along the major drainage ways. The
"A" area represents the regions of
predominantly thick loess. Areas "B"
and "C" and the "D," "E," "F," and "Q"
series represent areas in which the
loess is thinning to the east and the
southeast, and correspond to the con-
tours shown in Figure 1. It will be
noted that none of these areas appears
in the extreme northeastern corner of
the state where areas designated "G,"
"H," "I," "J," "K," and "S," "T," "U,"
and "V" indicate soils developed pri-
marily from glacial drift. These are
the areas where the loessial influence
is so minor that it affects at most
only the surface horizon.

On a larger scale map of northeast
Illinois the variations in parent mate-
rial can be shown in more detail.[4]
Six different textures of drift (mostly
tills) have been mapped by the agrono-
mists preparing soil surveys in this
area. These vary from loamy gravel
till and outwash (Parent Material No.
1 in Reference 4) to clay till and
lacustrine sediments (Parent Material
No. 6). The texture designation used
is in accordance with the standard tri-
angular diagram of the U. S. Department
of Agriculture.

As part of a cooperative research
project with the Illinois Division of
Highways and the U. S. Bureau of Public
Roads, the validity of agricultural soil
maps using the parent material classi-
fication was tested from the standpoint
of physical properties pertinent to
engineering. Three counties in north-
eastern Illinois were selected for
study: DeWitt, Livingston, and Will.
All had relatively up-to-date county
agricultural soil reports and maps which
were used as a basis for selecting sites
at which samples could be taken. Using
the published soil map, the sampling
sites were selected in the office. A
field check was made only to determine
whether or not the profile corresponded
reasonably well with that described in
the soil report. This was necessary
since even recent soil maps cannot indi-
cate all the minor inclusions of slightly
varying soil types which occur within
a mappable unit. Samples were taken at
each site from each of the major hori-
zons encountered within 5 to 6 ft of
the surface. These samples were then
subjected in the laboratory to grain-
size analyses, Atterberg limit tests,
and moisture-density relations tests.
Since the "C" horizon samples generally
represented the parent materials, it
was possible, by combining data from
those soil types mapped on the same
parent material, to obtain a rather pre-
cise statistical indication of the vari-
ability in the major drift units.

The data presented in the following
figures were taken from a published
engineering soil report for Livingston
County.[5] In that county, the following
parent material areas were delineated:

No. 3, loam till; No. 4, silty clay loam till; No. 5, silty clay till; No. 6, clay till; No. 7, water- and/or wind-deposited sandy loams and sands; No. 8, medium and moderately fine-textured outwash; and No. 9, mixed bottomland terrace and bluff wash materials. In the western part of the county the loess is thick enough that it was also possible to obtain samples of some soils developed on relatively unweathered loessial material.

Average grain-size data on each of the parent material groups is plotted in Figure 5. The numbers in parentheses indicate the number of samples tested in each group. It is apparent that on the average there are distinct differences in the characteristics of each of the groups. Curves for loess and sandy windblown soils (No. 7) show textural characteristics which can be obtained only through sorting by wind action. Parent Material Nos. 9 and 8, recent alluvium and medium to moderately fine-textured outwash, respectively, are obviously coarser than the materials constituting the four textural classifications of till. A comparison of the tills shows that the percent of fines increases progressively from loam till through silty clay loam till, and silty clay till to clay till.

In Figure 6 the average plasticity values are plotted on a plasticity chart divided according to the AASHO classification system. Parent Material Nos. 3, 4, 5, and 6 increase progressively up the chart. A similar pattern is shown in Figure 7, a plot of the average moisture-density relations for each of the eight different parent

materials. As one would expect, the highest values of maximum dry density were obtained with the granular materials. The loam till and the loess showed almost identical results and the other maximum dry density values decreased progressively from the No. 4 through No. 6 materials.

Statistical data for each parent material were summarized, as partly shown for Parent Material No. 3 in the table on p. 5. In addition, statistical data were also obtained as indicated at the bottom of Table 1 in terms of the estimate of range of 85 percent probability. It was felt that this range was more meaningful from the engineering standpoint than one, two, or three standard deviations. It will be noted that even at 85 percent probability there is a fairly wide range of values for each of the three properties. One might therefore question whether there is any value to the differentiation of the various parent materials from the engineering standpoint. In order to test this hypothesis, each parent material was compared with each one of the others with respect to a number of different physical properties (see Figure 8). Where the symbol of a particular property appears in the comparison box relating two different materials, there was a statistically significant difference between the two materials with respect to this property. The single asterisk represents significance at the 10 percent level and the double asterisk, significance at the 5 percent level. Statistically significant differences were obtained in every case, with the exception of Parent Material Nos. 8 and 9

STATISTICAL EVALUATION OF PARENT MATERIAL NO. 3, LIVINGSTON COUNTY.

LOAM TILL

Statistical Data

Index Property	No. of Samples	Mean	Standard Deviation	Coefficient of Variation
Liquid Limit, percent	39	34.5	6.8	19.8
Max. Dry Density, lbs per cu ft	40	110.8	5.7	5.1
Optimum Water Content, percent	40	16.3	3.0	18.2

Estimate of Range, 85 Percent Probability

Liquid Limit, percent	25-44
Max. Dry Density, lbs per cu ft	102-119
Optimum Water Content, percent	12-21

and Parent Material Nos. 5 and 6. Parent Material Nos. 7 and 9 show statistical differences only with respect to the textural characteristics of the material passing the No. 10 and No. 40 sieve. On the basis of this analysis it was felt that without a doubt the field separations made by the agricultural soil survey are significant from the standpoint of engineering. The highway engineer should be familiar with these differences and be prepared to alter his design and construction methods accordingly.

Using the information obtained from the test data, joined with a knowledge of the other characteristics of the soil profiles developed on the various parent materials, it is possible to present the engineer with certain quali-

tative design and construction information. This can be utilized especially during the preliminary planning stage for a highway facility to be located in any part of the state where soil conditions are similar to those already examined. Items which were normally considered are

(a) design and construction information,

(b) alignment problems,

(c) water table position,

(d) frost action susceptibility,

(e) seepage problems,

(f) excavation problems,

(g) stability of cut slopes,

(h) compaction characteristics,

(i) erosion of slopes,

(j) source of borrow,

(k) source of granular material,

6

(1) special recommendations. This list does not differ greatly from those which are seen in other engineering soil reports or in the more recent reports of the Soil Conservation Service. This does not mean, however, that evaluation of these items is of any less value to the engineer. Certainly such information should facilitate the planning and construction of new highway facilities and the improvement of older ones.

REFERENCES

1. Thornburn, T. H., Surface Deposits of Illinois, Engineering Experiment Station Circular No. 80, University of Illinois, Urbana, 1963.

2. Horberg, Leland, Pleistocene Deposits Below the Wisconsin Drift in Northeastern Illinois, Illinois State Geological Survey Report of Investigations No. 165, 1953.

3. Fehrenbacher, J. B., Walker, G. O., and Wascher, H. L., Soils of Illinois, Agricultural Experiment Station Bulletin No. 725, University of Illinois (in cooperation with Soil Conservation Service, U.S.D.A.), Urbana, 1967.

4. Wascher, H. L., Alexander, J. D., Ray, B. W., Beavers, A. H., and Odell, R. T., Characteristics of Soils Associated with Glacial Tills in Northeastern Illinois, Agricultural Experiment Station Bulletin No. 665, University of Illinois, Urbana, 1960.

5. Thornburn, T. H., Morse, R. K. and Liu, T. K., Engineering Soil Report, Livingston County, Illinois, Engineering Experiment Station Bulletin No. 482, University of Illinois, Urbana, 1966.

Pg. 7 Is Blank

BLANK
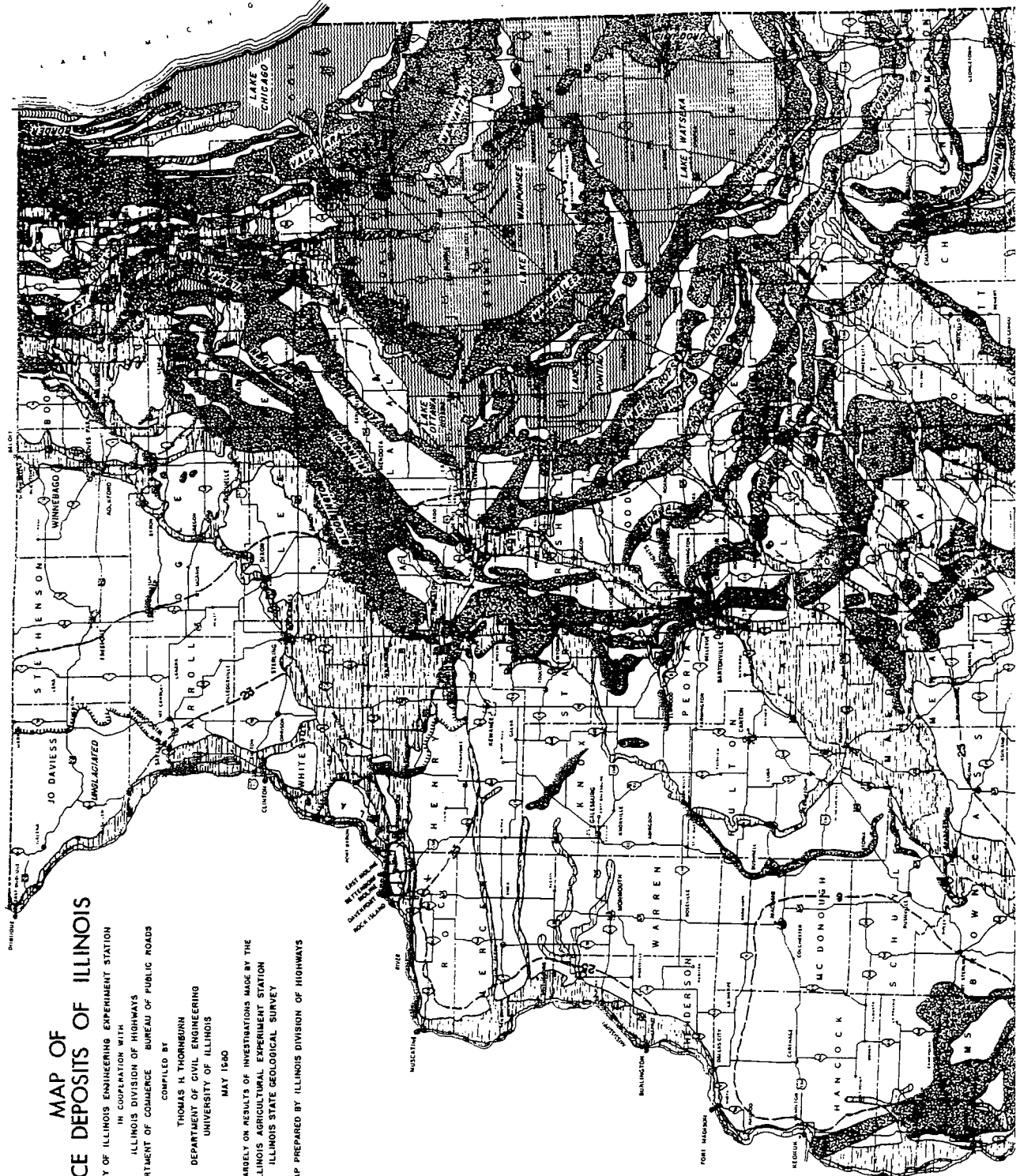
MAP OF
SURFACE DEPOSITS OF ILLINOIS

UNIVERSITY OF ILLINOIS ENGINEERING EXPERIMENT STATION

IN COOPERATION WITH

ILLINOIS DIVISION OF HIGHWAYS

U.S. DEPARTMENT OF COMMERCE   BUREAU OF PUBLIC ROADS

COMPILED BY

THOMAS H. THORNBURN

DEPARTMENT OF CIVIL ENGINEERING

UNIVERSITY OF ILLINOIS

MAY 1960

BASED LARGELY ON RESULTS OF INVESTIGATIONS MADE BY THE

ILLINOIS AGRICULTURAL EXPERIMENT STATION

ILLINOIS STATE GEOLOGICAL SURVEY

BASE MAP PREPARED BY ILLINOIS DIVISION OF HIGHWAYS

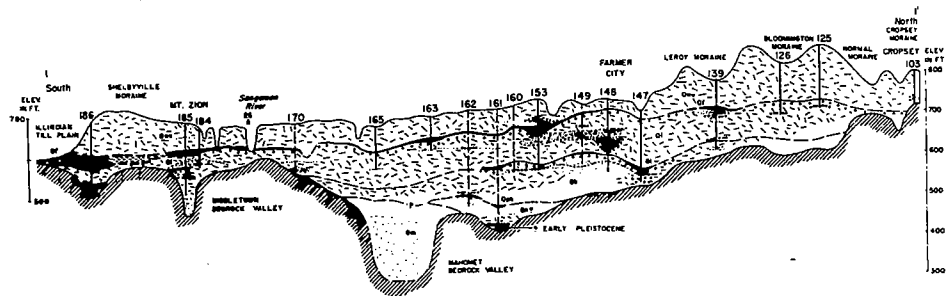FIGURE 1. SURFACE DEPOSITS OF ILLINOIS (AFTER THORNBURN).
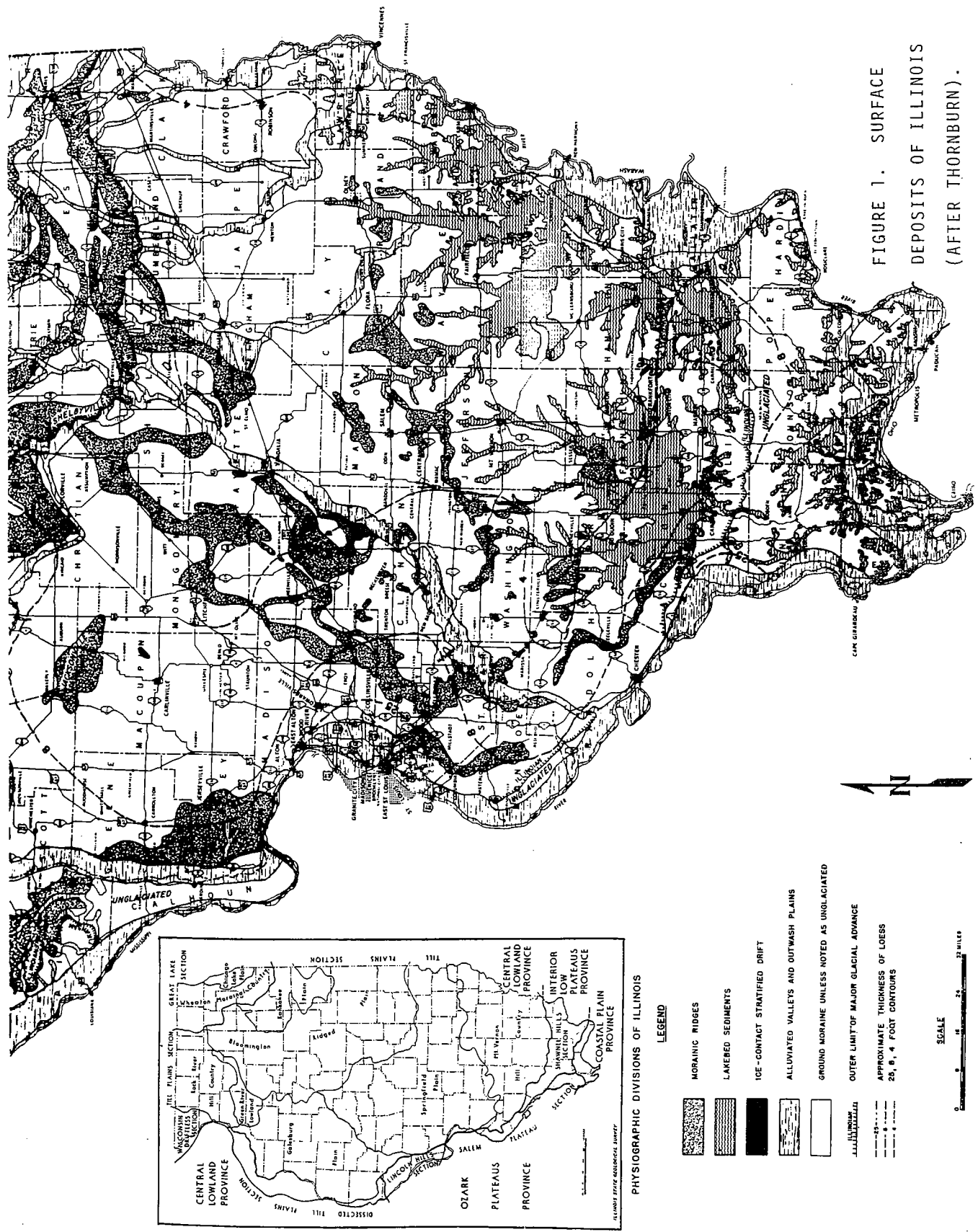
FIGURE 2.   CROSS SECTION THROUGH GLACIAL DEPOSITS,
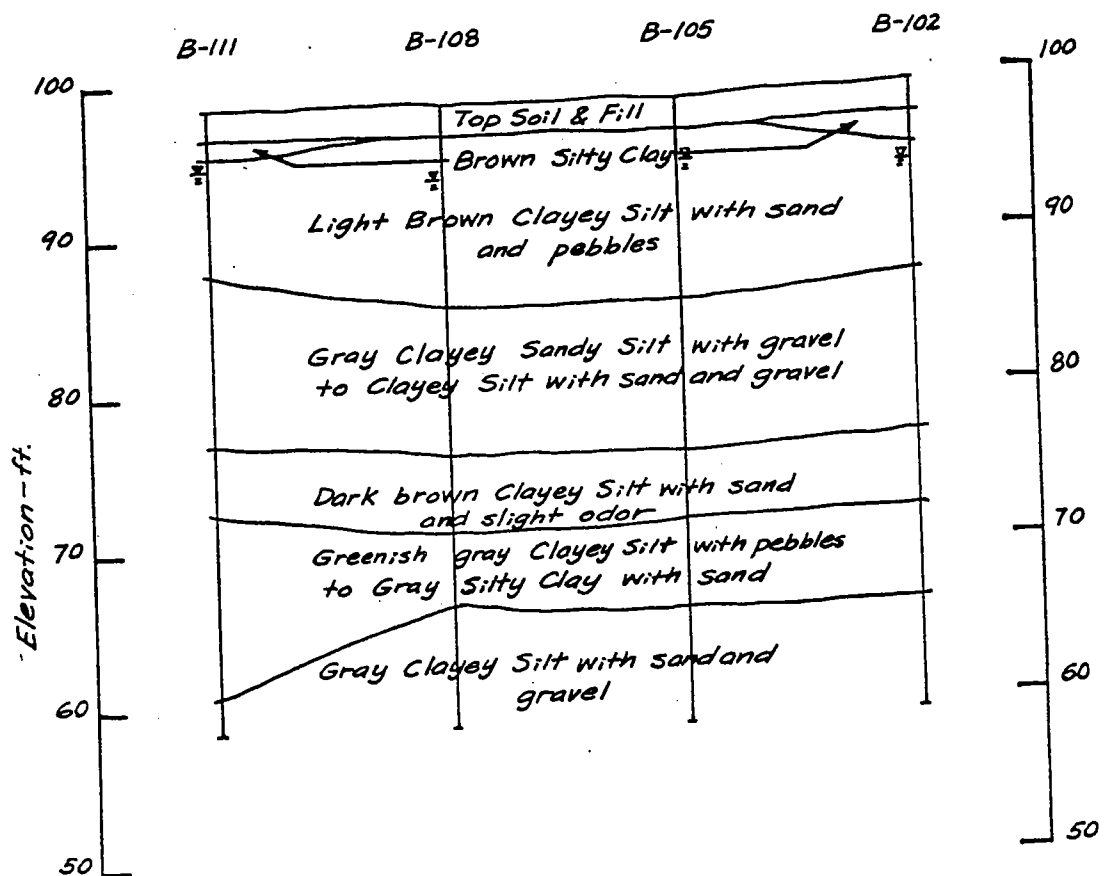EAST CENTRAL ILLINOIS (AFTER HORBERG).

FIGURE 3.   DETAILED SOIL PROFILE, FARMER CITY, ILLINOIS.

GENERAL SOIL MAP OF ILLINOIS

Legend

DARK-COLORED SOILS

DEVELOPED PRIMARILY FROM LOESS

A Joy - Tama - Muscatine - Ipava - Sable
B Sidell - Catlin - Flanagan - Drummer
C Wenona - Rutland - Streator
D Harrison - Herrick - Virden
E Oconee - Cowden - Piasa
F Hoyleton - Cisne - Huey

DEVELOPED PRIMARILY FROM GLACIAL DRIFT

G Warsaw - Carmi - Rodman
H Ringwood - Griswold - Durand
I La Rose - Saybrook - Lisbon
J Elliott - Ashkum - Andres
K Swygert - Bryce - Clarence - Rowe

LIGHT-COLORED SOILS

DEVELOPED PRIMARILY FROM LOESS

L Seaton - Fayette - Stronghurst
M Birkbeck - Ward - Russell
N Clary - Clinton - Keomah
O Stookey - Alford - Muren
P Hosmer - Stoy - Weir
Q Ava - Bluford - Wynoose
R Grantsburg - Robbs - Wellston

DEVELOPED PRIMARILY FROM GLACIAL DRIFT

S Fox - Homer - Casco
T Mc Henry - Lapeer - Pecatonica
U Strawn - Miami
V Morley - Blount - Beecher - Eylar

DARK- AND LIGHT-COLORED SOILS

DEVELOPED PRIMARILY FROM MEDIUM- AND FINE-TEXTURED OUTWASH

W Littleton - Proctor - Plano - Camden - Hurst - Ginat

DEVELOPED PRIMARILY FROM SANDY MATERIAL

X Hagener - Ridgeville - Bloomfield - Alvin

DEVELOPED PRIMARILY FROM MEDIUM-TEXTURED MATERIAL ON BEDROCK

Y Channahon - Dodgeville - Dubuque - Derinda

DEVELOPED PRIMARILY FROM ALLUVIUM

Z Lawson - Beaucoup - Darwin - Haymond - Belknap

SCALE IN MILES
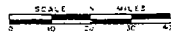
UNIVERSITY OF ILLINOIS AGRICULTURAL EXPERIMENT STATION
In Cooperation With
U. S. DEPARTMENT OF AGRICULTURE SOIL CONSERVATION SERVICE

FIGURE 4. GENERAL SOIL MAP OF ILLINOIS (AFTER FEHRENBACHER, ET AL).

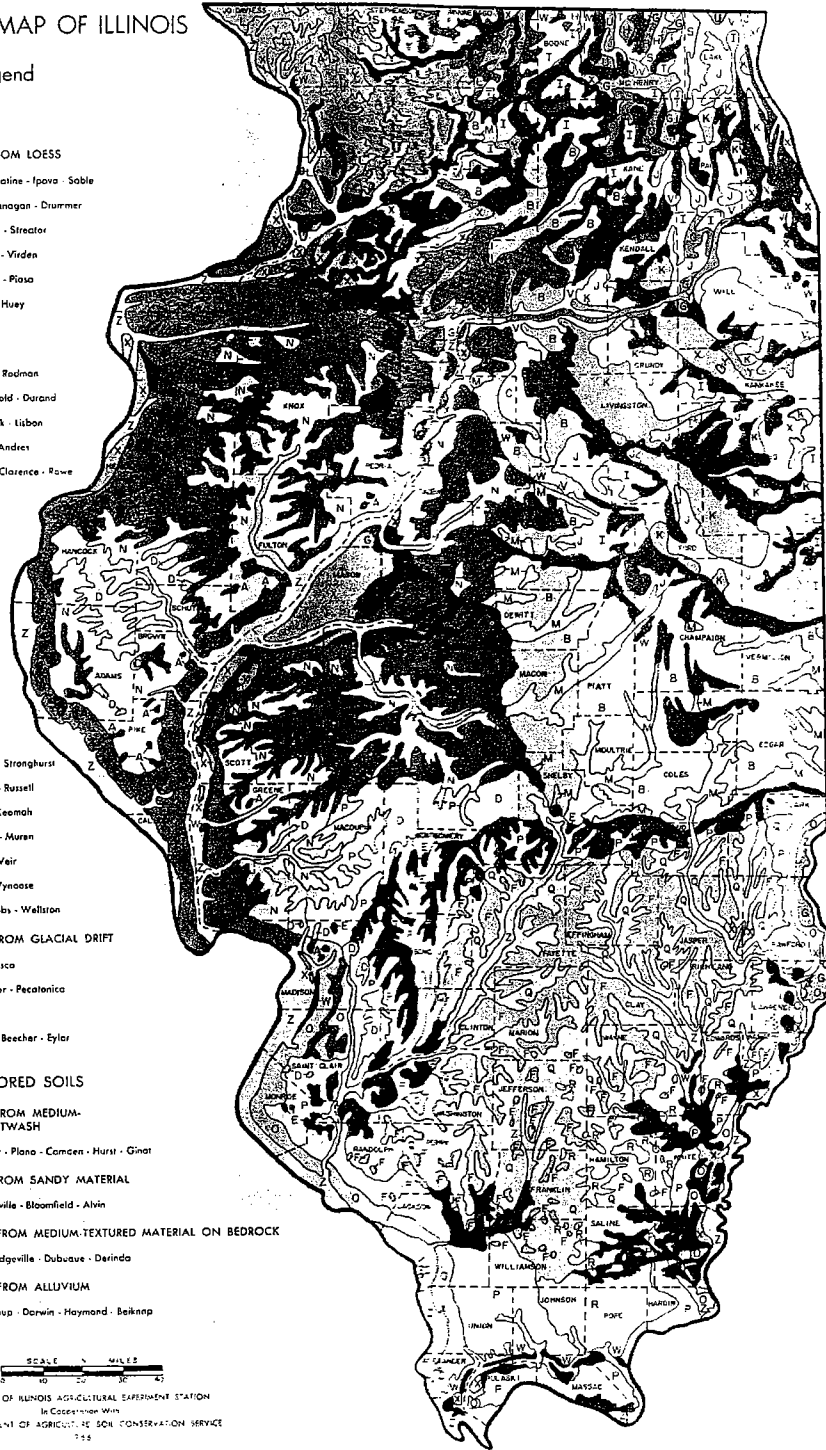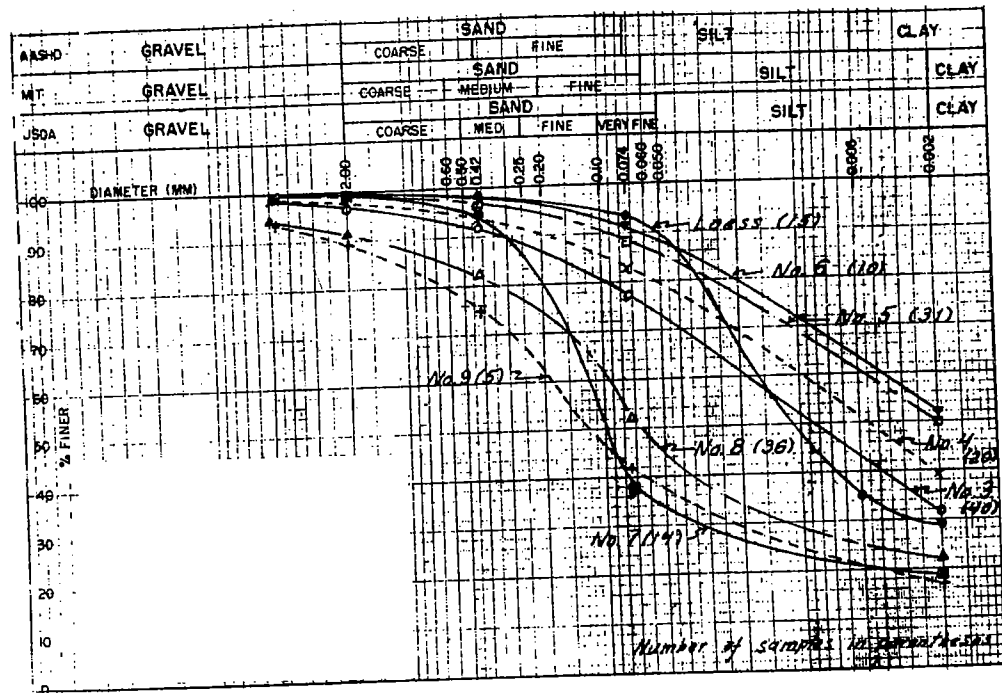FIGURE 5. AVERAGE GRAIN SIZE DISTRIBUTION CURVES
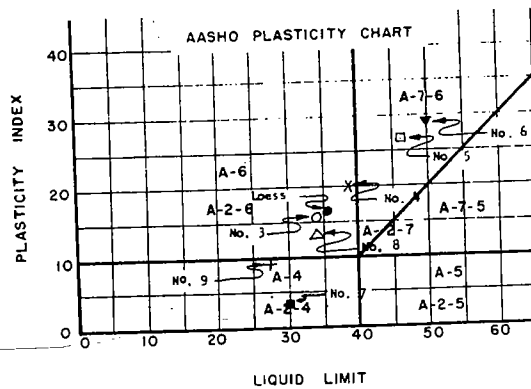FOR LIVINGSTON COUNTY PARENT MATERIAL GROUPS.

FIGURE 6. AVERAGE PLASTICITY
PROPERTIES FOR LIVINGSTON COUNTY
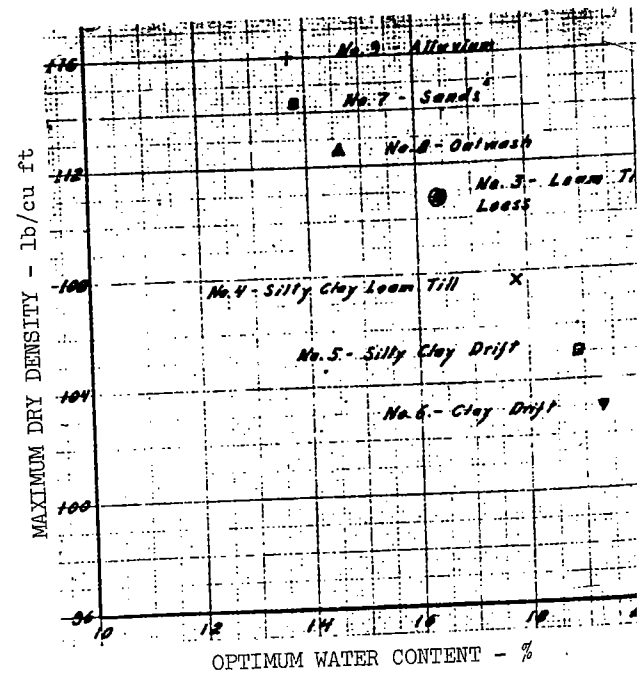PARENT MATERIAL GROUPS.

FIGURE 7. AVERAGE MOISTURE-DENSITY RELATION
FOR LIVINGSTON COUNTY PARENT MATERIAL GROUPS

Based on Average
C Horizon Values

Legend

10	Percent passing No. 10 sieve
40	Percent passing No. 40 sieve
200	Percent passing No. 200 sieve
C	Percent clay < 2μ
LL	Liquid Limit
PI	Plasticity Index
γ	Maximum Dry Density
0	Optimum water content
*	Significant at the 10% level
**	Significant at the 5% level

9	7	8	Loess	3	4	5	6	Parent Material
	10** 40**		10** LL** / 40** PI* / 200** γ** / C** 0**	10** LL* / 40** PI** / 200** γ* / C** 0*	10** LL** / PI** / 200** γ** / C** 0**	10** LL** / 40** PI** / 200** γ** / C** 0**	10** LL** / 40** PI** / 200** γ** / C** 0**	9
		10* 40** PI** 200*	PI** / 200** γ* / C** 0**	10** / PI** / 200** γ* / C** 0**	LL** PI** / 200** γ** / C** 0**	LL** PI** / 200** γ* / C** 0**	LL** PI** / 200** γ* / C** 0**	7
			10** 40** 200** C** 0**	10** 40** 200** C** 0**	10* LL** / 40* PI** / 200** γ** / C** 0**	10** LL** / 40** PI** / 200** γ** / C** 0**	10* LL** / 40** PI** / 200** γ** / C** 0**	8
				10** 40** 200**	10** / 40** PI** / 200** γ** / C** 0**	LL** PI** γ** C** 0**	LL** PI** γ** C** 0**	Loess
					LL** PI** γ** C** 0*	10** LL** / 40** PI** / 200** γ** / C** 0**	10** LL** / 40** PI** / 200** γ** / C** 0**	3
						40* C**	10* LL** / 40* PI** 200** γ** / C**	4
								5
								6

FIGURE 8.   STATISTICAL COMPARISON OF LIVINGSTON COUNTY PARENT MATERIAL GROUPS.

II. A GEOTECHNOLOGY PROFILE IN JO DAVIESS COUNTY, ILLINOIS

Robert L. Brownfield*

INTRODUCTION

Few areas on the face of the earth have been as favored by nature and geologists as has been the Upper Mississippi Valley zinc-lead district (Figure 1). Diverted by highlands and deep pre-glacial valleys, ice lobes of the Illinoian and Wisconsin glaciers bypassed the Driftless Sector. The entrenched and well-integrated stream system of the area, its rugged, mature to submature relief, and its fragile landforms are in marked contrast with the glaciated plains that surround it. Jo Daviess County, in the northwest corner of Illinois, is a part of this district.

Mining in the area goes back at least three centuries. In 1658 the Sioux Indians are reported to have had lead mines in the area. American operations there began in 1819. By 1830 this was the leading lead-producing district in the United States and it remained so till 1871.

Geological investigations in the vicinity began in 1839 when the United States Congress commissioned Dr. David Dale Owens to conduct a geological reconnaissance there. Since then some 300 papers have been written on the are or have made a significant reference to it. Recently, 1942 to 1950, the Unitec States Geological Survey with the co-operation of the State Geological Surveys of Illinois, Iowa, and Wisconsin studied its lead and zinc deposits extensively. For references to these studies and to much of the earlier lit erature, see the Bibliography and Inde. of Illinois Geology through 1965. [1]**

The first part of the present stu is a review of the existing literature on the geological environment of the county. The second part applies this data to highway engineering.

THE GEOLOGICAL ENVIRONMENT

The geological environment of Jo Daviess County will be considered unde three headings: bedrock strata and la forms, streams, and soils.

Bedrock Strata and Landforms

Agnew,[2] Buschbach,[3] and Templ ton and Wilman[4] have studied the bec rock stratigraphy of the area and have

---

**Superscript numbers in parentheses refer to the References at the end of this paper. The observations and conclusions of the authors listed in the references have been employed freely. Justice and our own wishes require that we acknowledge our indebtedness.

d
d
-

rea
to
ed

-

t-
ex
*
udy
e

er
and-

le-
d-
e

assigned group status to the Silurian Dolomites, the Maquoketa Shale, the Galena Dolomites, and the Platteville Dolomites. It suits our purpose to refer to them simply as units (Figure 2). All four units listed above outcrop in the county, but the Platteville outcrops only in a small area in the Galena river four miles upstream from Galena.[5]

The structure of the area is dominated by the southwest regional dip of about 15 ft per mile. There are local folds with local dips up to 7° and a system of joints which seem to have some influence on straight stretches and right angle bends in streams.[6,7]

The erosion of these beds has formed two upland surfaces: cuestas with bold cliffs (Figure 3) and outliers. The outliers are called mounds in the area. As the land surfaces form flat skylines or accordant summits, as they bevel the rock structure, and as their dip varies in degree and direction from that of the bedrock, some authors have attributed these surfaces to different periods of erosion and have named them the Dodgeville and Lancaster Peneplains. The Dodgeville is an erosional surface developed on the top of the Silurian Dolomites and the Lancaster a similar surface developed on the Galena Dolomites. Both surfaces are well dissected; their relief is about 100 ft. Most of the area is in slopes. Whether these uplands are the remnant of one or more peneplains does not seem to have engineering significance and was not considered in this study.

The geologic map of Jo Daviess County in Figure 4 shows the distribution of strata and the uplands developed upon them. The black pattern represents the outcrop of the Silurian Dolomite, which caps the ridges and high mounds of the Dodgeville Surface and defines the area of that surface. The unmarked pattern represents the outcrop of the Maquoketa Shale, whose erosion undermines the Silurian Dolomites. As a result of that erosion, the shale outcrops on the slopes of the ridges and high mounds and on the entire surface of the lower mounds. The Galena Dolomite is represented by the dot pattern; its outcrops on the Lancaster Surface are the most extensive in the county and extend northward into Wisconsin to within ten miles of the Wisconsin River.

The Streams

The streams of the area flow to the southwest and are entrenched 100 to 300 ft below the uplands where they enter the Mississippi river. Except for the glaciated eastern part of the county, the drainage is well integrated. Branching is generally dendritic but some right angle bends and straight stretches seem related to synclinal axes and joint systems. The incised meanders of the main stream are much wider than their floodplains as a result of rejuvenation in Pliocene times. They also have slip-off slopes, as meandering attended uplift.

Terraces composed mostly of varved clays and fine silts are present on many streams near their junction with the Mississippi Valley. These were formed during the Wisconsin glaciation when outwash in the main valley dammed its tributaries and induced slackwater deposition. Such terraces are found at the town of Hanover and at the old fairgrounds at Galena.

The Soils

The Soil Association Map shows the principal soils of the area (Figure 5), which reflect the influence of vegetation, loess (silt loam soil) thickness, bedrock, and stream deposition. Except for organic accumulations in depressions on the glacial till, the effects of vegetation have no engineering significance. The influence of the other factors will be considered in order.

The loess is wind-blown sand, silt, and clay picked up on the flood plains of the Mississippi, carried inland and deposited on the land surface. In mildly eroded topography, its thickness varies from a possible 50 ft in the river bluffs to about 8 ft in the northeast corner of the county. The texture of the loess also becomes finer with distance from the river. The loess thickness map, constructed by combining soil patterns from the Soil Association Map with equal thicknesses of loess, shows the inferred thickness distribution of loess (Figure 6). The heavy dot pattern shows the distribution of thick loess in the river bluffs. The unmarked pattern is the loess thickness, 5 to 15 ft in the mildly eroded topography on the Lancaster Surface. The small dot pattern represents the thin areas of loess caused by erosion, either from the steep slopes and narrow ridges of the Dodgeville Surface or from the stream margins on the Lancaster Surface.

The influence of bedrock can be determined from the geologic map (Figure 4) by differentiating the areas of thin loess underlain by dolomite from those underlain by shale. The Engineering Soil Interpretation Map, Figure 7, does just this. The unmarked pattern indicates areas of mild erosion with silt loam soils over 5-ft thick. (Five feet was adopted because it is the demarcation line on the Soil Association Map.) The small dot pattern shows the distribution of loess over dolomite a configuration occurring at stream margins on the Lancaster Surface and on the high dolomite ridges of the Dodgeville Surface. The dash pattern shows the distribution of thin silt loam soils on shale. These soils are characteristic of the low mounds and the unforested slopes beneath the high ridges and mounds of the Dodgeville Surface.

A fourth soil type, shown on the Engineering Soil Interpretation Map by the black pattern, is the alluvial or water-laid soil. Generally the alluvial soils are thin. Bridge foundation borings at eight stream crossings revealed a maximum depth to bedrock varying from 20 ft to more than 80 ft. On that basis the following thicknesses of alluvium are inferred: main stream near the Mississippi Valley, 100 ft or more; main streams 10 mi upstream from their mouths, 20 to 40 ft; minor stream normally less than 20 ft. These alluvial soils are generally silt loams with dolomite rubbish and chert chips with some clays.

The above soils are delineated on the Soil Association Map. In addition its text and table list other soils of engineering significance: the organic silty clay loams of depressions in the glacial till east of Stockton, and the

:ed
ion
,
the
-
ows
ite,

n

e

gh

ie
by
ɔr
ʌvi-
ɔn
ɛ-

ft.
sses
eams
or
rom
reams
luvial

th

on
ion
of
nic
the
the

silty clay loams in the poorly drained, backswamp, areas on the flood plains.

APPLICATION: THE GEOTECHNICAL PROFILE

Thus, the principal elements of the geological environment of Jo Daviess County are the two upland surfaces, the Dodgeville and the Lancaster (Figure 3). Both are controlled by shallow bedrock, mantled with loess, and drained by a well-integrated stream system whose lower reaches flow through rock-walled gorges and contain glacial lake deposits of varved clays and fine silts.

With the aid of two geotechnical profiles, these elements are applied to highway engineering under the following headings: subgrade, foundations, cuts and fills, stability and settlement, and water supply for rest areas.

Subgrades

The subgrade character of materials along a proposed route is a principal concern in route planning. In the design stage this is done with soil borings; in reconnaissance, it is done with aerial photographs and agricultural soil maps.

As conditions along Illinois Route 84 Relocated are typical of the driftless portions of Jo Daviess County, a geotechnical profile of this route is shown as an illustration (Figure 8). To examine subgrade and foundation conditions, this profile combines an engineering soil map with profiles on the ground surface and the bedrock units. The engineering soil types are drawn from the Soil Association Map (Figure 5) and the geologic map of the area.[5] Data on bedrock elevations are derived from publications of the Illinois State Geological Survey.[8,5,9]

In terms of subgrade, the unmarked pattern in Figure 8 represents the distribution of silt loam soils over 5 ft thick. These generally occur on mildly eroded and gently sloping terrain. In such areas the normal subgrade will be on loess and the Illinois Division of Highway Standards for loess subgrades and cuts will apply. An exception is made for depressions in the glacial till northeast of Stockton. Where organic soils have accumulated in depressions, removal must be considered.

Areas with the small dot pattern are thin silt loam soils overlying the Galena Dolomites at depths less than 5 ft. This occurs near the margins of the larger valleys on the Lancaster Surface. The roadway will usually be in a rock cut with a dolomite subgrade. The dolomite has good internal drainage. With a granular subbase, the subgrade performance should be excellent.

Areas with the large dot pattern are similar silt loams overlying the Silurian Dolomites at depths less than 5 ft. This occurs on the top of the ridges and high mounds of the Dodgeville Surface, where terrain is steep to rugged. The roadway will be in deep cuts which extend into the underlying shale. As the shale is impervious and becomes plastic when wet, the cuts will have to be graded to keep water from ponding on the subgrade. So treated, the shale cuts should perform satisfactorily with a granular subbase.

Areas with the dash pattern are thin silt loam overlying the Maquoketa Shale at depths less than 5 ft. This occurs on the slopes of the high ridges below the Silurian Dolomites and on the lower mounds. The terrain is rugged and

the subgrade will be on fills and in shale cuts. The fills will be subject to design controls but the shale will require the treatment described above.

Foundations

Foundations or adequate bearing for highway structures are our next concern. While the Galena River, Smallpox Creek, and other major streams have cut their valleys deep into the more-than-competent Galena Dolomites, the bridges that span these streams will have most of their footing on alluvium. This, as has already been noted, was ponded in glacial times and may contain an appreciable quantity of low cohesive soils, requiring long pile lengths.

Irish Hollow is probably representative of minor streams; its alluvium is thin. Footings in the upper reaches will be on the Maquoketa Shale, which will provide good bearing if water is kept from accumulating around the footings. In the lower reaches, the footings will be in the Galena Dolomite and the bearing will be more than adequate.

The silt loam soils in the unmarked pattern both east and west of Galena are probably adequate to support rest area structures (Figure 8, 1 and 2). At both places the view is probably scenic and a water supply of 200 gal per min may be anticipated from the St. Peter Sandstone. This aquifer is at depths of approximately 300 ft for the west location and 400 ft for the east location.

Cuts and Fills

Cuts and fills are functions of relief and Jo Daviess County is an area of considerable relief for Illinois. The Galena River flows 300 ft below its upland and Smallpox Creek 400 ft below

the Dodgeville Surface. The relief in Irish Hollow is only 60 ft along the alignment of the profile but the land surface normal to the alignment rises 230 ft in a quarter of a mile. With relief of this order, cuts and fills required to maintain a reasonable grade will be excessive.

A 130-ft cut being considered for the high ridge east of Smallpox Creek (Figure 8,3) would involve voluminous rock excavation, a problem in disposal of shale waste, and the expense of long hauls over steep and winding gravel roads with the attendant hazard to life and property.

A tunnel through the Maquoketa Shale about 180 ft below the Dodgeville Surface is an alternative consideration. Preliminary estimates indicate that we may come out ahead in construction cost on a tunnel, only to have the savings offset by maintenance costs. In the case of a tunnel, rock slides would be a problem only at the portals rather than along the entire length.

Cuts in the Galena Dolomite will be required at major stream approaches. Though dolomite rubble can be incorporated into fills, the cuts will be dee and classed as rock excavation.

Fills up to 60 ft will be require at minor stream crossings and up to 90 ft at major stream crossings; and fills will be needed to bring the grad on the Lancaster Surface up to the gra of cuts (or tunnels) crossing the ridg and mounds of the higher surface (Fig-ure 8, 4). There is no ready source c granular material in the county and quarry run material may be required t supplement material from the dolomite cuts.

Stability and Settlement

Perhaps the principal stability problem in the area is rock slides associated with the undermining of the Silurian Dolomite ledges of the Dodgeville Surface. A geotechnical profile, combining the profiles of the preceding geotechnical profile with the geologic map by Trowbridge and Shaw[5], is employed to investigate stability and ground water supplies (Figure 9).

The Silurian Dolomite outcropping in the black pattern on the geologic map is creviced, water bearing, and subject to slides. Huge blocks of this dolomite are present at various positions on the slopes underlain by Maquoketa Shale. The principal cause of slides of Silurian Dolomite is the undermining of the subjacent strata by erosion. When support is removed past the center of gravity, the rock block tilts and, depending on the inclination of the slopes, creeps, slides, or falls downward. Alternate freezes and thaws, which shove the outermost blocks further and further slopeward, also contribute to the slides, as do rock glides of the large blocks themselves, powered by their own weight and overriding a wetted and plastic shale surface that tilts up to 7°.

Associated with this problem are seepage at the lower contact of the Silurian Dolomite, debris slides which involve both the weathered, thin-bedded dolomite beds in the lower part (Edge-wood Formation) of the Silurian and the Maquoketa Shale, and soil creep in the debris at the toe of the slope.

The tentative treatment for rock cuts involving the Silurian Dolomite consists of:

(a) a 20-ft bench at the base of the Silurian Dolomites with a gully to divert seepage away from the face of the cut;

(b) a 1:1 slope on the Maquoketa Shale with a 20-ft wide bench every 20 to 35 ft to restrict sheet erosion of the face; and

(c) a 50-ft bench at the toe of the slope to contain the slide debris.

For rock cuts involving only dolomite, vertical faces and only 20-ft benches are being considered.

Stability and settlement may be serious problems in the fills crossing the flood plains of the Galena River and Smallpox Creek. Both streams were ponded in glacial times and may contain appreciable quantities of soil low in shear strength and high in compressibility. As the terraces rise to an elevation of 640 ft, ponding did not occur above that level. Adding an estimated 40-ft thickness of alluvium yields an elevation of 680 ft as the demarcation contour. Flood plains above this elevation are probably free of ponded sediments; the lower a flood plain is below 680 ft, the more likely it is to contain ponded material.

As 90 ft in height is the economic breaking point between a fill and a bridge, and as most of the major stream crossings will be more than 90 ft above their flood plains, stability and settlement problems will not be common.

Rest Area Water Supply

Rest area sites require a water supply of 40 gal per min to meet peak demands without costly storage facilities.[10] The Silurian Dolomites, the Galena-Platteville Dolomites, and the St. Peter Sandstones are proved aquifers in the area.

The Silurian Dolomites outcrop in the black pattern in Figure 9. As has been mentioned earlier, these are vesicular and creviced, and most springs in the county issue at their base. Some farm wells secure water from this source.[11] Unless a rest area is built on the high ridges of the Dodgeville Surface, wells in this aquifer will not be possible.

The Galena-Platteville Dolomites are interconnected and form a single aquifer. Where erosion has removed the overlying Maquoketa Shale and allowed solution to enlarge the rock openings, the probability of securing an adequate water supply is good.[12] This condition is present in areas with the small dot pattern on the geologic map. The town of Elizabeth, a mile northeast of the area in Figure 9, is pumping 100 gal per min from this aquifer.[12]

The St. Peter Sandstone is a clean, white, and very pure quartz sandstone. It is 300 to 350 ft below the top of the Galena and is widely used as an aquifer in northern Illinois. It is reliable for water supplies up to 200 gal per min.[12] The lower dashed line on the geotechnical profile shows its approximate elevation. Subtracting this elevation from the ground elevation gives the approximate depth of a well to the St. Peter Sandstone.

CONCLUSION

The geotechnical profile is an experimental presentation of earth science data to location engineers. As used in the Illinois Division of Highways it is a combination of maps and profiles (Figure 10). As much data

as possible is compiled from existing literature. Field checks, including seismic and earth resistivity, are used where needed to supplement the data secured from publications.

To date three sets of profiles have been prepared by the Bridge Office for the use of location engineers in District Offices. So far the feedback has been favorable.

REFERENCES

1. Bibliography and Index of Illinois Geology through 1965, Illinois State Geological Survey Bulletin No. 92.

2. Agnew, A. F., et al, Stratigraphy of Middle Ordovician Rocks in the Zinc-lead District of Wisconsin, Illinois, and Iowa, United States Geological Survey Professional Paper No. 274-K, 1956, pp. 251-312

3. Buschbach, T. C., Cambrian and Ordovician Strata of Northeastern Illinois, Illinois Geological Survey Report of Investigations No. 218, 1964.

4. Templeton, J. S., and Willman, H. B., Champlain Series (Middle Ordovician) in Illinois, Illinois Geological Survey Bulletin No. 89, 1963.

5. Trowbridge, A. C., and Shaw, E. W. Geology and Geography of the Galen and Elizabeth Quadrangles, Illinoi Geological Survey Bulletin No. 26, 1916.

6. Heyl, A. V., Jr., et al, The Geolc of the Upper Mississippi Valley Zinc-lead District, United States Geological Survey Professional Paper No. 309, 1959.

7. Mullens, T. E., Geology of the Cut City, New Diggings, and Shullsbur Quandrangles, Wisconsin and Illin(United States Geological Survey Bulletin No. 1123-H, 1964.

8. Bradbury, J. C., Grogan, R. M., ar Cronk, R. J., Geologic Structure Map of the Northwestern Illinois Zinc-lead District, Illinois Geological Survey Circular No. 20(1956.

9. Willman, H. B., and Reynolds, R. R., Geological Structure of the Zinc-lead District of Northwestern Illinois, Illinois Geological Survey Report of Investigations No. 124, 1947.

10. Cartwright, Keros, Groundwater Supplies along the Interstate Highway System in Illinois, Illinois Geological Survey Environmental Geology Notes No. 11, 1966.

11. Hackett, J. E., and Bergstrom, R. E., Groundwater in Northwestern Illinois, Illinois Geological Survey Circular No. 207, 1956.

12. Walton, W. C., and Csallany, Sandor, Yields of Deep Sandstone Wells in Northern Illinois, Illinois State Water Survey Report of Investigations No. 43, 1962.

BIBLIOGRAPHY

Chryssafopoulos, Nicholas, "Engineering Soils of Part of Jo Daviess County," Illinois Cooperative Highway Research Program, Project IHR-12, Report Q-1-57, 1957.

Fehrenbacher, J. B., et al, Soils of Illinois, Agricultural Experiment Station Bulletin No. 725, University of Illinois, Urbana, 1967.

Thornburn, T. H., Surface Deposits of Illinois - A Guide for Soil Engineers, Engineering Experiment Station Circular No. 80, University of Illinois, Urbana, 1963.

Wascher, H., and Rehner, R., Soil Associations of Jo Daviess County, Agriculture Cooperative Extension Service Circular No. 927, University of Illinois, Urbana 1966.

22

FIGURE 1.   UPPER MISSISSIPPI VALLEY
ZINC-LEAD DISTRICT AND THE DRIFTLESS
SECTOR OF THE CENTRAL LOWLANDS.

BEDROCK STRATA

System	Group Or Formation	Graphic Log	Description (Thickness)
Silurian	Hunton Megagroup: Joliet Kankakee Edgewood		Dolomite (0-197')
Ordovician	Maquoketa		Shale (110-210')
	Galena		Dolomite (260')
	Platteville		Dolomite (45-70')
	St. Peter		Sandstone (40-400')
	Knox Megagroup		

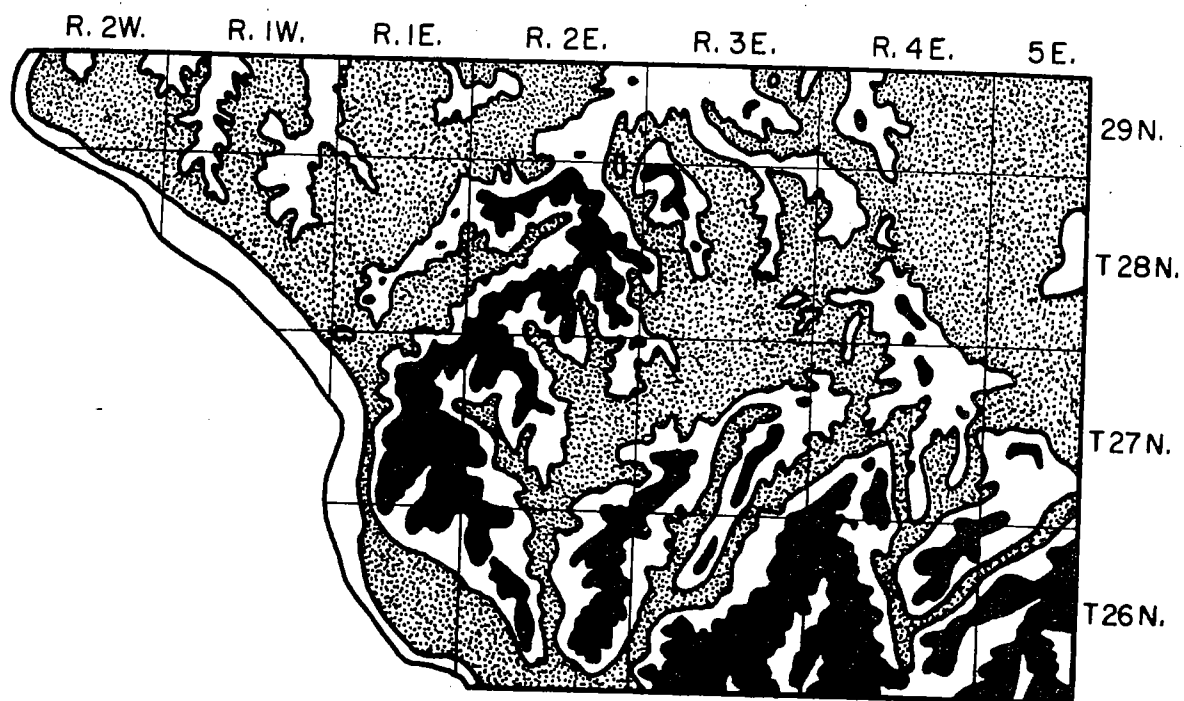▲ Cherty,   ๘ Vuggy,   — Shaly

FIGURE 2.   STRATIGRAPHIC COLUMN,

JO DAVIESS COUNT
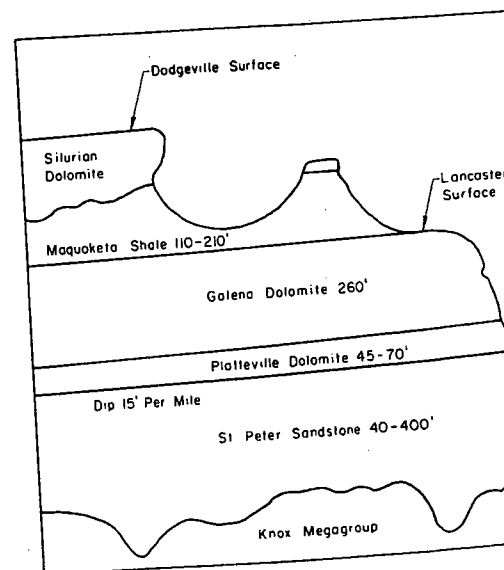
FIGURE 3.   RELATION OF LANDFORMS
AND BEDROCK, DRIFTLESS SECTOR.

R. 2W. R. IW. R. IE. R. 2E. R. 3E. R. 4E. 5E.

29 N.

T 28 N.

T 27 N.

T 26 N.

Geologic Map

Pattern	Bedrock
◢◤	Silurian Dolomites
▭	Maquoketa Shale
▨	Galena Dolomites

from Illinois Geol. Survey 1967 Edition
Geologic Map of Illinois

FIGURE 4.   GEOLOGIC MAP, JO DAVIESS COUNTY.

R. 2W. R. IW. R. IE. R. 2E. R. 3E. R. 4E. 5 E.

29 N.

T 28N.

T27N.

T 26 N.

Cir. 927,
University of Illinois
College of Agriculture
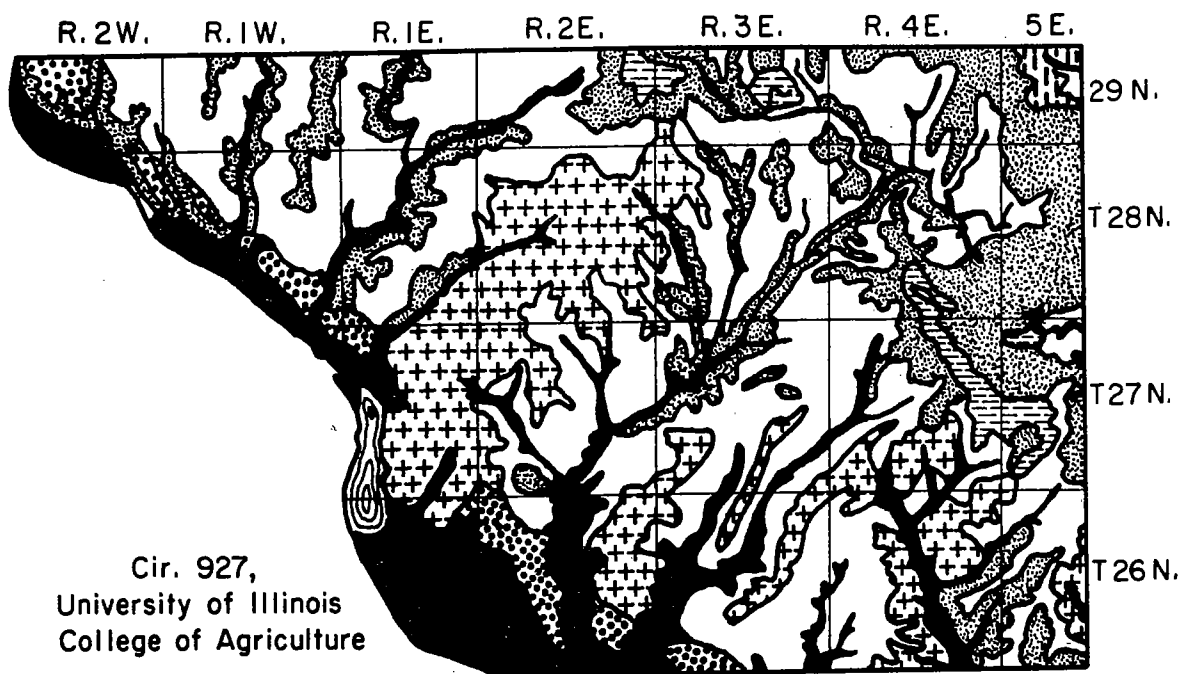
Parent Material	Pattern	Internal Drainage			
		Well	Moderate	Imperfect	Poor
Loess > 5'		Seaton (F) Tama (P) Fayette (F) Roxetta (F)		Muscatine (P) Sable (H) Stronghurst (F)	
Loess with Dolomite at 2-1/2'- 4' Dolomite at 0'- 2-1/2'		Palsgrove (F) Dodgeville (P) Dubuque (F)			
Loess with Shale at 0'-2-1/2'		Schapville (P) Derinda (F)			
Terrace		Camden (F)			
Alluvium: Calc. Silt Loam Silt Loam Silt Clay Loam		Dorchester Huntsville	Lawson	Otter Sawmill	

(P) Prairie Soils   (F) Forest Soils   (M) Mixed Soils   (H) Humic Glei Soils
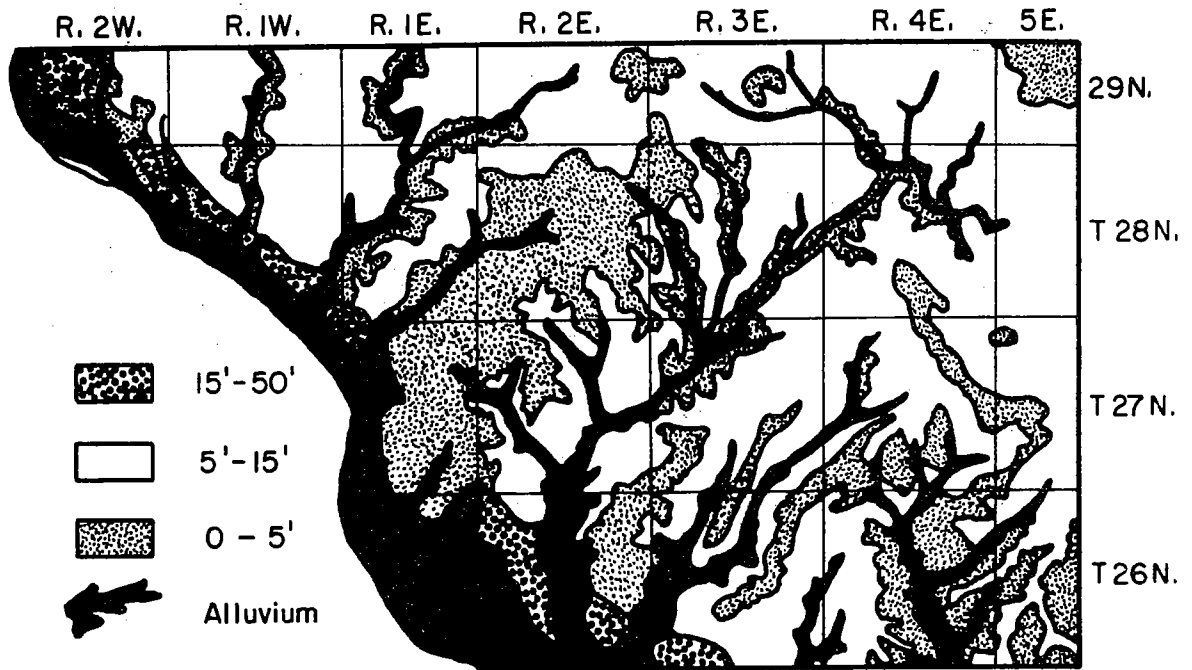
FIGURE 5.   SOIL ASSOCIATION MAP - JO DAVIESS COUNTY.

FIGURE 6.   MAP ON INFERRED THICKNESS OF LOESS, JO DAVIESS COUNTY
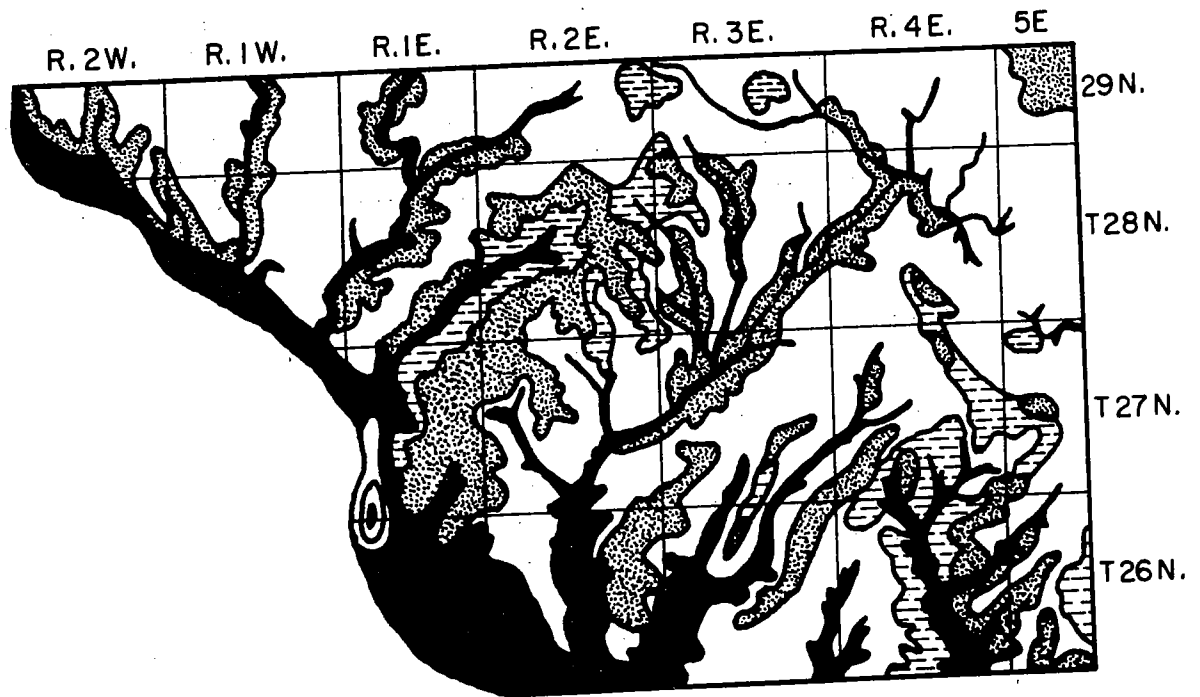
ENGINEERING SOIL INTERPRETATION
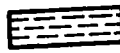
Pattern	Description
	Silt Loam (Loess) Over 5' Some Silt Clay Loam in Depressions
	Dolomite Bedrock at Less Than 5'
	Shale Bedrock at Less Than 5'
	Alluvium: Mostly Silt Loam with Silt Clay Loam in Backswamps

FIGURE 7. ENGINEERING SOIL INTERPRETATION, JO DAVIESS COUNTY.

ENGINEERING SOIL INTERPRETATION

FIGURE 8. GEOTECHNICAL PROFILE (SOILS) ILL. ROUTE 84 RELOCATION.

GEOLOGIC MAP (Bulletin 26 Ill. Geol. Surv.)

FIGURE 9. GEOTECHNICAL PROFILE (BEDROCK) ILL. ROUTE 84 RELOCATION.

FIGURE 10. FLOW SHEET FOR A GEOTECHNICAL PROFILE.

III. PROBLEMS WITH HIGHWAY CUTS IN LOESS NEAR EAST ST. LOUIS, ILLINOIS

Kenneth R. Keene*
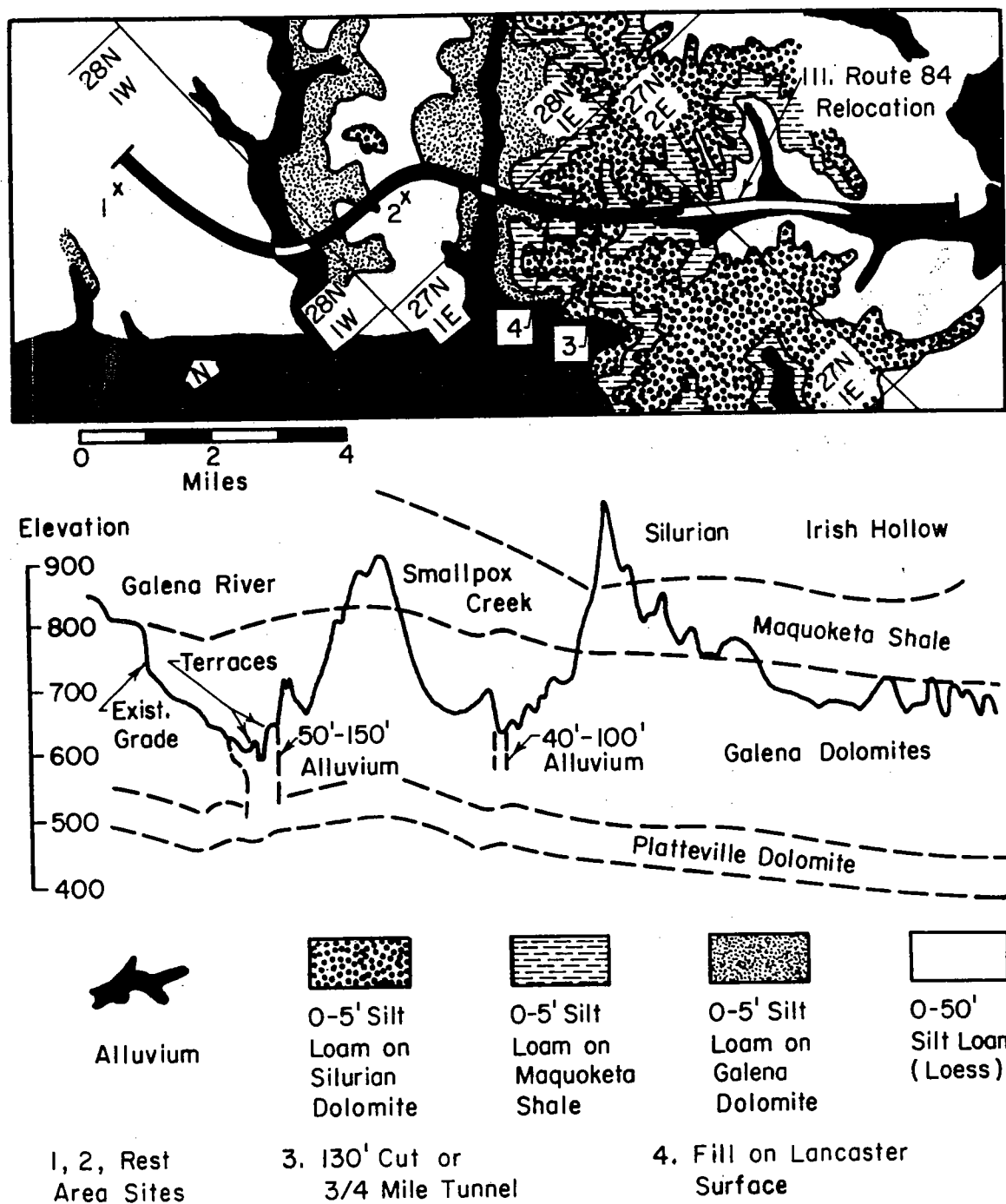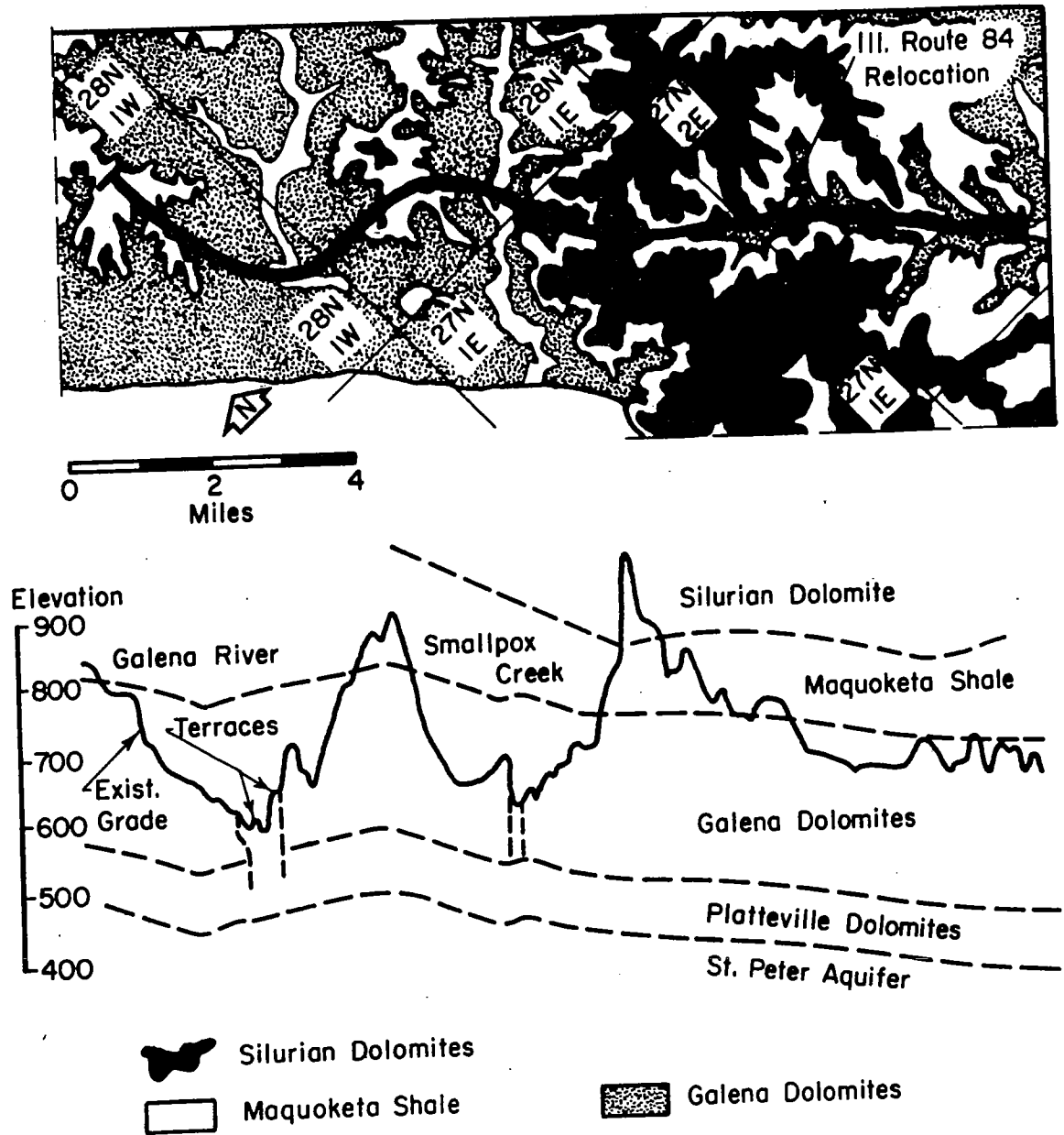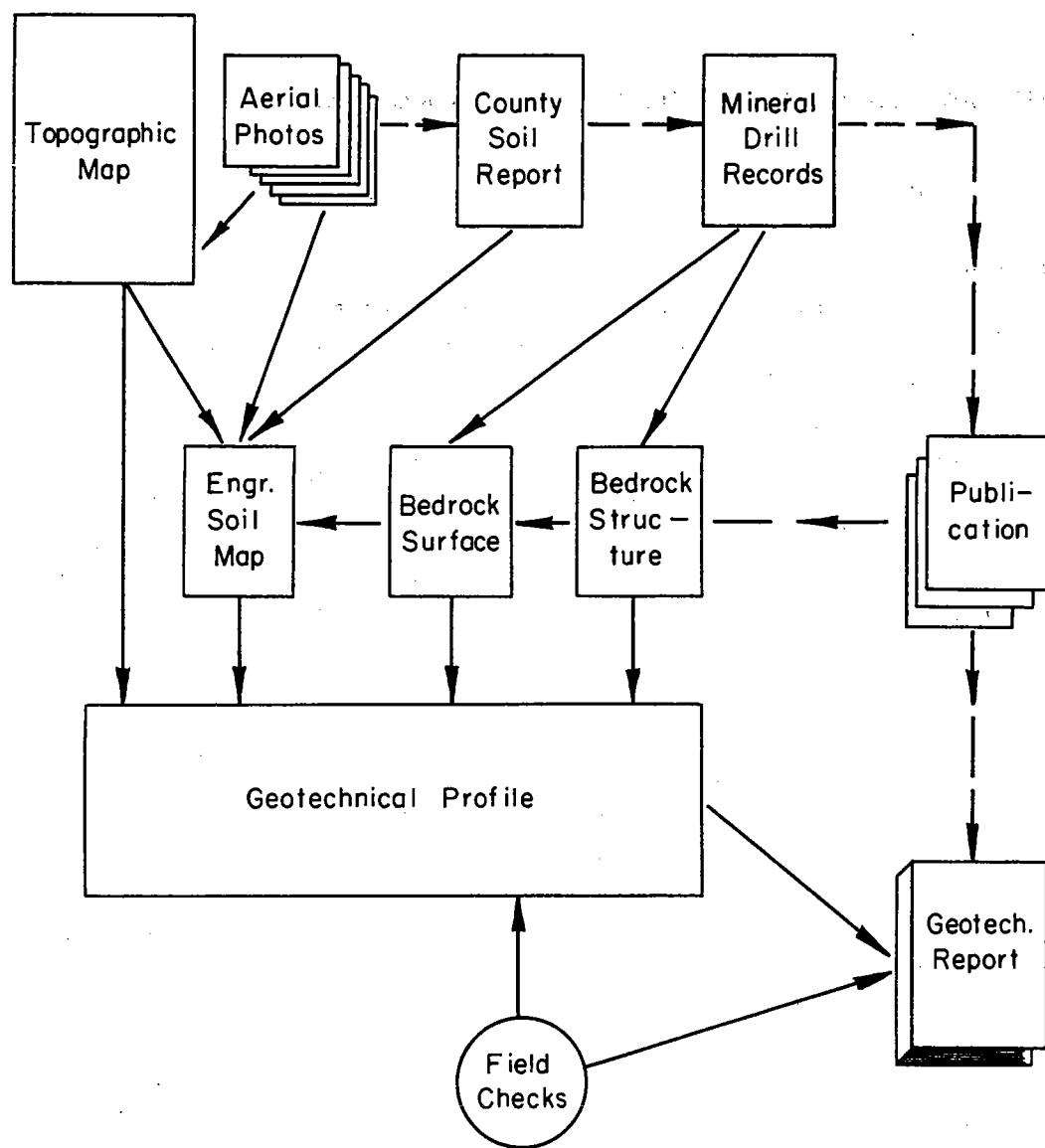
INTRODUCTION

I'm sure that many of you come from areas where you have certain soil problems that seem to plague you eternally on much of the construction within that area. Around East St. Louis we must continually construct highways in loess cuts and loess embankments. Our biggest problem to date has involved the excavation of deep cuts in thick loess. The nature of that problem is two-fold:

(a) Erosion control of slopes flatter than vertical has proven extremely difficult in most of the deep cuts.

(b) Slopes of 2:1 and 2.5:1 (horizontal to vertical) have proven to be very unstable in saturated loess. Today I am going to acquaint you with some of the problems we have encountered in the construction of three deep cuts in loess and describe for you some of the procedures and techniques to be used on a fourth project currently under construction.

GENERAL GEOLOGY OF THE AREA

The projects to be discussed here

today are all situated on the loess bluffs along the east side of the Mississippi River Valley near East St. Louis, Illinois. (See Figure 1 for the geographical location of the East St. Louis District.) Basically, the geology of the Pleistocene deposits is quite similar for all of the project with 30 to 50 ft of Peoria Loess overlying 30 to 50 ft of Roxana Loess underlain by Illinoian till.

The Illinoian till in these deposits has tentatively been identifie as a basal till deposited beneath the glacier and subsequently overridden by an ice sheet of considerable thickne

Loess overlying the till is an aeolian deposit, a result of several periods of deposition corresponding to the several periods of advance and retreat of the Wisconsinan age. Certa of the loessial units can be individua identified and even traced back to the particular till from which they originated. In the area of the subject projects, the loess units are divided, in descending order, into Peoria, Roxana IV, Roxana III, Roxana II, and Roxana I. Roxana IV Loess has been correlated with the Winnebago till of northern Illinois, while Roxana II Loe

*Assistant Engineer of Materials,
Illinois Division of Highways,
East St. Louis.

has been correlated with the tenta-
tively identified "Danville" till.
The Roxana I frequently has distinc-
tive lower and upper zones, Ia and Ib,
with Ia resting directly on the
Illinoian till. Roxana Ia is a silt
formed primarily of loess that has been
translocated and redeposited as
alluvium or colluvium.

The age of the loess deposits in
the area has been estimated at 10,000
to 20,000 radiocarbon years for the
Peoria Loess and 30,000 to 70,000
radiocarbon years for the Roxana Loess.
As in the case of most loesses, the
cementing agents are primarily clay
minerals and calcium carbonate with
Montmorillonite the principal clay
mineral in both the Peoria and Roxana
Loesses.

The usual engineering index
properties are of little value in dis-
tinguishing between the various loess
units, especially between Roxana II,
III, and IV. Perhaps the easiest
method of differentiation is by color.
Peoria Loess, a light yellow-tan,
consists predominantly of coarse silt,
though it does contain pockets of fine
sand at some locations (such as near
Collinsville). In contrast, the under-
lying Roxana IV is pinkish-gray. The
generally light grayish-tan color of the
Roxana III distinguishes it from the
pink layer above and the pink to
reddish-brown Roxana II below. This
Roxana II generally displays a marked
reduction in carbonates compared to
the overlying layers and contains silt
particles of finer grain size. Roxana
I is generally dark gray and possesses
a higher clay content and more plastic-
ity than the overlying units. Table I

illustrates the typical profile found
in this area and gives a color descrip-
tion of each unit.

PAST CONSTRUCTION PROJECTS AND THEIR
TREATMENTS
I-70 Cut

In April of 1960, construction was
begun on a deep cut for I-70 through
the loess bluffs northwest of Collins-
ville. The original design called for
a system of alternate horizontal berms
and nearly vertical slopes for the
entire depth of the 75- to 100-ft excava-
tion (Figure 2).
Geology of the Deposit

The soil profile for this project
generally consists of 50 to 70 ft of
loess containing pockets of fine sand
and underlain by very wet, gray, clayey,
and sandy silt. Figure 3 is a profile
of the natural ground, pavement grade,
and soil strata; as the figure shows,
there is a maximum of approximately
60 ft of Peoria Loess. Below an eleva-
tion of 510 ft, Roxana I is present,
often blending indeterminably into
underlying soil and gley. In this
instance, Roxana II, III and IV were
not present as continuous, readily
identifiable layers within the exca-
vation. There were numerous sand pock-
ets within the Peoria Loess. Neither
the excavation nor any of the soil
borings was deep enough to locate the
depth of the Illinoian till which under-
lies the soil and gley.
Construction Problems

Soon after construction began, a
two-fold problem came to light. At a
depth of 20 ft below the ground surface,
soft unstable material was encountered
and at 26 ft, free water was found.

TABLE 1. AVERAGE THICKNESSES AND COLOR DESCRIPTION OF THE LOESS UNITS OF THE EAST ST. LOUIS THICK LOESS DEPOSITS.

G R O U N D   S U R F A C E

20 to 50 Ft   Peoria Loess

Light Yellow-Tan

— — — — — — — — — — — — — — — — —

5 to 20 Ft   Roxana IV Loess

Pinkish-Gray

— — — — — — — — — — — — — — — —

5 to 30 Ft   Roxana III Loess

Gray - Tan

— — — — — — — — — — — — — — — — —

5 to 30 Ft   Roxana II Loess

Pink or Reddish - Brown

— — — — — — — — — — — — — — — —

10 to 30 Ft   Roxana I Loess

Dark Gray

— — — — — — — — — — — — — — — —

Illinoian Till

In addition, we opened up numerous sand pockets within the Peoria Loess. Because of the presence of the shallow water table and the sand pockets, it was impossible to construct the first vertical bench called for in the original design.

Re-examination of the subsurface conditions indicated the probability that the sides of the excavation would be stable if they were laid back on a reasonable angle. Due to the limited right-of-way available, the flattest slope which could be achieved was a 2:1 (horizontal to vertical).

Further deepening of the excavat revealed that the groundwater was mov laterally through the southern slope of the excavation. With this in minc we decided to install a perforated pi in a trench along the toe of the southern slope to help draw down the

groundwater and increase slope stability.

A perforated pipe was installed at the top of the slope to intercept surface runoff. This pipe was backfilled to the ground surface with crushed stone. The section of pipe at the toe of slope was backfilled with coarse sand to within 1 ft of the surface of the slope, with the remaining 1 ft backfilled with soil. To help prevent surface erosion caused by runoff from the slope, we placed erosion netting resembling a badminton net over the straw mulch after seeding operations were complete. This netting was held secure with metal staples driven into the ground at regular intervals.

Post-Treatment Failures

Within one month after shaping, seeding, and mulching of the southern slope, silt-flow type failures had occurred in varying degrees over approximately 75 percent of the back-slope (Figure 4). Most of the movements occurred overnight.

The following construction season corrective treatment was begun on the southern slope. Additional perforated pipe was placed in two excessively wet areas part of the way up the slope, resulting in the treatment seen in Figure 5. After the pipe and proper backfilling were placed, all of the slump failure locations were re-shaped, seeded, mulched, and again covered with erosion netting.

Within two weeks after completion of the re-construction, failures in the form of silt flows occurred, beginning after a rainfall of 1.24 in. in a 24-hr period (see Figures 6 and 7). A relatively shallow escarpment (about 5 ft deep) indicated a shallow slip circle failure within the slope itself. This slip circle failure was about 150 ft long, with most of the slope affected only by silt flows.

Final Corrective Treatment

Inasmuch as the problems encountered appeared to be due primarily to excess moisture in the soil, we sought a method of treatment which would remove this moisture. In line with this attempt, black locust seedlings were planted in staggered rows on 4-ft centers over the entire slope. Prior to actual planting of the seedlings, over 4,000 cu yds of soil was brought in to re-shape the slope, and the area was seeded with an 80-lb-per-acre mixture of Kentucky bluegrass, perennial rye grass, creeping fescue, brome grass, and redtop.

The use of the rapidly-growing black locust seedlings had two advantages:

(a) the root systems of the trees "anchor" the upper portion of the slope, and

(b) the trees remove large quantities of water from the ground for their growth.

Since completion of the final corrective treatment in 1963, there have not been any major movements of the slope. It would seem that a combination of time, perforated pipe underdrains, and locust seedlings has drawn down the water table enough to allow stabilization of the upper portion of the slope surface. The only thing which has not been completely overcome at this time is surface erosion due to runoff (see Figure 8). Some of the seedlings originally planted have been cut to thin out the growth.

34

I-270 Cut

In the spring of 1963, construc-
tion was begun on the excavation for
I-270 through the loess bluffs northwest
of Glen Carbon just east of Ill. Rte.
157. Maximum height of the cut was to
be approximately 80 ft with the exca-
vation to include the alignment of the
mainline as well as two of the inter-
change ramps.

Original Design

The plans originally called for
a series of nearly vertical faces
(1:10 slope) and horizontal berms on
the sideslopes of the excavation. All
berms were to be 20 ft wide with the
vertical faces a maximum height of
20 ft. Before the start of excavation
the plans and soils investigation were
reviewed for possible changes in cross
section in view of the earlier experi-
ences with I-70. On the basis of the
soils borings we decided to modify the
backslope for the sourthern side of
the excavation, since the borings
indicated free water about 35 ft below
the ground surface.

This modification was the use of
vertical cuts, variable in height up
to a maximum of 20 ft, with 12-ft wide
berms to a point near the ground water
table as determined by the borings.
Between the pavement grade and the base
of the lowest vertical face, a slope of
approximately 2:1 was intended. The
back-slope angle and berm widths were,
of course, dictated by available right-
of-way.

Since the soils borings along the
northern limits of the excavation did
not indicate any free water in that
area, we decided to build that back-
slope in accordance with the plans.

Results of Excavation

As the excavation neared comple-
tion to a rough grade, problems develop
on both backslopes. On the southern
slope, the contractor experienced loss
of ground and a subsequent slope fail-
ure which appeared to center itself in
the Roxana II; he was thus unable to
cut the ditch to grade.

On the northern slope considerabl
difficulty developed in maintaining
the vertical faces as the base of the
lowest one was reached. Whether it wa
coincidental or not, a major portion o
the bottom two vertical faces collaps
on the night of a massive explosion i
a propellent plant in nearby Edwards-
ville. An interim slope of about
1.5:1 was attempted in lieu of the tw
lower benches which had collapsed. T
resulted ultimately in failure of the
slope near the toe, due to both seepa
and lack of support by the softer und
lying material.

Corrective Treatments

Separate corrective treatments
selected for each backslope.

(a) On the northern slope the
of the upper vertical cut was moved
back as far as right-of-way permitte
Then a series of nearly vertical fac
a maximum of 10 ft high, and nearly
horizontal berms, 14 ft wide, were
constructed to a point within 5 ft
the saturated zone corresponding to
top of the Roxana II. From that po
downward a slope of 2:1 was used in
conjunction with a minimum berm wid
of 12 ft behind the ditch. The res
tant cross section is shown in Figu
This treatment proved very effecti
in establishing slope stability.
ure 10 shows this slope as it now

(b) On the southern slope it was impossible to flatten the backslope much more, inasmuch as all of the available right-of-way had previously been utilized. In an effort to stabilize the 2:1 backslope we decided to construct a counterweight of the heaviest material available near the toe of slope. Open hearth slag was selected as the material, since it possessed a loose weight of 3500 lbs per cu yd. The resultant cross section is shown in Figure 11.

This treatment extended a distance of 900 ft along the base of the southern slope. The slag toewall extended a depth of approximately 12 ft into the underlying material. At some points along the length of the toewall, it penetrated the undulating surface of the underlying Illinoian till.

At the westerly limit of the toe wall a 12-in. perforated pipe was installed to provide drainage from the trench across the infield area into the drainageway adjacent to mainline I-270. After a period of several months this pipe began to discharge water which had apparently accumulated in the toe wall.

This treatment appeared to be very satisfactory as far as future slope stability was concerned. Figure 12 shows this slope as it now exists.

Experimental Slope Treatments on U.S. 460

In the spring of 1964, construction was begun on enlarging the excavation for existing U.S. 460 to permit the construction of a diamond interchange at Ill. Rte. 157. To permit construction of the interchange it was necessary to make a deep excavation into the existing hill in the northeast quadrant of the proposed interchange. At this location a vertical face about 60 ft high had remained stable on the southern side of U.S. 460 for many years. On the basis of this experience of stable vertical faces at this site, the original plans called for construction of vertical faces and horizontal berms.

As in past cases, however, construction according to plans resulted in failure of the vertical faces once the zones of capillarity and saturation were encountered. To correct the failure, a treatment similar to the one used on the southern slope of the I-270 cut was used. This meant construction of vertical faces and horizontal berms in the upper, dry Peoria Loess, a 2:1 slope in the unstable Roxana Loess, and an open hearth slag toe wall at the base. (See Figure 13 for a cross section and soil profile.)

Alternate Slope Treatments

In order to obtain much-needed information regarding the erosion control of loess slopes, we decided to install several types of erosion control treatments over the slope between the slag toe wall and the vertical faces. An area about 600 ft long, from Station 238+50 to 244+50, was selected for testing five different types of treatment for control of surface erosion. The base treatment for relative comparison was a special seeding mixture prepared for soil conditions normally existing in the local loessial deposits. The various types of treatment were divided in plots as follows:

(a) special seeding mixture with

ag lime, fertilizer nutrients, and asphalt-coated straw mulch,

    (b) a three-media inverse filter,

    (c) locust seedlings placed 2 ft apart in staggered rows with the special seeding, fertilizer nutrients, ag lime, and straw mulch,

    (d) special seeding with ag lime, fertilizer nutrients, ag lime, and jute matting, and

    (e) stabilization of the upper 12 in. of soil with 10 percent hydrated lime and the special seeding.

These experimental plots were laid out in a pattern as shown in Figure 14. The special seeding mixture was the same for all the plots and consisted of:

Vernal Alfalfa	20 lbs / acre	
Brome Grass	30 "	"
Perennial Rye Grass	20 "	"
Kentucky 31 Fescue	30 "	"

The straw mulch was applied at a rate of 2 tons/acre. None of the seeding, ag lime, fertilizer nutrients, or straw mulch were, of course, applied to the inverse filter plot.

Analysis of the Results

    Initial observation of the experimental plots revealed that:

    (a) an appreciable slope failure occurred within the inverse filter following a period of heavy rainfall, and

    (b) germination was poor in the lime-stabilized plot and survival of the grasses even poorer.

About a year after the installation of the various plots, an evaluation was made by the Bureau of Research and Development. The evaluation was made on the bases of slope stability, control of soil washing, and quality of plant cover. The comparative rati are shown in Table 2.

DEVELOPMENT OF SLOPE DESIGN FOR I-64

    Results of treatments used on th three previously mentioned projects were evaluated for application in the design of the roadway cross section f the loess cut for I-64 between Frencl Village and Caseyville near Ill. Rte. 157. In addition, a special soils investigation was conducted to obtai vital information regarding the vari soil units. Data from the soil bori

TABLE 2. EVALUATION OF EXPERIMENTAL SLOPE TREATMENT PLOTS ON LOESS CUT AT U.S. 460.

TREATMENT	SLOPE STABILITY	CONTROL OF SOIL WASHING	QUALITY OF PLANT COVER
Special Seeding	Fair	Fair	Excellent
Locust Planting	Good	Excellent	Excellent
Jute Matting	Good	Excellent	Excellent
Inverse Filter	Failure	-	-
Lime Stabilized	Excellent	Fair	Poor

er-

ure
fol-
and
he
f

s

y,

y

tings

4

the

he

for

ch

e.

in

ious

ings

were used to evaluate the slope stability of various angles of repose in saturated Roxana Loess.

Slope Stability

From past experience we have learned that a series of nearly vertical (1:10) and horizontal berms are relatively stable in dry Peoria Loess. It is imperative, however, that surface runoff be kept from flowing over the faces of the vertical cuts. Some minor sloughing which occurs basically on vertical cleavage planes is more significant on slopes facing north than on those facing south.

Triaxial tests indicate that saturated Roxana Loess is virtually cohesionless; what is more, the soil is highly unstable below the water line. These characteristics, combined with the boundary condition imposed by excavating the soil for a roadway cut from the ground surface to a point below the water table, all lead to the conclusion that the slope failures are due to seepage pressures near the face of the excavation slope during and shortly after construction.

Once the water table has been drawn down below the face of the cut slope, the infiltration of heavy rainfall into the cut slope can cause a temporary state of seepage. In this case the soil for a shallow depth beneath the cut surface would behave as if it were below a free groundwater table.

The factors of safety for various values of backslope were calculated on the basis of rapid drawdown, steady seepage, and an infinite, cohesionless slope (Figure 15). These values are correct at the mid-height of the slope, liberal near the toe of slope, and conservative near the top--hence, average over the slope. From these values it may be seen that a slope of 4.5:1 is needed to provide an ample factor of safety near the toe.

Erosion Control

Information gained from the experimental slope treatments employed on the U.S. 460 project was utilized to select a slope treatment to minimize surface erosion on I-64. The plots of special seeding with jute matting and of locust seedlings were initially rated nearly equal with regard to erosion control.

Both treatments were selected for the I-64 project. The lower portion of the slope within the saturated loess will be treated with special seeding and jute matting while the upper portion will be treated with special seeding and locust seedlings.

A series of small, 3:1 slopes with intermediary berms was selected to reduce the amount of surface runoff on the slope. The over-all effective slope of this series of slopes and berms is 4.5:1 (Figure 16). Each of the horizontal berms is V-shaped and sodded to prevent erosion which would occur while seeding was becoming established. Figures 17 and 18 show the construction of the first two verticals and the placement of the sod, respectively.

SUMMARY

From these three extensive excavations in thick loess, we have gained considerable knowledge about the

treatment of loess cuts for highways. We have found that dry, Peoria Loess is relatively stable in nearly vertical (1:10) cuts and in this configuration it naturally negates the need for erosion control. Saturated Roxana Loess is highly unstable for slopes of 3:1 or steeper. In addition, erosion control is an important consideration for any loess slope flatter than about 1/2:1.

In order to achieve a stable slope and minimize surface erosion in loess cuts, the following treatments are suggested:

(a) The amount of surface runoff over the face of the slope must be minimized. This may be accomplished by placing a dike or paved ditch at the top of the cut and by placing sodded waterways or paved ditches on each berm.

(b) A good cover of vegetation must be established as soon as possible. A heavy rate of application of seeding and as many re-applications as necessary help to achieve this. Use of a hydro-seeder for the reseeding keeps any existing turf in place. Brome grass, crown vetch, and fescue appear to provide excellent turf in the East St. Louis area.

(c) The water table can often be drawn down a safe distance below the toe of slope with granular toe wal or perforated underdrains.

(d) Sodded waterways and paved ditches can be utilized extensively to reduce erosion.

(e) Employment of slopes of 4:1 or flatter generally eliminates slope failures in saturated loess.

BIBLIOGRAPHY

Frye, John C., Glass, H. D., and Willman, H. B., Statigraphy and Miner ogy of the Wisconsinan Loesses of Illinois, Illinois State Geological Survey Circular 334, Urbana, 1962.

Leighton, Morris M., and Willman, H. Loess Formations of the Mississippi Valley, Illinois State Geological Survey Report of Investigations No. 149, Urbana, 1950.

"Report of Subsurface Investigation Slope Stability Problem FAI 64, East St. Louis, Illinois," Layne-Western Company, Aurora, Illinois, 1965.

Turnbull, W. J., "Construction Probli Experienced with Loess Soils," High-way Research Board Record No. 212, Washington, D. C., 1968.

walls

d

to

:1
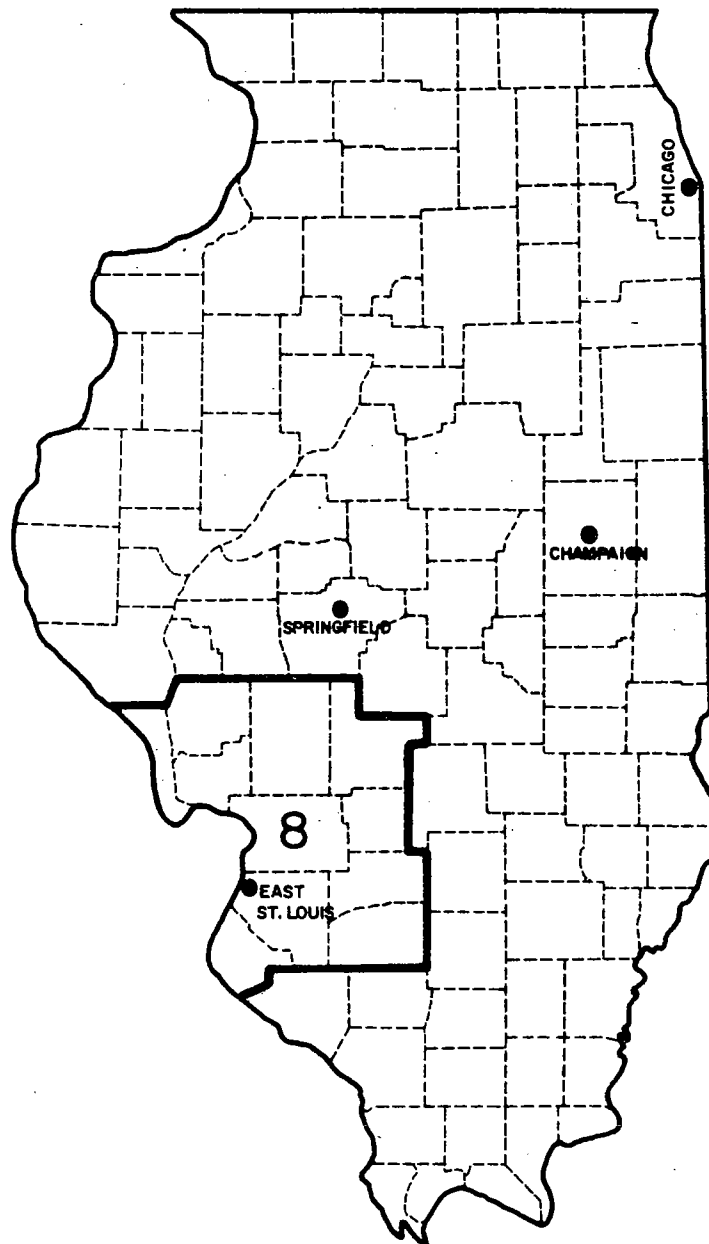
pe

ıeral-

f. B.,

ן -
st
ר

ɔlems
ר-

FIGURE 1.   LOCATION SKETCH OF DISTRICT NO. 8.

40

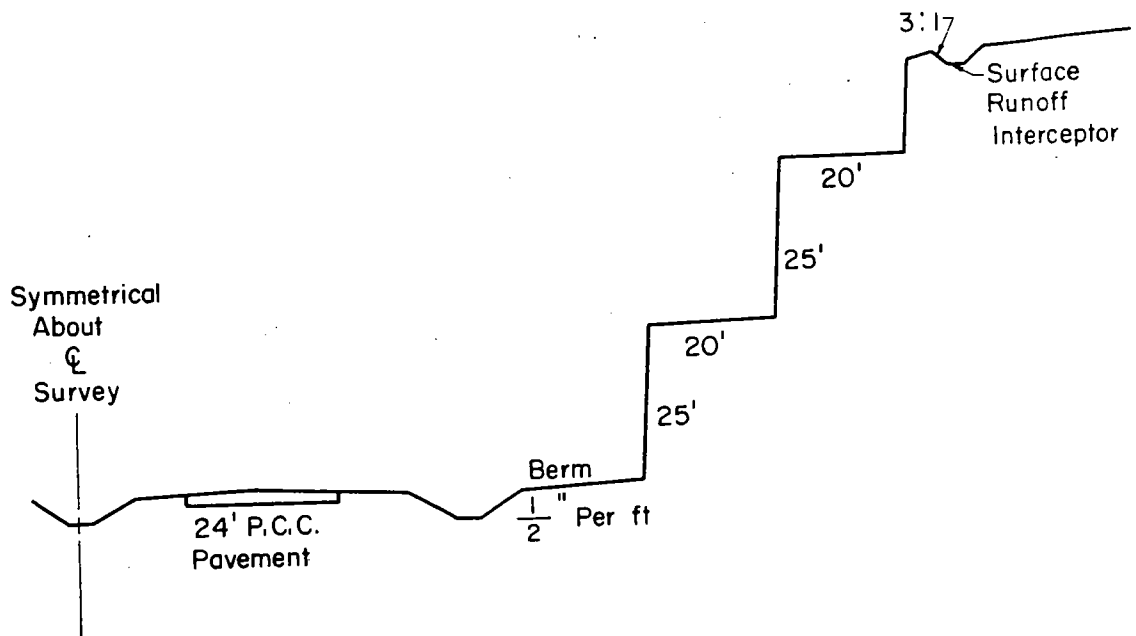FIGURE 2.   ORIGINAL DESIGN FOR I-70 LOESS CUT.

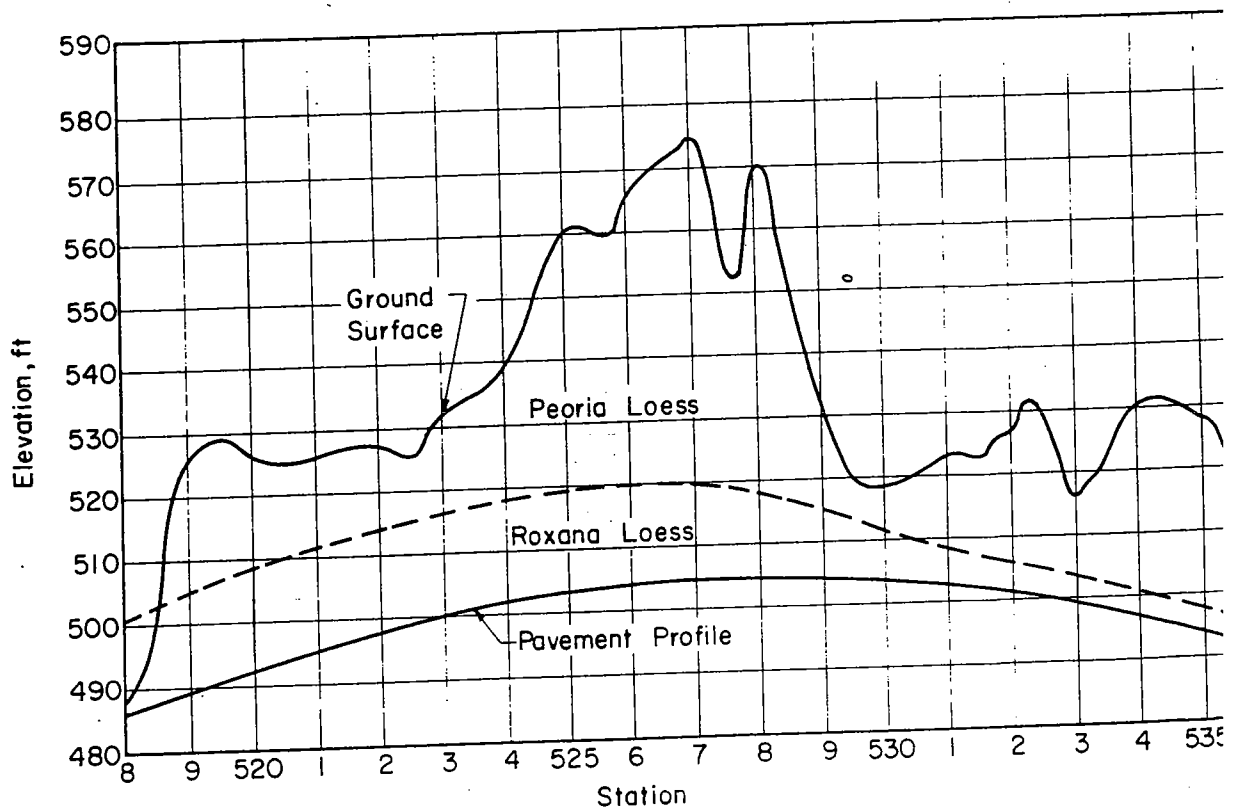FIGURE 3.   PROFILE OF I-270 CUT.
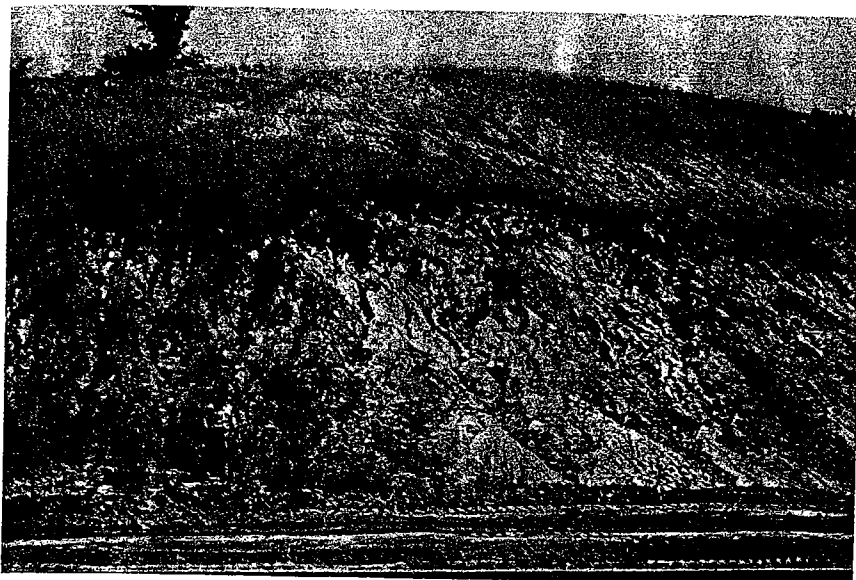
FIGURE 4. INITIAL
SILT FLOW FAILURES
ON I-70 CUT.

Note: Dotted Areas In Trenches Denote
Granular Backfill
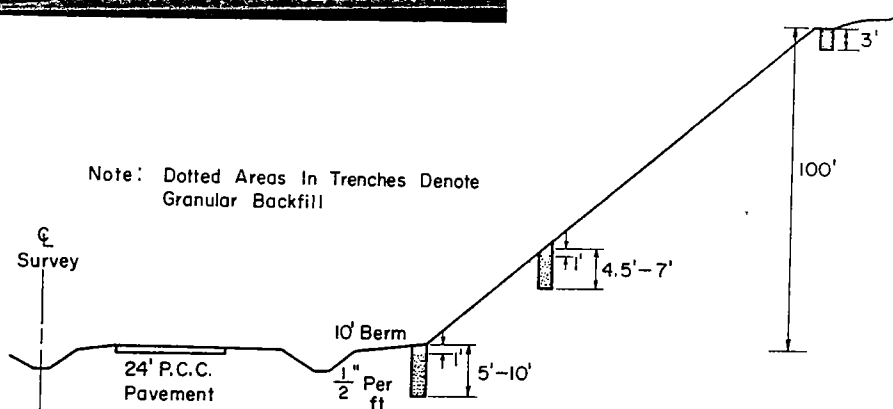
FIGURE 5. REVISED CROSS SECTION FOR I-70 CUT.

FIGURE 6. SILT FLOWS
ON RECONSTRUCTED SLOPES
OF I-70 CUT.

42
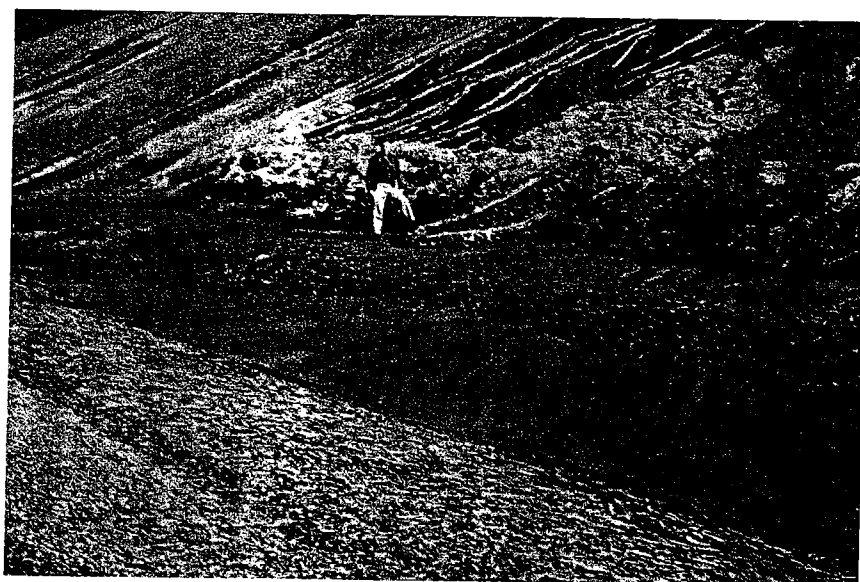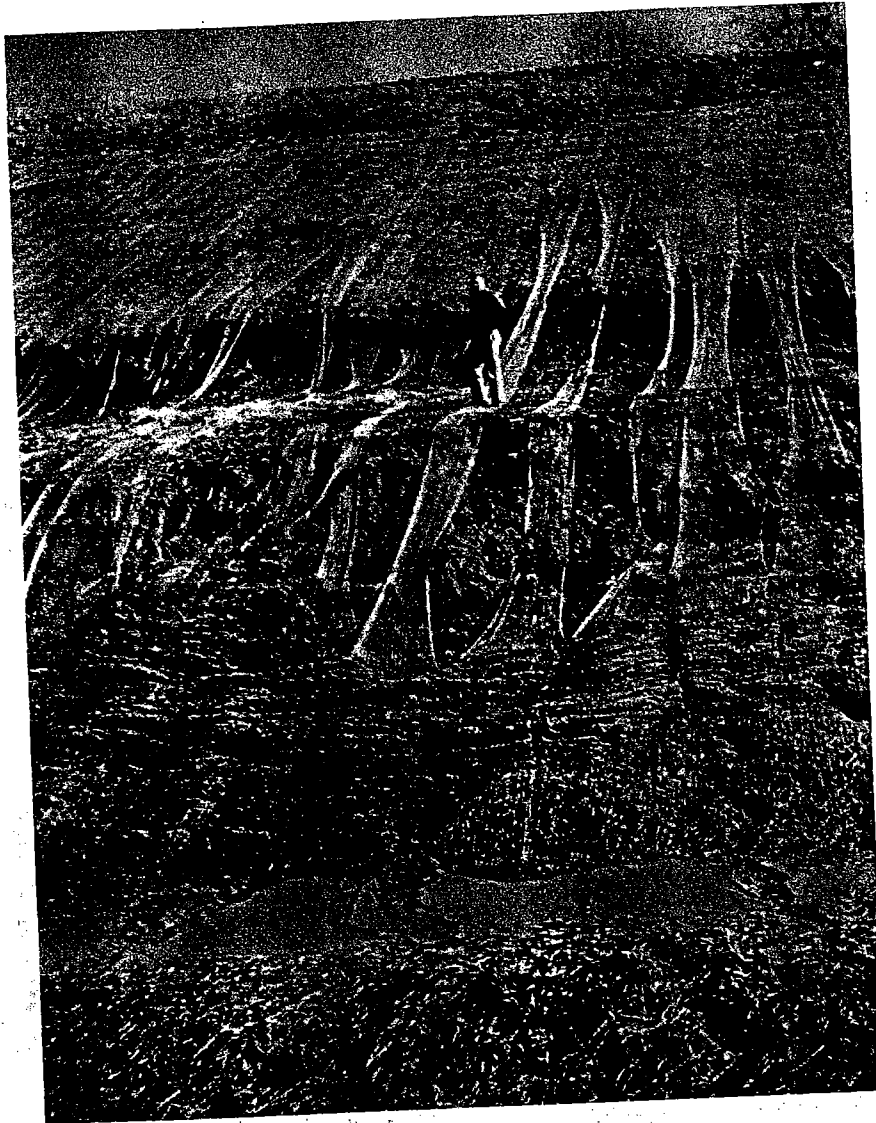
FIGURE 7. SLIPCIRCLE
FAILURE ON RECONSTRUCTE
SLOPES OF I-70 CUT.

FIGURE 8. EXIST:
SOUTHERN SLOPE
ON I-70 CUT.

Row

Peoria

Roxana   IV

Roxana   III

Roxana   II

Roxana   I

Illinoian Till

Original Ground

Original Design

1.5:1

2:1

Slope After Failure Of
Original Benches

Final Corrective
Slope

Edge Of
Pavement

Scale:
Vert. 1"= 20'-0"
Horiz. 1"= 20'-0"
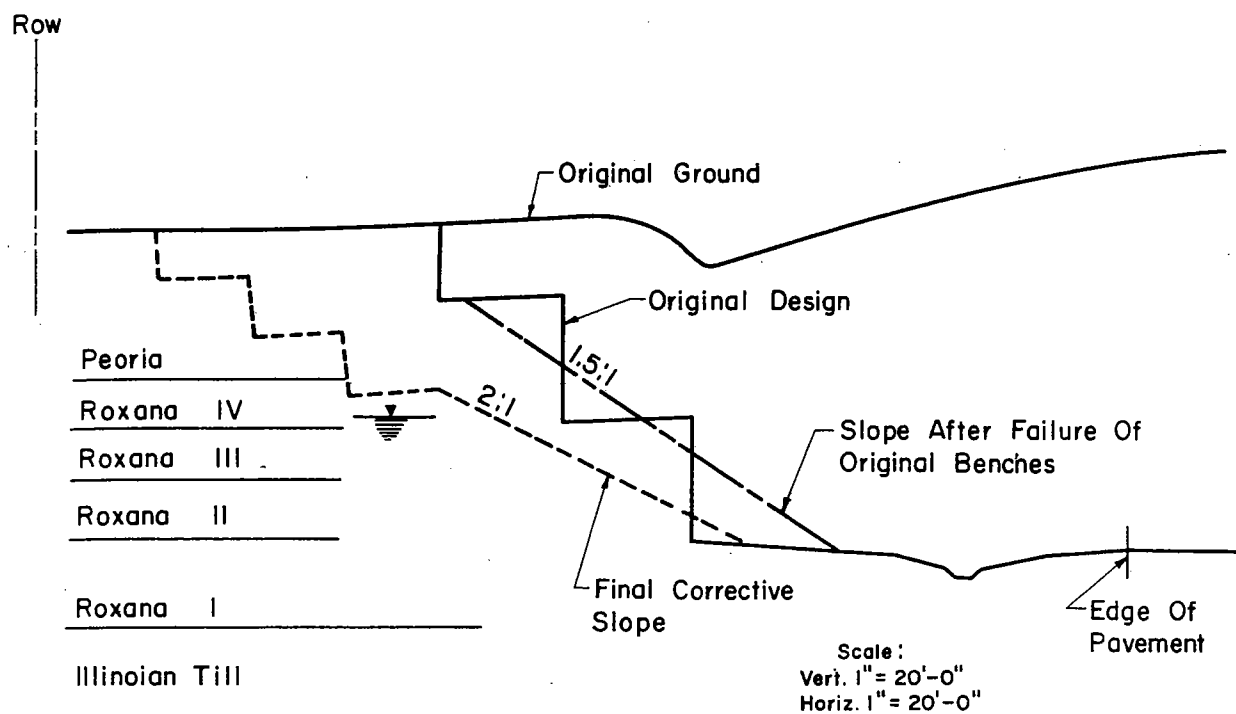
FIGURE 9.   CROSS SECTION OF NORTH SLOPE ON I-270 CUT
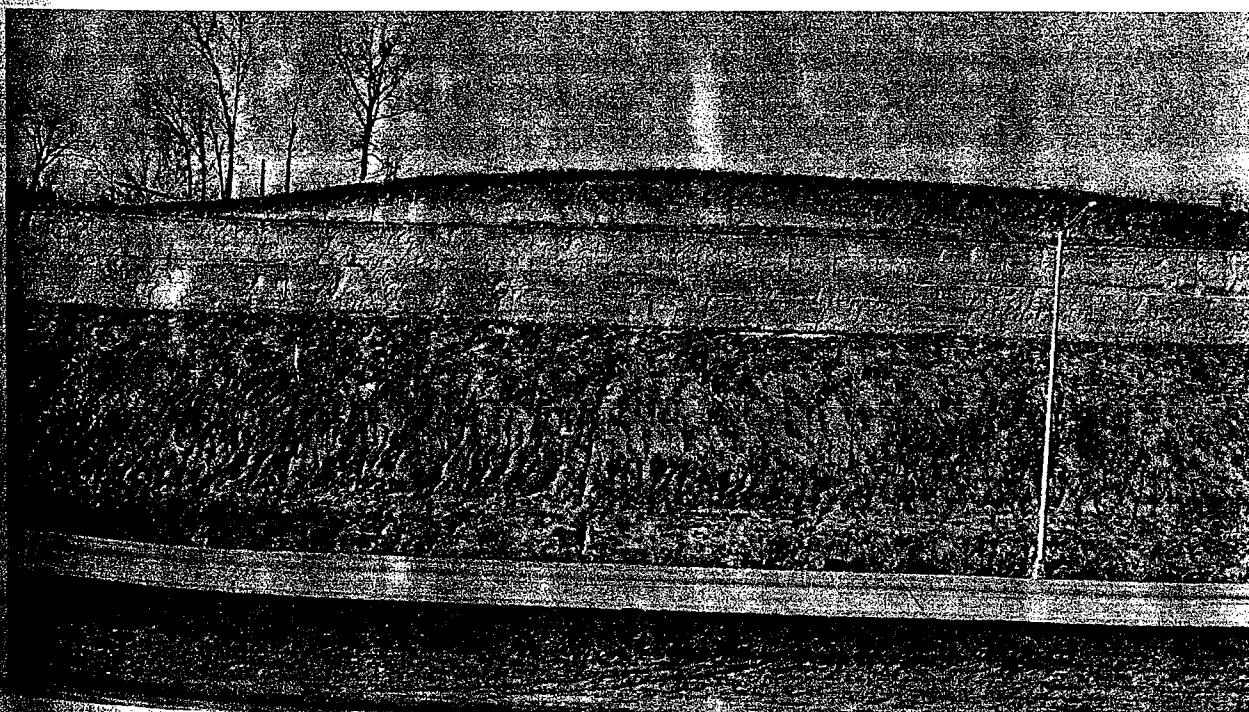
FIGURE 10.   EXISTING SOUTH FACING SLOPE ON I-270 CUT.

44

Original Ground

Var. 20'

551.0'

20'

Original Plan Section

20'

20'

Peoria

20'

Roxana IV

508'

Roxana III

Elevation 501.8

20'

As Built

2:1 ±

Roxana II

20'

Roxana I

1.5:1 ±

20'

Illinoian Till

Elevation 474

12' ±

12' ±

FIGURE 11. CROSS SECTION OF SOUTH SLOPE OF I-270 CUT.

FIGURE 12. EXISTING NORTH FACING SLOPE ON I-270 CUT.

Ground
Surface

40'

Peoria
Loess

|←10'→|

|←12'→|

|←12'→|

14' Roxana IV Loess

8' Roxana III Loess

9' Roxana II Loess

6' Roxana I Silt

Illinoian Till

Shale

2:1

Open
Hearth
Slag
Toe Wall

Edge
Ramp

20th. Annual Highway
Geology Symposium

FIGURE 13.   CROSS SECTION FOR U.S. 460 LOESS CUT.

Vertical Face

Vertical Face

Vertical Face

| Slope | | Special Seeding | Inverse Filter | Locust Seedlings & Special Seeding | Special Seeding | Jute Matting & Special Seeding | Lime Stabiliza- tion | Special Seeding |

Open Hearth Slag Toe Wall

240+50   241+00   241+50   242+00   242+50   243+00   243+50   244+00
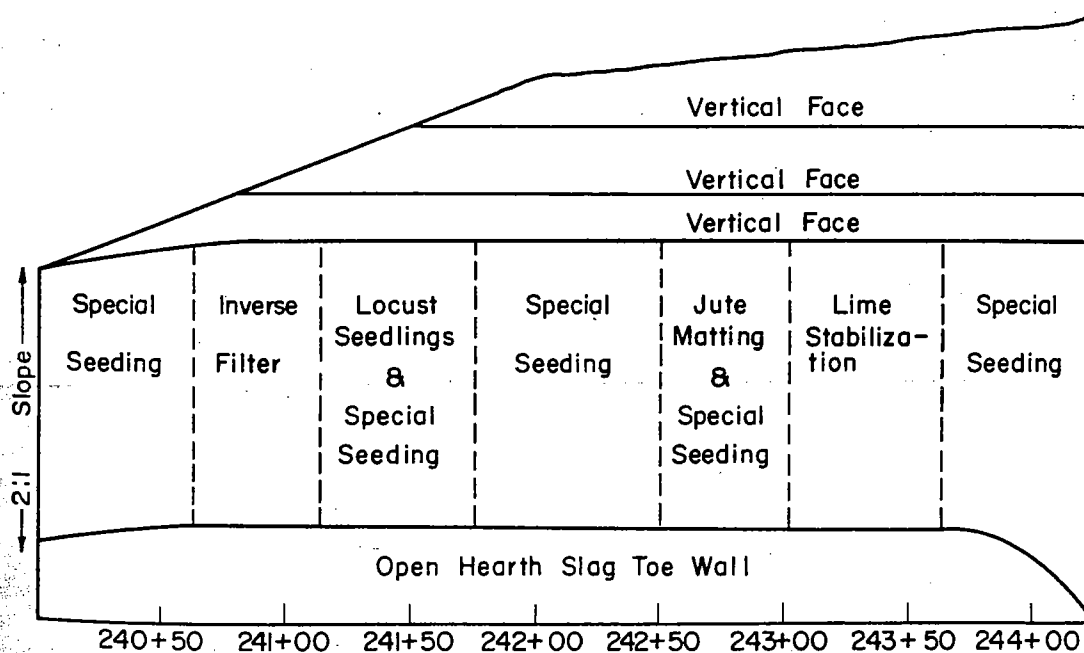
FIGURE 14.   ELEVATION VIEW OF LOESS SLOPE

TREATMENT FOR U.S. 460 NEAR ILL. RTE. 157.

Ground Surface &
Water Table

$$F.S. = \frac{Z\,(\gamma_t - \rho)\,(\cos^2 I)\,(\tan \phi)}{Z\,(\gamma_t)\,(\sin I)\,(\cos I)} \quad \text{On Plane A-B}$$
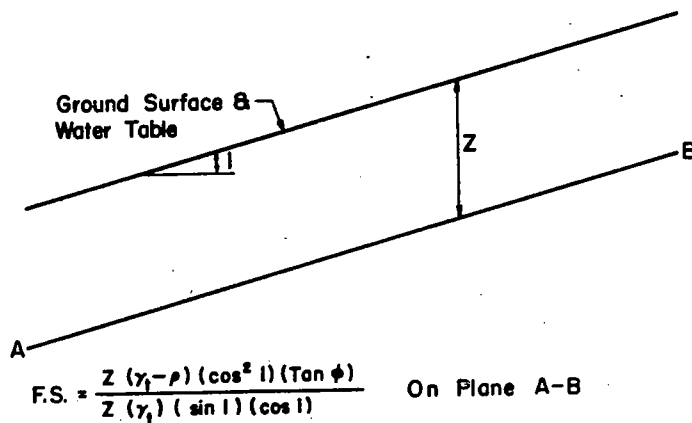
Where: γ_t = Saturated Soil Density — P.C.F. = 130 P.C.F.

ρ = Pore Pressure — Feet Of Water x 62.4

ϕ = Effective Angle Of Internal Friction = 32°

Factors Of Safety For Various Backslopes :

Slope	Factor Of Safety
3:1	0.97
3.5:1	1.14
4:1	1.31
4.5:1	1.46

FIGURE 15.   STABILITY ANALYSES FOR VARIOUS BACKSLOPES FOR RAPID DRAWDOWN CASE

Jute Matting | Black Locust
And Seeding, Cl. III | Seedlings And Seeding, Cl. II

15' Var.
20' Peoria
15'
Roxana IV
Roxana III
Roxana II

Till | Sat. Loess

Limits Of Rough Excavation

15' 3:1

3:1
10'

Sat. Loess | Dry Loess
Roxana I

Illinoian Till

15' 3:1
10'

17' 3:1
10'
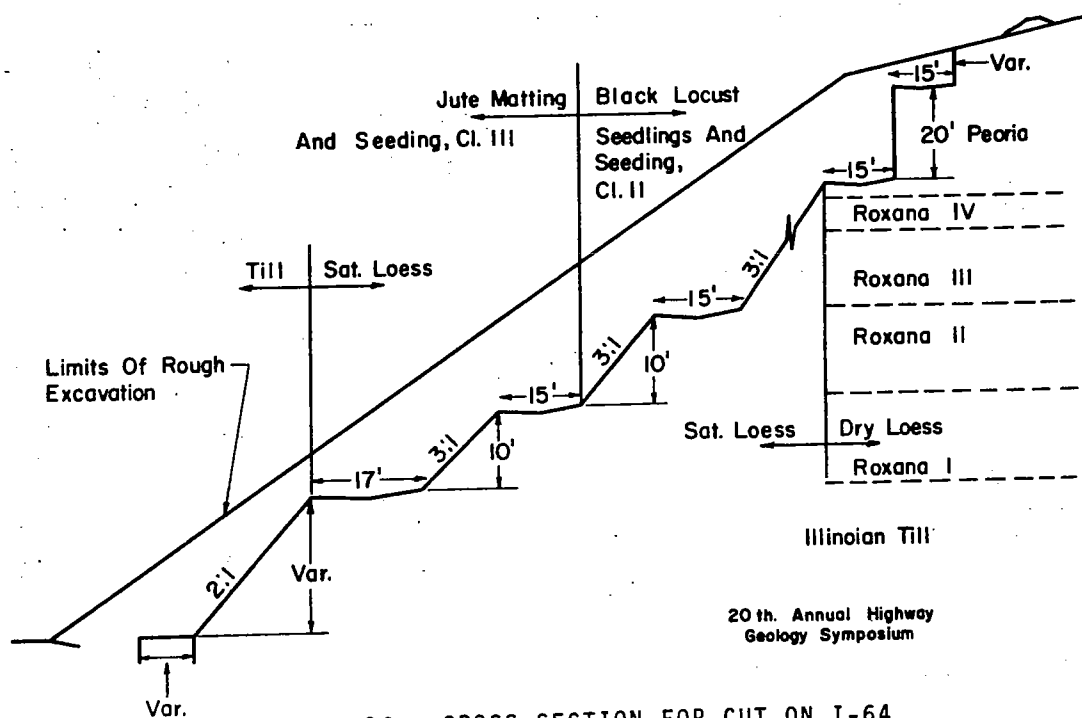
2:1

Var.

Var.

20 th. Annual Highway
Geology Symposium

FIGURE 16.   CROSS SECTION FOR CUT ON I-64.

FIGURE 17. CONSTRUCTION OF
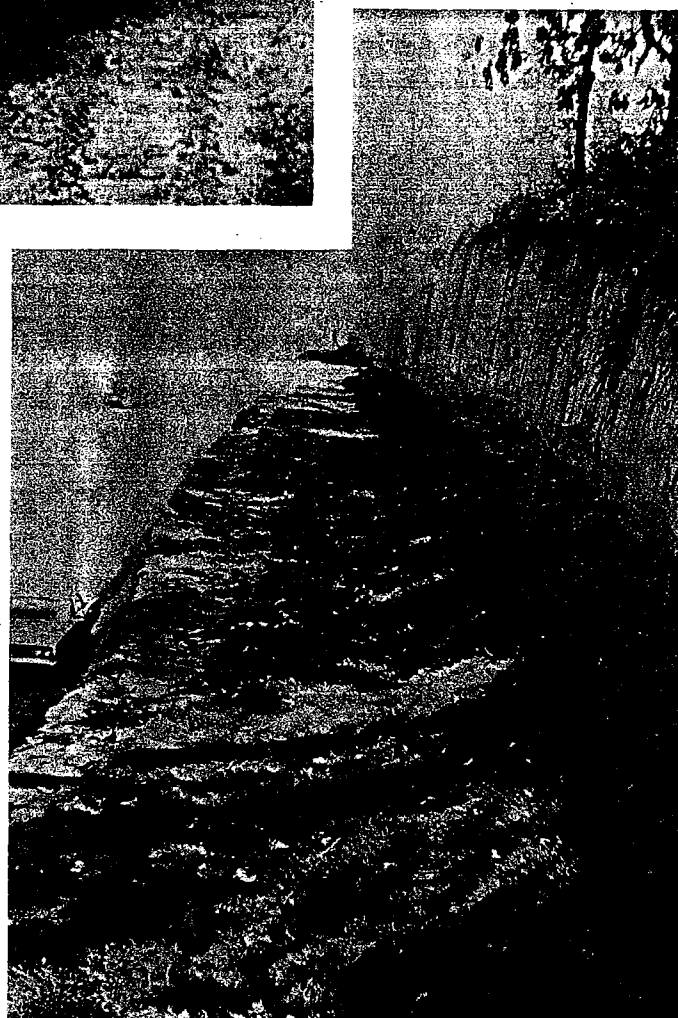VERTICAL FACES ON THE I-64 CUT.

FIGURE 18. PLACEMENT OF SOD
ON BERMS ON THE I-64 CUT.

CASE.

IV. FRACTURE SURFACES OF CARBONATE AGGREGATES: A SCANNING ELECTRON MICROSCOPE STUDY*

Richard D. Harvey**

INTRODUCTION

Because physical properties of carbonate rocks vary considerably, some limestone and dolomite deposits make better concrete aggregates than others, even though their mineral components may be essentially identical. Many characteristics of an aggregate influence its quality in concrete; an important one of these is the aggregate surface. Hsu and Slate[1]*** measured the tensile bond strength between aggregates and hardened cement paste and found that this strength was affected by the surface roughness of the aggregate. Moreover, the strength of the bond between cement paste and a hard, brittle, homogeneous, fine-grained limestone was 45 to 65 percent greater than that of a medium- to coarse-grained oolitic limestone.

***Superscript numbers in parentheses refer to the References at the end of this paper.

Studies by Gaynor[2] and Wills[3] show that the principal effect of differences in shape and surface texture of coarse and fine aggregate particles is on the water requirements of concrete. Several other published works on the effects of surface texture and shape of aggregates on concrete are discussed by Mather.[4]

Measurements of the surface texture of rocks and other materials have been made using various mechanical, electrical, and optical devices.[5,6,7] The relative shape and surface texture are indirectly measured by the flow rate of aggregates through an orifice.[2,3,8]

Microscopic observation of the surfaces is most helpful in interpreting surface texture and roughness data; without it, incomplete or inaccurate interpretations may result.[9]

Purpose

The purpose of this project is to survey the fracture surfaces of Illinois carbonate rocks at high magnification and to describe and classify the feature observed.

Scanning Electron Microscope

Samples were examined with a relatively new type of electron microscope--tively new type of electron microscope--

a scanning electron microscope. The combination of electromagnetic lenses with direct examination of the specimen, rather than a replica, produces an enhanced three-dimensional image. A rock specimen up to about 1 cu cm in size may be examined in the instrument; useful magnifications range from 20 to more than 20,000 times. To describe its operation briefly: the scanning microscope produces an electron beam that impinges on the surface of the specimen, and the reflected and scattered electrons are detected, amplified, and displayed on cathode ray tubes for visual observation and photographic recording. For a detailed description of the scanning electron microscope, the reader is referred to Thornton[10], Smith and Oatley[11], or Nixon.[12]

Preparation of rock specimens for study in this microscope has one complication. As the electron beam strikes the specimen, an electron cloud is produced on the specimen surface; if the charge were not conducted away, this cloud would completely disguise the specimen. Since carbonate rocks are nonconductors, they must be coated with a thin film of conducting metal to eliminate the unwanted charge. Specimens for this report were coated with gold and palladium, approximately 100 to 300 angstroms thick, deposited by simultaneously vaporizing gold and palladium wires under high vacuum.

Fracture of Samples

In the "Brazilian" or indirect tensile test commonly used in testing concrete[13,14] and rocks[15,16,17], a cylindrical specimen is compressed along opposite ends of a diameter. The speci-

men fails by extension--that is, by splitting parallel to the direction of load because of tensile stresses acting at right angles to the direction of load-- and in shear in a small portion of the specimen immediately under the points of loading.[18]

Fracture surfaces for this study were produced by breaking a specimen with a pair of ceramic nippers. The rock splits between the opposing wedges of the nippers and therefore fails in tension along a major portion of the failure surface. High compressive stresses induced in a small volume of rock immediately under the wedge of the nippers produce local shear fractures.

The fracture surfaces produced this way were examined under a binocular light microscope, so that several areas considered to be representative of the entire surface, as well as some showing special features, could be selected for detailed study at high magnifications. These surfaces were coated with gold-palladium as outlined earlier and were studied in the scanning electron microscope.

To date, seven samples of carbonate rocks commonly used as concrete aggregates in highways and eight samples not generally used in concretes have been examined. The samples are listed by geologic units and described in the table on pp. 12-13. The table also includes an index of the electron micrographs by figure numbers.

MICROSCOPIC OBSERVATIONS
Extension Fracture Surfaces in Limestones

Electron micrographs of extension fracture surfaces of calcite grains in

limestones can best be interpreted by comparing them with extension fractures of single crystals. The three unique and nonparallel cleavage planes possible in calcite contribute to the complexity of fracture markings. Figure 1 shows a portion of an extension fracture surface of a single crystal of iceland spar calcite, broken along rhombohedral cleavage planes. Cleavage steps indicated by the letter "C" in this figure characterize transgranular fractures, or fractures that pass through individual grains, as distinct from intergranular fractures, or fractures that pass along grain boundaries. Fracture surfaces lacking these markings may or may not be transgranular, but when the markings are present, transgranular fracturing is definitely indicated.

In metals, the direction of propagation of cleavage cracks is parallel to the lineation of the cleavage steps, especially in cases where two cleavage steps coalesce to produce a "river" pattern.[19,20,21] The same pattern has been detected in quartzite stone.[22] Coalescence of cleavage steps also occurs on calcite surfaces, faintly shown in the upper left-hand corner of Figure 1. Interpretation of these cleavage steps, based on behavior of metals, would indicate that the fracture was initiated along the lines AB and AD and was propagated as shown by the arrows.

An extension fracture surface of a large grain of calcite (crinoid fossil fragment) in the Ullin Limestone (Figure 2) shows cleavage surfaces and steps oriented left-to-right on the micrograph.

micrograph negative. Small grains of calcite dust derived from nearby areas of the rock during failure appear as highlighted particles on the crystal surface.

Most coarse-grained limestones contain large crystalline particles of calcite derived from fossil crinoids. When viewed with the unaided eye, coarse-grained stones have very rough surfaces compared with fine-grained limestones; however, a high percentage of the coarse surfaces are rather smooth when examined at high magnification, as in Figure 3. This micrograph shows a surface of a crinoid fossil from the Burlington Limestone. A very large cleavage step is shown in the left half of the micrograph, and numerous small steps occur over the entire grain. A few relatively loose particles derived from the specimen at the time of fracturing appear as highlighted particles weakly attached to the surface of the specimen.

The irregular holes seen on the specimen are portions of intragranular voids that occur within the grains. These voids are the same type of structure as the fluid inclusions illustrated by Lamar and Shrode.[23] Occasionally, liquid is observed in similar voids in specially-prepared thin sections of Burlington and other limestones. Most of the intragranular voids have one or more planar boundary surfaces parallel to cleavage intersections.

The Kimmswick Limestone contains many coarse-grained particles, and extension fracture surfaces of these particles closely resemble the one shown in the Burlington sample in Figure 3.

filling, sparry calcite. An example of
its extension fracture surface appears
in the specimen of Salem Limestone in
Figure 4. The fracture path in the
sparry calcite of this sample is trans-
granular and the cleavage steps are
varied in pattern and height.

Extension fracture surfaces of the
fine-grained components in high purity
crinoidal limestones are shown in Fig-
ures 5 and 6. The fine-grained bryozoan
fossil material in the Ullin Limestone
(Figure 5) mainly consists of euhedral
grains of calcite; that is, the grains
are bounded by rhombohedral crystal
faces. Only a few of the grains show
evidence of transgranular fracture
(arrow, Figure 5). On the basis of the
preponderance of euhedral grains, it is
interpreted that the path of the frac-
ture was mainly along grain boundaries,
or intergranular.

The euhedral shape of these grains
is not seen in routine thin-section
study with transmitted polarized light.
The size of the fine-grained calcite is
approximately 1 to 3 μ, and although
these particles can be seen with light
microscopes, the very small depth of
field and the possible alteration of
grain surfaces during grinding and pol-
ishing inhibit detailed observations.

A high pore volume in the Ullin
specimen is strongly suggested by the
micrographs, especially of the fine-
grained components (Figure 5). Labora-
tory measurements indicate 11 to 12 per-
cent porosity in the sample studied,
which accounts for the preponderance of
intergranular failure surfaces.

The fine-grained component of the
sample of Kimmswick Limestone has a

grain-size distribution between about
7 and 16 μ. An extension fracture sur-
face of this material is shown in Fig-
ure 6, where the grains average 8 μ,
are mainly euhedral, and are rhombic in
shape. There is little evidence of
transgranular fracturing, although sev-
eral grains have tiny rectangular pits
on their uppermost surfaces. These
pits may have been points of direct con-
tact with grains on the opposite side
of the fracture, perhaps slightly inter-
grown. Micrographs of other areas of
the fine-grained calcite show fewer
euhedral grains; however, cleavage
steps and other transgranular fracture
markings were rarely observed.

Very fine-grained micritic lime-
stones (Figures 7-15) are in distinct
contrast to the general euhedral shapes
of fine-grained components that occur
in dominantly medium- to coarse-grained
crinoidal limestones. The surface of
the sample of St. Louis Limestone (Fig-
ure 7) contains mainly anhedral grains
(grains with very few or no morphologic
crystal boundaries). A planar polished
and etched surface of this limestone
shows a mosaic texture with curvilinear
grain boundaries. The fracture surface
reflects this texture. Micrographs of
the sample show few or no pore spaces.
One of the few large grains of calcite
widely scattered throughout this sam-
ple is seen in the upper center of Fig-
ure 7. The grain has been cleaved dur-
ing fracturing, and many of the small
surrounding grains appear to have been
similarly broken. However, only a few
cleavage steps were observed on the
small grains (arrows, Figure 7), the
most abundant particles in this sample.

Fractures of specimens of the very fine-grained (lithographic) Wapsipinicon Limestone show similar surfaces (Figure 8); however, in this case, transgranular fracture markings are more abundant.

The Cedar Valley Limestone sample is typified by the surface shown in Figure 9. The large grains seen on the top and right of the figure represent only about 10 percent of the rock; the remainder consists of fine-grained calcite, as seen in the left side of the micrograph. Extension fracture surfaces of this specimen are characterized by the highly irregular grain surfaces and the occurrence of minute particles adhering to both fine and coarse particles. These minute particles are thought to be produced at the time of fracture.

Much of the oolitic Ste. Genevieve Limestone consists of very fine-grained calcite. The fracture surface of a small part of an outer band of an oolite shown in Figure 10 is characterized by intergranular fracture, the most common mode of fracture in fine-grained components of the oolites.

Figure 11 depicts an extension fracture surface of the sample of Kinkaid Limestone; its fracture mode is mainly transgranular. A close-up of the area in the center of Figure 11, shown in Figure 12, reveals clay flakes on the surfaces of calcite grains. In addition to the clay, about seven percent very fine-grained quartz and chert-like material is also found along calcite grain boundaries.

The limestone samples discussed above were taken from Ordovician, Devonian, and Mississippian strata. Pennsylvanian limestones have not proved to be major sources of concrete aggregates in Illinois; generally, those that are fine-grained have excessive soundness losses. Figure 13 is typical of the extension fracture surfaces of the specimen of Pennsylvanian Seville Limestone (Spoon Formation), broken parallel to the bedding. A close-up of the specimen (Figure 14) shows a poorly defined grain structure over most of the surface. The highlighted surface shown is mainly clay material. Also, three rhombs of carbonate grains stand above the general level of the fracture surface.

Figure 15 shows a surface of the Lonsdale Limestone (Modesto Formation), which also contains clayey material along the extension fracture, oriented parallel to the bedding. The center of the figure shows a cylindrical and wax-looking structure that also is observed in other Pennsylvanian limestones and is possibly organic in origin. Note a similar structure near the center of Figure 13. Such structures may weaken the cement-aggregate bond.

Shear Fracture Surfaces in Limestones

As stated above, high compressive stresses are produced in the rock specimen immediately under the wedges of the nippers, and shear failures occur in this area of the stone. These areas always produce high intensity electron reflections under the scanning electron beam, mainly because of the large surface area of the powdery material on the sheared surface. Figures 16 and 17 are typical examples of sheared surfaces of very fine-grained specimens of the Wapsipinicon and Cedar Valley Limestone. The crystalline particles are flattened due to the shearing, which is espe-

tes
re
s

pec-
one
o
imen
rain
 The
clay
bon-
evel

e
n),

ed
 of
axy-
ved
d
 a

en

s
ve
eci-
the

on
ron
r-
 the
show
 in
ap-
s.
red
ally

noted when examined at ultra-high mag-
nification (Figure 17). The one speci-
men of sheared dolomite examined (Racine,
Sample #65-36) also had much very fine
powder and in addition contained a num-
ber of very small "V" or cone-shaped
structures (Figure 18) pointing in the
opposite direction of the load applica-
tion.

Extension Fractures in Dolomites

Extension fracture surfaces in
dolomites reflect a fairly uniform rhom-
bic mosaic grain structure more commonly
found in dolomites than in limestones.
Examples of this rather uniform texture
are observed in the Racine Dolomite of
Silurian age (Figure 19, Sample #65-36).
Nevertheless, abundant cleavage steps
and fracture markings resemble those
observed in limestones (Figure 20).
The samples of Racine Dolomite clearly
failed by transgranular fracture mode.
Pore spaces, common in dolomites, are
frequently lined with euhedral crystals
(Figure 21), and the distinction between
grain-boundary failure and failure sur-
faces that include such pores cannot
always be made with certainty.

Extension fractures in the Joliet
Dolomite of Silurian age (Sample #62-
16A) from northeastern Illinois general-
ly show numerous fine particles weakly
adhering to the surface (Figure 22).
Samples of the Joliet from northwestern
Illinois (Sample #67-303) have low
density and high abrasion and soundness
losses, and do not meet present speci-
fications as aggregates for concrete
highways in Illinois. The rock from
this area contains kernels of hard,
dense dolomite, 1 to 4 in. across,
bounded by friable, porous dolomite.

An extension fracture in one of the hard
kernels (Figure 23) shows dolomite
grains surrounded by very fine-grained
porous material that is aggregated into
spherical structures 1 to 2 μ across.
Judging by its structure, this material
would be very susceptible to deteriora-
tion in freeze-thaw and sulfate sound-
ness tests.

Intragranular voids contribute to
the surface roughness of dolomites and
are particularly abundant in some speci-
mens of the Racine and Joliet Dolomites
(Figures 19, 20, and 24). No such
voids were observed in the dolomite
specimen examined from the Mississippian
Salem Formation in western Illinois
(Figure 25); there, several grains
failed by transgranular cleavage, and
a close-up view (Figure 26) of the grain
in the center of Figure 25 shows two
sets of cleavage steps. One set is
oriented in a NW-SE direction, the
other in a NE-SW one. The theory that
propagation is parallel to the direction
of cleavage steps leaves some doubt in
determining the direction of fracture
propagation in this case. The NE-SW
set appears far less regular than the
other set, and the NW-SE set has some
"river" patterns in the lower left of
the figure. For these reasons, a NW-
SE fracture interpretation seems most
reasonable, but the evidence is not
conclusive.

CONCLUDING REMARKS

The surfaces of carbonate rock
specimens broken in tension along a
plane between two wedges of a pair of
nippers are thought to simulate surfaces
of aggregate produced by commercial

crushers. Examination of these surfaces at high magnifications with a scanning electron microscope shows they are highly variable, and details of grain surfaces show complex arrangements of fracture markings characteristic of brittle materials.

Cleavage steps appear to originate in carbonate crystals in a manner similar to that in brittle silicon-iron and aluminum.[21,24] The path of the fracture mainly follows one set of cleavage planes, but the fracture frequently takes short jumps to another plane. When this path change occurs in calcite and dolomite, it commonly does so on one or the other of two {1011} crystallographic cleavage planes. Two and sometimes three cleavage steps on calcite crystals coalesced to form one large step; this was also observed by Frechette.[25] In limestones and dolomites examined to date, however, the step markings rarely coalesced on either the calcite or the dolomite grains.

The distinction between transgranular and intergranular modes of grain failures is in most cases easily made on scanning electron micrographs, although the presence of crystal-lined pores in some rocks makes it difficult to determine which mode of fracturing occurred.

Details of the shapes of intragranular voids or fluid inclusions are readily observed with the scanning electron microscope. Intragranular voids were observed mainly in the larger calcite particles of crinoid fossils in the Kimmswick and Burlington Limestones and in the Racine and Joliet Dolomites. Voids exposed on the fracture surfaces are sites for bonding with cement paste. On the other hand, they reduce the strength of the grains and, when abundant, tend to increase the abrasion loss of aggregates.

Carbonate rocks--especially limestones--that have failed by shearing yield a fine powdery material that has a flat or flaky morphology. Ultra-small cones or "V"-shaped markings were observed on shear failure surfaces in dolomites.

On the basis of this work, extension or tensile fracture surfaces in fine-grained, non-porous, lithographic-type constituents in limestones appear to contain more abundant little nooks and crevices in which hydrated cement paste could harden than do coarse-grained sparry limestone constituents. This would account for the relatively high tensile bond strength Hsu and Slate[1] observed in fine-grained limestone.

The micrographs shown in this report represent most of the common types of carbonate aggregates and form a basis for further analyses of surface texture of these rock types as it affects their behavior in concretes.

REFERENCES

1. Hsu, T. T. C., and Slate, F. O., "Tensile Bond Strength between Aggregate and Cement Paste or Mortar," American Concrete Institute Proceedings, Vol. 60, 1963, pp. 465-486.

2. Gaynor, R. D., "Aggregate Properties and Concrete Strength," a paper presented at the 49th Annual Convention of the National Sand and Gravel Association, Jan. 28, 1965, Miami Beach, Fla.

3. Wills, M. H., Jr., "How Aggregate Particle Shape Influences Concrete Water Requirements and Strength," Journal of Materials, Vol. 2, No. 4, pp. 843-865.

4. Mather, Bryant, "Concrete Aggregates--Shape, Surface Texture, and Coatings," in Concrete and Concrete-making Materials, ASTM STP 169-A, American Society for Testing and Materials, Philadelphia, Pa., 1966, pp. 415-431.

5. Herschmann, H. K., "Replica Surface Analyzer," National Bureau of Standards Technical News Bulletin, Vol. 31, No. 3, 1947, pp. 29-32.

6. Horino, F. G., Hoskins, J. R., and Ellickson, M. L., "A Method of Measuring Surface Texture of Rock," United States Bureau of Mines Report of Investigations 7095, 1968.

7. Merchant, H. D., "Influence of Metal Roughness on Surface Texture of Glass," American Ceramic Society Bulletin, Vol. 42, No. 2, 1963, p. 57.

8. Huang, E. Y., "An Improved Particle Index Test for the Evaluation of Geometric Characteristics of Aggregates," Michigan Highway Research Project No. 86546, Department of Civil Engineering, Michigan Technological University, Houghton, Michigan, 1965.

9. Tucker, R. C., Jr., and Meyerhoff, R. W., "An SEM Study of Surface Roughness Measurement," in Scanning Electron Microscopy-1969: 2nd Annual Scanning Electron Microscope Symposium Proceedings, Illinois Institute of Technology Research Institute, Chicago, Ill., 1969, pp. 391-396.

10. Thornton, P. R., Scanning Electron Microscopy, Chapman and Hall Ltd., London, 1968.

11. Smith, K. C. A., and Oatley, C. W., "The Scanning Electron Microscope and Its Field of Application," British Journal of Applied Physics, Vol. 6, 1955, p. 391-399.

12. Nixon, W. C., "Twenty Years of Scanning Electron Microscopy, 1948-1968, in the Engineering Department Cambridge University, England," in Scanning Electron Microscopy--1968: 1st Annual Scanning Electron Microscope Symposium Proceeding, Illinois Institute of Technology Research Institute, Chicago, Ill., 1968, pp. 55-62.

13. Mitchell, N. B., Jr., "The Indirect Tension Test for Concrete," Materials Research and Standards, Vol. 1, No. 10, 1961, pp. 780-788.

14. "Splitting Tensile Strength of Molded Concrete Cylinders," ASTM Designation C 496-66, in the Book of ASTM Standards, American Society for Testing and Materials, Philadelphia, Pa., 1968, pt. 10, p. 351-354.

15. Hobbs, D. W., "An Assessment of a Technique for Determining the Tensile Strength of Rock," British Journal of Applied Physics, Vol. 16, No. 2, 1965, pp. 259-269.

16. Jaeger, J. C., and Hoskins, E. R., "Rock Failure under the Confined Brazilian Test," Journal of Geo-Physical Research, Vol. 71, No. 10, 1966, pp. 2651-2659.

17. Hiramatsu, Y., and Oka, Y. "Determination of Tensile Strength of Rock by Compressive Test of an Irregular Test Piece," International Journal of Rock Mechanics and Mining Science, Vol. 3, No. 2, 1966, pp. 89-99.

18. Fairhurst, Charles, "On the Validity of the 'Brazilian' test for Brittle Materials," International Journal of Rock Mechanics and Mining Science, Vol. 1, 1964, pp. 535-546.

19. Crussard, C., Borione, R., Plateau, J., Yorillion, Y., and Maratroy, F., "A Study of Impact Tests and the Mechanism of Brittle Fracture," Iron and Steel Institute Journal, Vol. 183, 1956, pt. 2, pp. 146-177.

20. Low, J. R., Jr., "A Review of the Microstructural Aspects of Cleavage Fracture," in Fracture, ed., B. L. Averbach et al, John Wiley & Sons, New York, 1959, pp. 68-90.

21. Berry, J. M., "Cleavage Step Formation in Brittle Fracture Propagation," Transactions of the American Society for Metals, Vol. 51, 1959, pp. 556-581.

22. Willard, R. J., "Scanning Electron Microscope Gives Researchers a Closer Look at Rock Fractures," Mining Engineering, Vol. 21, No. 6, 1969, pp. 88-90.

23. Lamar, J. E., and Shrode, R. S, "Water Soluble Salts in Limestones and Dolomites," Economic Geology, Vol. 48, No. 2, 1953, pp. 97-112.

56

24. Beachem, C. D., and Pelloux, R. M. N., "Electron Fractography--A Tool for the Study of Micromechanism of Fracturing Processes," in Symposium on Fracture Toughness Testing and its Applications, ASTM Special Technical Publication 381, Phila-delphia, Pa., 1965, pp. 210-245.

25. Frechette, V. D., "Characteristic of Fracture-exposed Surfaces," British Ceramic Society Proceedin No. 5, 1965, pp. 97-106.

Pg 57 Is Blank

(57)

BLANK

TABLE

SAMPLE DESCRIPTIONS AND SOURCES, AND FIGURE NUMBERS OF ELECTRON MICROGRAPHS

Fig. no.	Geologic unit	Source	Nearest town (Illinois)	Use	Remarks on physical properties	Lithology
1	Iceland-spar calcite					
	LIMESTONES					
2 & 5	Ullin	quarry	Mill Creek	$A^{(1)}$	High abrasion loss	Coarse brownish-gray grains of crinoidal fragments irregularly interstratified with fine-grained light gray, bryozoan fragments; cc 95, do 4,(2) organics + cl + qt 0.6.
3	Burlington	mine	Quincy	A	High abrasion loss	Coarse crinoid fragments and fine bryozoan fragments; cc 96, do 3.
4	Salem	outcrop	Mt. Sterling	A	37% abrasion loss (3) 9% soundness loss (3)	Light gray, medium-grained, fossiliferous fragmental cc mainly; qt + cl 15.
6	Kimmswick	outcrop	Thebes	A	52% abrasion loss	Coarse partly recrystallized crinoid fragments with some fine bryozoan fragments and microspar; cc 96, do 3.
7	St. Louis	quarry	Mt. Sterling	CA^{4}		Brownish-gray, very fine-grained and equant granular; cc 95 qt 5.
8 & 16	Wapsipinicon (Davenport Member)	quarry	Milan	CA		Brownish-gray, very fine-grained and equant granular (lithographic); cc 97+, qt + cl 1.
9 & 17	Cedar Valley (Solon Member)	quarry	Milan	A	High soundness loss	Gray, very fine-grained, granular, micro-laminated; cc major, do minor, qt + cl + organics 6.

No.	Formation	Type	Quarry	CA/A	Test results	Description
10	Ste. Genevieve (Fredonia Member)	quarry	Anna	CA		Gray, oolitic, medium- to coarse-grained particles surrounded by very fine-grained particles; sparry cc cement; cc 98-99.
11 & 12	Kinkaid	quarry	Buncombe	CA		Dark gray, fine-grained, micro-laminated; cc 78, do 9, cl + qt 13.
13 & 14	Seville	quarry	Viola	A	High soundness loss	Dark gray, fine and equant granular.
15	Lonsdale	quarry	Princeville	A	High soundness loss	Gray, fine and equant granular.
	DOLOMITES					
18 & 19	Racine (Sample #65-36)	quarry	Osborne	CA		Gray, medium-grained mosaic, macro-porous; do 99.
20 & 21	Racine (Sample #65-41A)	quarry	Kankakee	CA		Gray, fine-grained mosaic, macro-porous; do 97, cc 2, qt + cl 1.
22	Joliet (Sample #62-16A)	quarry	Jollet	CA		Gray, fine-grained and equant mosaic, thinly laminated, non-porous; do 90, qt + cl 10.
23 & 24	Joliet (Sample #67-303)	quarry	Sterling	A	High soundness loss	Brown, medium rhombs surrounded by fine grains, porous; do 90+.
25 & 26	Salem	quarry	Brooklyn	A	43% abrasion loss (3) 5% soundness loss (3)	Brown, fine-grained and equant mosaic, micro-porous; do 93, cc 5, qt + cl 2.

1. CA = crushed stone of this lithology is generally used for concrete aggregates. A = crushed stone of this lithology is not generally used for concrete aggregates. Illinois Division of Highways maximum limits for quality A aggregates: Na_2SO_4 soundness, 15%; Los Angeles abrasion, 40%.

2. Mineral abbreviations: cc, calcite; do, dolomite; qt, quartz; ct, chert; cl, clay. The numbers following the mineral abbreviation are the percentages of minerals in the sample.

3. Illinois Division of Highways, Bureau of Materials, test results on ledge rock collected by the author.

4. The product from this quarry is not used as a concrete aggregate by Illinois Division of Highways, although the lithology of the specimen is identical to St. Louis Limestone strata near Alton, Illinois, that do pass specifications for CA.
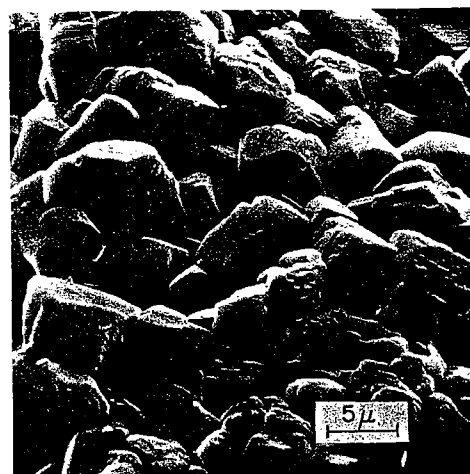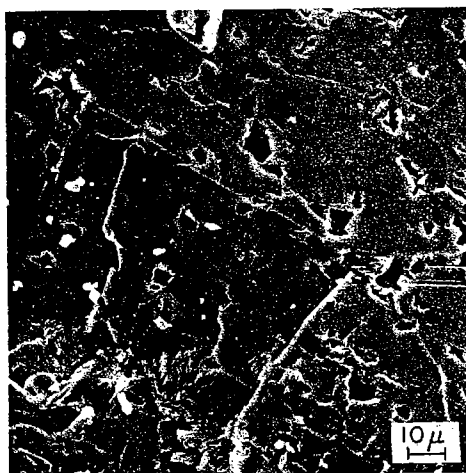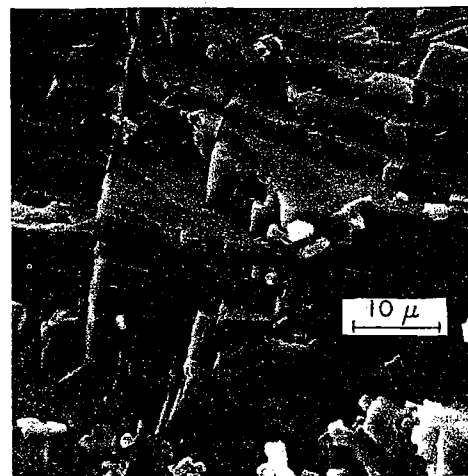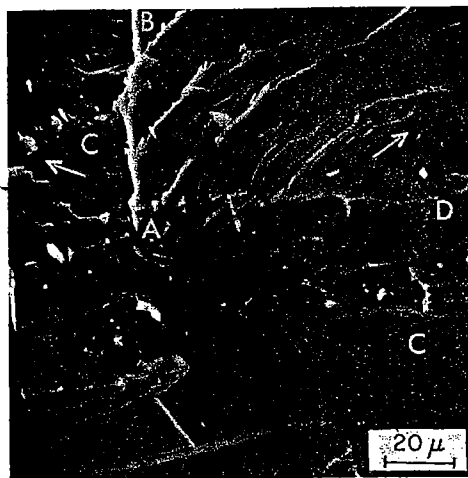
UPPER LEFT

FIGURE 1.   TRANSGRANULAR FRACTURE ON RHOMBOHEDRAL CLEAVAGE PLANE IN CALCITE CRYSTAL ICELAND-SPAR TYPE WITH CLEAVAGE STEPS (C).   THE ARROWS ARE THE INFERRED DIRECTION OF CRACK PROPAGATION BASED ON THE PATTERN OF CLEAVAGE STEPS.

UPPER RIGHT

FIGURE 2.   TRANSGRANULAR FRACTURE OF A CRINOID FRAGMENT IN THE ULLIN LIMESTONE SHOWING CLEAVAGE STEPS OF A VARIETY OF SIZES.   SMALL GRAINS OF CALCITE DUST DERIVED FROM THE ROCK DURING FAILURE ARE SEEN AS HIGHLIGHTED PARTICLES. -

CENTER LEFT

FIGURE 3.   TRANSGRANULAR FRACTURE OF A CRINOID STEM IN THE BURLINGTON LIMESTONE, SHOWING A LARGE CLEAVAGE STEP AND NUMEROUS INTRAGRANULAR VOIDS.

CENTER RIGHT

FIGURE 4.   TRANSGRANULAR FRACTURE OF SPARRY CALCITE IN THE SALEM LIMESTONE.

LOWER LEFT

FIGURE 5.   MAINLY INTERGRANULAR FRACTURE IN THE FINE-GRAINED COMPONENT IN THE ULLIN LIMESTONE.   NOTE THE NUMEROUS RHOMBIC-SHAPED GRAINS AND THE RARITY OF CLEAVAGE STEPS (ARROW).

LOWER RIGHT

FIGURE 6.   INTERGRANULAR FRACTURE SURFACE IN THE FINE-GRAINED CALCITE IN THE KIMMSWICK LIMESTONE.
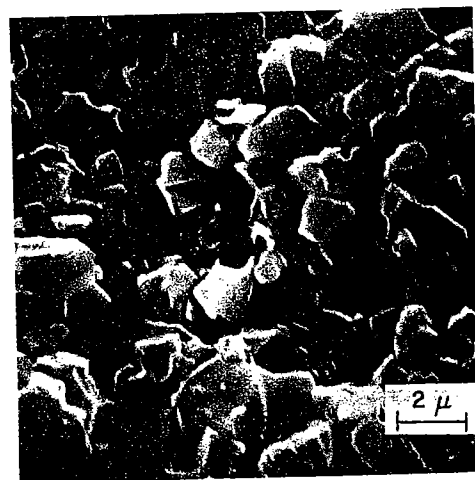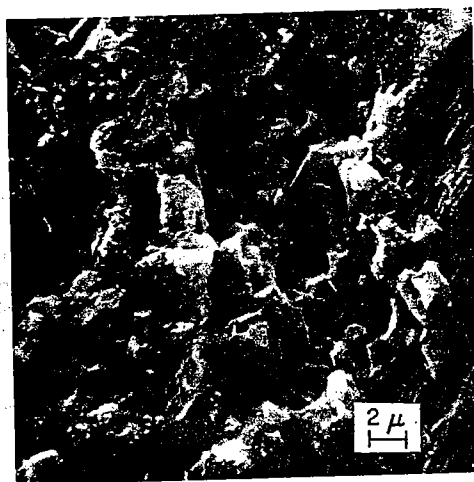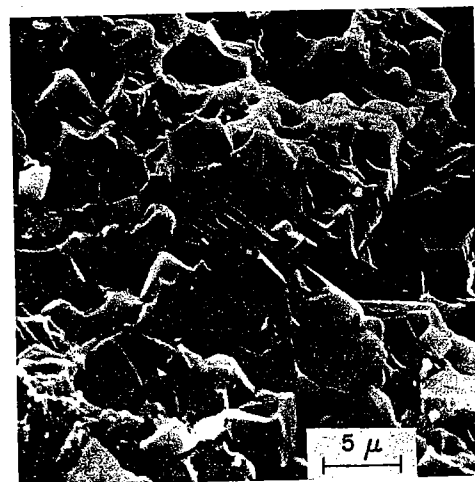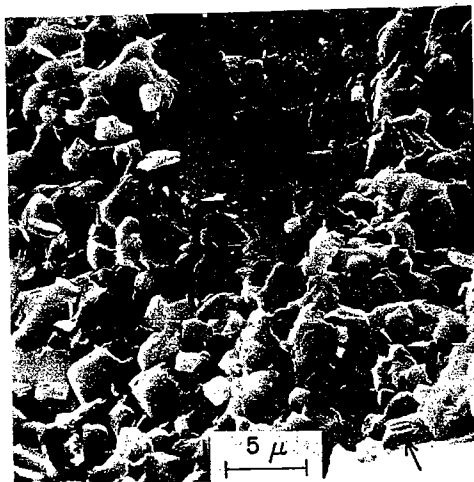
UPPER LEFT

FIGURE 7. TYPICAL EXAMPLE OF TENSILE FRACTURE SURFACES OF MICRITIC
COMPONENTS OF VERY FINE-GRAINED CALCITE IN THE ST. LOUIS LIMESTONE. THE FRACTURE
IS A MIXTURE OF INTERGRANULAR AND TRANSGRANULAR MODES. ARROWS POINT TO EXAMPLES
OF GRAINS THAT WERE DEFINITELY BROKEN.

UPPER RIGHT

FIGURE 8. MAINLY TRANSGRANULAR FRACTURE MODE IN VERY FINE- AND
EVEN-GRAINED CALCITE IN THE WAPSIPINICON LIMESTONE.

CENTER LEFT

FIGURE 9. MIXED FRACTURE MODE IN UNEVEN GRANULAR LIMESTONE IN THE CEDAR
VALLEY LIMESTONE. NUMEROUS DUST PARTICLES ARE ADHERING TO THE SURFACE.

CENTER RIGHT

FIGURE 10. MAINLY INTERGRANULAR FRACTURE IN AN OUTER BAND OF AN OOLITE IN
THE STE. GENEVIEVE LIMESTONE.

LOWER LEFT

FIGURE 11. MAINLY TRANSGRANULAR FRACTURE IN FINE-GRAINED KINKAID LIMESTONE.
SEE CLOSE-UP VIEW OF CENTER OF THIS SAMPLE IN FIGURE 12.

LOWER RIGHT

FIGURE 12. CLAY MATERIAL ALONG GRAIN BOUNDARIES OF CALCITE PARTICLES IN
THE KINKAID LIMESTONE.

64
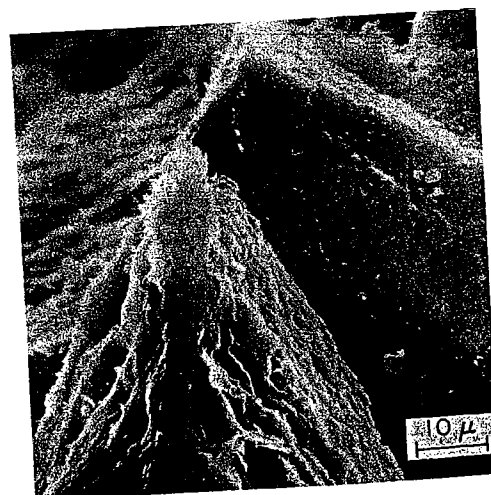
UPPER LEFT

FIGURE 13. INTERGRANULAR TENSILE FRACTURE OF THE BEDDING SURFACE IN A TYPICAL SPECIMEN OF THE SEVILLE LIMESTONE. MUCH OF THE HIGHLIGHTED MATERIAL SHOWN IS CLAY.
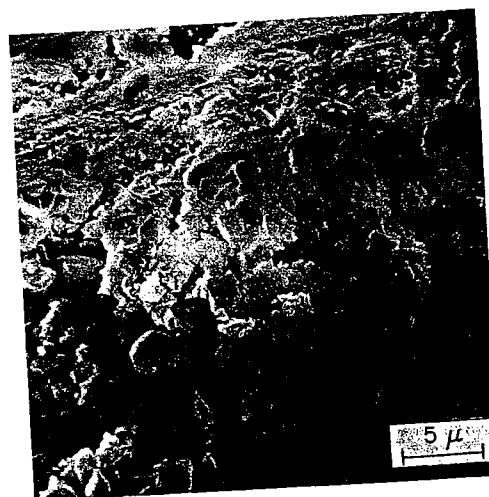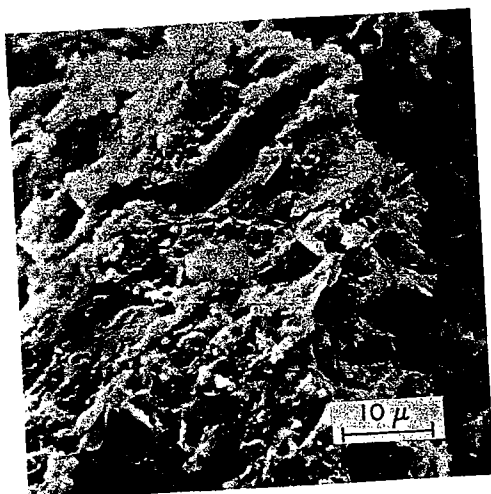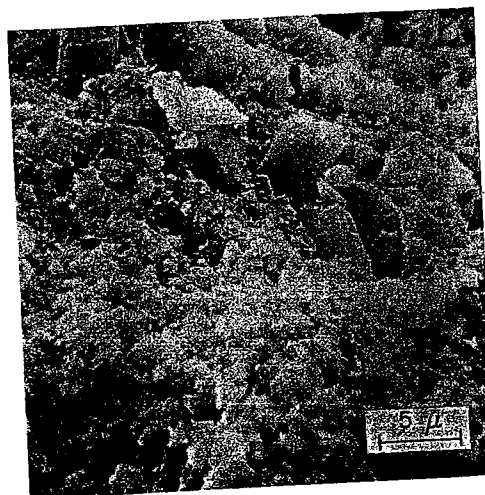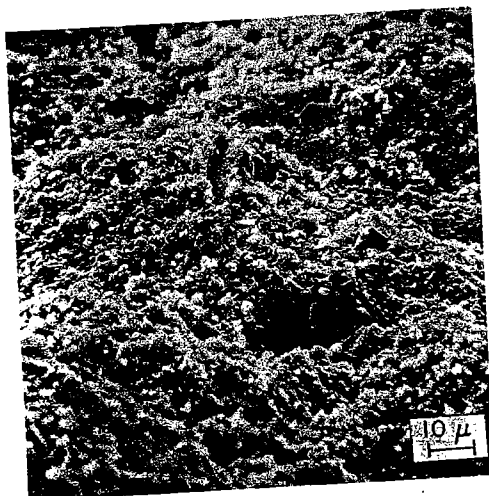
UPPER RIGHT

FIGURE 14. CLOSE-UP VIEW OF THE SPECIMEN IN FIGURE 13, SHOWING MUCH CLAY MATERIAL AND THREE RHOMBS OF DOLOMITE TYPICAL OF THOSE SCATTERED THROUGHOUT THE SAMPLE.

CENTER LEFT

FIGURE 15. TENSILE FRACTURE ALONG A BEDDING SURFACE OF THE LONDSDALE LIMESTONE. MUCH OF THE HIGHLIGHTED MATERIAL IS PROBABLY CLAY, AND THE ELONGATED STRUCTURE IN THE CENTER IS THOUGHT TO CONSIST OF ORGANIC MATTER. A SIMILAR STRUCTURE IS ALSO SHOWN IN FIGURE 13.

CENTER RIGHT

FIGURE 16. TRANSGRANULAR SHEAR FRACTURE OF VERY FINE-GRAINED CALCITE IN THE WAPSIPINICON LIMESTONE.

LOWER LEFT

FIGURE 17. TRANSGRANULAR SHEAR FRACTURE IN VERY FINE-GRAINED CALCITE OF THE CEDAR VALLEY LIMESTONE, SHOWING FLATTENED AND SHEARED GRAINS.

LOWER RIGHT

FIGURE 18. SHEAR CONE PRODUCED DURING FRACTURE OF A SPECIMEN OF THE RACINE DOLOMITE. THE SHEARING LOAD WAS APPLIED TO THE SPECIMEN FROM THE TOP, TOWARD THE BOTTOM OF THE FIGURE.

66
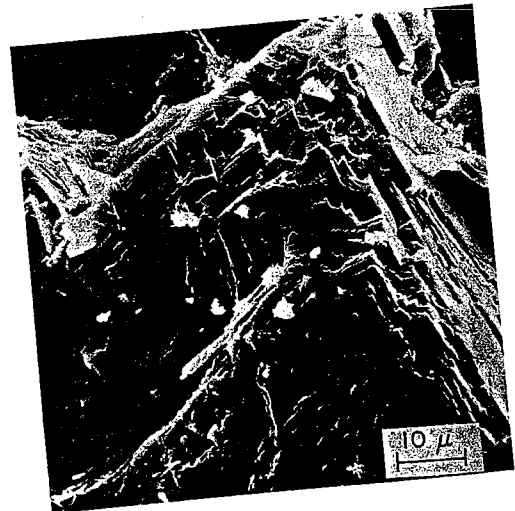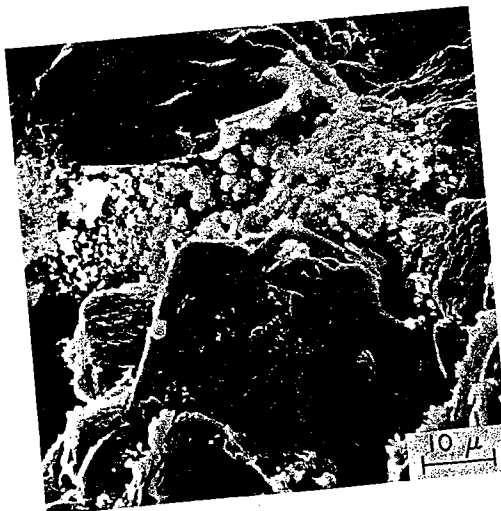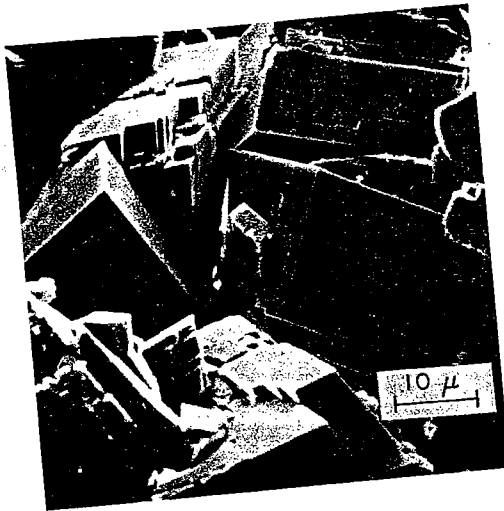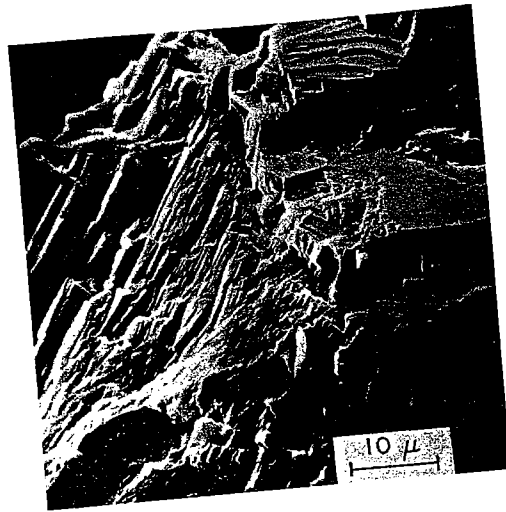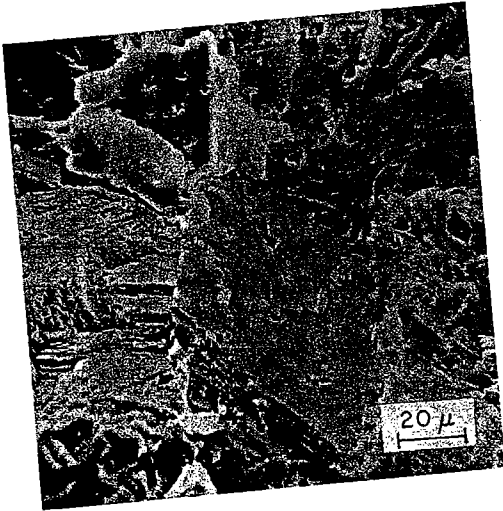
UPPER LEFT

FIGURE 19. TRANSGRANULAR FRACTURE SURFACE SHOWING CLEAVAGE STEPS AND INTERGRANULAR VOIDS IN THE RACINE DOLOMITE (SAMPLE #65-36).

UPPER RIGHT

FIGURE 20. CLEAVAGE FRACTURE OF TWO DOLOMITE GRAINS IN THE RACINE DOLOMITE (SAMPLE #65-41A).

CENTER LEFT

FIGURE 21. RHOMBIC CRYSTALS OF DOLOMITE ON A SURFACE OF A PORE IN THE SAME SPECIMEN SHOWN IN FIGURE 20.

CENTER RIGHT

FIGURE 22. TENSILE FRACTURE OF THE JOLIET DOLOMITE, SHOWING DUST PARTICLES PRODUCED DURING FRACTURE THAT ADHERE TO THE SPECIMEN SURFACE.

LOWER LEFT

FIGURE 23. INTERGRANULAR FRACTURE SHOWING TYPICAL TEXTURE OF A "HARD" KERNEL OF JOLIET DOLOMITE (SAMPLE #67-303). NOTE SPHERICAL STRUCTURES 1 TO 2 μ IN DIAMETER SITUATED BETWEEN LARGE GRAINS OF DOLOMITE.

LOWER RIGHT

FIGURE 24. TRANSGRANULAR FRACTURE OF DOLOMITE GRAIN IN SAMPLE #67-303 OF THE JOLIET DOLOMITE, SHOWING NUMEROUS INTRAGRANULAR VOIDS.

68
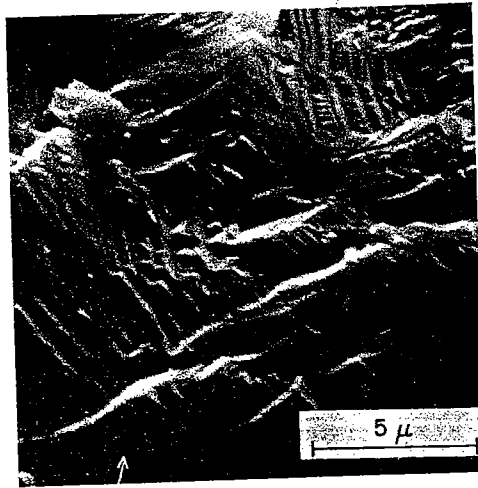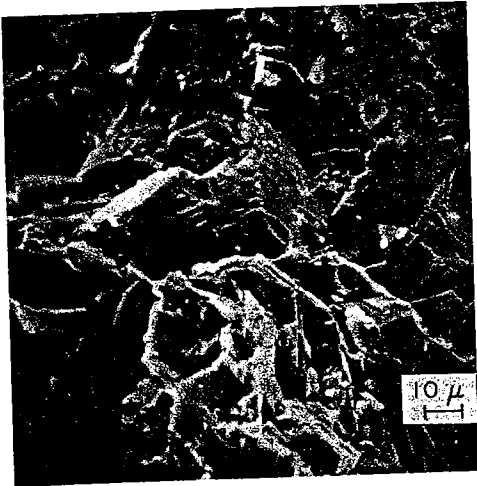
LEFT

FIGURE 25. MAINLY TRANSGRANULAR FRACTURE OF A SPECIMEN OF DOLOMITE FROM THE SALEM FORMATION.

RIGHT

FIGURE 26. CLOSE-UP VIEW OF THE CENTER OF FIGURE 25, SHOWING CLEAVAGE STEPS WITH MINUTE "RIVER" PATTERNS (ARROW).

V. FOUNDATION EXPLORATION FOR INTERSTATE 280 BRIDGE OVER MISSISSIPPI RIVER NEAR ROCK ISLAND, ILLINOIS

James C. Gamble,* A. J. Hendron, Jr.,** and Grover C. Way***

INTRODUCTION

DeLeuw, Cather & Company of Chicago are in the final stage of designing for the state of Illinois a bridge to cross the Mississippi River near Rock Island, Illinois, and Davenport, Iowa, as part of Interstate 280. Three test boring programs have been conducted to obtain subsurface information for the bridge piers and foundations. In situ pressuremeter tests were included in the third boring program, and shale samples were obtained for laboratory testing at the University of Illinois. The laboratory tests included one-dimensional consolidation tests, drained and undrained triaxial tests, and direct shear tests, for the determination of the compressibility and strength properties of the shales at the site.****

LOCATION AND DESCRIPTION OF STRUCTURE

The proposed bridge is located on a bypass route south and west of Moline, Rock Island, and Davenport, crossing the Mississippi River about one mile downstream of the juncture of the Rock River (Figure 1). At the crossing, the Mississippi is about 2400 ft wide and 10 to 15 ft deep at normal pool. High flood level in 1965 reached 18 1/2 ft above normal pool.

The bridge will be about 2400 ft long from abutment to abutment (Figure 2). Crossing the main channel is a 570-ft tied-arch span with 63 ft minimum vertical clearance. The approach spans are of continuous welded-plate girder design, supported by 27 piers--200, 150, or 100 ft apart. All the piers in the river are to be founded on shale, while the land approach piers will be founded on H-piles driven to bedrock. Design dimensions for pier footings on shale are: 128 ft x 28 ft for the two navigation channel piers, 96 ft x 22 ft for

*Research Assistant, Department of Civil Engineering, University of Illinois, Urbana.

**Associate Professor, Department of Civil Engineering, University of Illinois, Urbana.

***Chief Soils and Materials Engineer, DeLeuw, Cather & Company, Engineers, Chicago, Illinois.

****Professor Don U. Deere was principal consultant to DeLeuw, Cather & Company, Engineers, on this project. He and Drs. R. F. Coon and A. H. Merritt did much of the preliminary geology and planning of the exploratory program. Dr. G. Mesri performed much of the testing and aided in analysis of the results.

approach piers in the river, and 80 ft x 20 ft for the land approach piers.

GEOLOGY

The geology at the site consists of river alluvium and possibly some lacustrine sediments resting on bedrock (Figure 3). The alluvial deposits, ranging in thickness from 5 to 25 ft in the river to about 40 ft on the Illinois river bank, consist of interbedded silts, sands, gravels, and clay, with some boulders reported. A zone of limonite-cemented sand and gravel (conglomerate) was encountered at the base of the alluvium above bedrock in borings at the navigation channel pier on the Illinois side.

In this region, the river runs through the lower part of the Mississippi river narrows. Prior to the Wisconsin Glaciation, the Mississippi river flowed east of the Rock Island area and emptied into the Illinois river near Hennepin. It was not diverted into its present course until about 20,000 years ago, which accounts for the relatively shallow bedrock channel in the Rock Island area. Borings indicate 40 to 60 ft or more of Pennsylvanian rocks overlying an irregular surface of Middle Devonian limestone. The Rock Island area is at the northwest boundary of the Illinois Basin and the Pennsylvanian rocks probably belong to the Caseyville Formation. The Devonian limestones and dolomites form Rock Island and also outcrop downstream from the site.

The bridge piers or piles are to be founded on the Pennsylvanian rocks, which consist primarily of light to medium gray silty shale and dark gray to black fissle shale, with lesser amounts of coal, underclay, sandy shale, siltstone, sandstone and conglomerate. A facies change from the gray to the black shale occurs in about the middle of the river. The upper beds have a general dip in the upstream direction of about one foot in ten.

The gray shales tend to be somewhat massive except for abundant plant material along many bedding planes. Grain size analyses showed compositions of 3-6 percent sand, 58-73 percent silt, and 23-32 percent clay (less than 2 microns). The underclays have similar grain size distributions (Figure 4).

The dark gray to black shales are fissle and generally blocky; they contain 13-20 percent sand, 37-47 percent silt, and 40-47 percent clay. One exception is an upper soft layer referred to in the field as a "clay" shale, which is half silt and half clay with only a trace of sand (Figure 4).

Both black and gray shales and the underclays have a tendency to crack upon drying from exposure to air and to soften, disaggregate, or slake in water.

Clay mineral analyses performed on ten samples of shales and underclays indicated the clays are mainly illite and chlorite with lesser amounts of kaolinite and mixed-layer clay minerals (see Table on p. 71). The analyses suggest that the gray shales may be slightly higher in illite content, while the underclays may be slightly higher in mixed-layer clay minerals.

EXPLORATION

There have been three stages in exploration for the proposed bridge. Phase 1 consisted of 19 borings mad

TABLE OF CLAY MINERAL ANALYSES.

(performed courtesy of Illinois State Geological Survey by W. A. White)

Boring	Depth	Rock Species	Illite	Mixed-Layer Clay Minerals	Chlorite	Kaolinite
				Clay Minerals in Parts in 10 of Diffraction Effects		
32A	27.8'-28.5'	Underclay	4-5	2	2	1
33	28.3'-28.8'	Gray clayey shale	5	2		3
34A	28.1'-29.0'	Gray shale	6	1-2	-	2-3
35	56.1'-56.4'	Gray shale	6	1	2-3	1
35A	40.3'-41.3'	Black shale	4	1	3	2
	47.5'-48.0'	Underclay	4-5	2-3	2	
36A	50.4'-51.4'	Black shale	4	3	2	
37A	36.1'-37.2'	Black clay shale	4	2	2	1
	39.7'-40.2'	Underclay	5	2-3		2-3
	52.7'-53.7'	Black shale	4-5	1	3-4	

In November and December, 1963. These were essentially soil borings with 2-in. spoon samples taken in the alluvium and the upper soft weathered shale. In four borings the shale was cored 2, 4, 5, and 13 ft, respectively; however, core recovery was low.

Phase 2 consisted of a program of 32 NX borings in the fall of 1965; these borings penetrated 10 to 20 ft into rock at locations shown in Figure 2. Core recovery was poor in many borings and drilling procedures were varied considerably in an attempt to obtain better core recovery and less sample disturbance. Changes were made in barrel and bit diameters and rate of flow and pressure of the wash water. Core recovery, drilling time, lithology, and compressive strengths and water contents of some split spoon samples

were included in the drilling reports.

The core was examined some time after drilling and logged in detail, noting lithology, color, hardness, and amount of disturbance. Split-spoon samples of upper weathered shale preserved in sealed bottles were tested for natural water content and Atterberg limits. Little other information could be obtained because of drying of the core.

On the basis of these borings, recommendations were made for estimated footing elevations for the bridge piers. However, at six pier locations with soft zones and/or high core loss, additional borings were recommended to determine footing elevations and to obtain information on strength and modulus of the shales.

Phase 3 consisted of the recommended

NX and 6-in. borings at six pier locations in September and October, 1968 (see Figure 2). Pressuremeter tests were also performed in the NX borings. The core was wrapped and sealed to preserve the natural moisture content of samples for laboratory testing. Rubber-mounted drill rigs were floated on a barge: two center units held the drill rig, while two additional units in back, one on either side, supported a plank working platform. The barge was anchored by two spuds, so large waves from passing boats or high winds caused some rocking. Three or four spuds to fix the platform completely would likely result in less core disturbance.

NX Borings

Six borings were located at the centerlines of piers and drilled 47 to 53 ft into rock. The borings went through river alluvium and upper weathered shale into shale where coring could begin. In all but one instance, NX casing, driven and cleaned out by a tricone roller bit, was used. On one boring, a hollow-stem auger was used for casing; however, it could not be seated tightly enough to prevent the drilling operation from working it loose. A Christensen D-3 double-tube NX core barrel with an offset bottom-discharge diamond bit was used for coring with an inner barrel extension and N-size drive rods. The bit had 6 waterways, 10 stones per carat, and cut the core 10/1000 in. undersize. A tapered face discharge bit was used on one boring.

---

*Superscript numbers in parentheses refer to the References at the end of this paper.

Water volume was kept to a minimum to prevent excessive erosion of the borehole for the pressuremeter testing. Generally the first core run was 2 ft and others 5 ft when possible. Drilling speed and water pressures were left to the experience of the driller, who had been on the previous drilling program.

Pressuremeter Tests

We ran pressuremeter tests after each 5-ft core run by lowering the pressure probe to the bottom section of the hole on A-size rod. An 18-in. long section of the borehole is stressed by the probe, which has two flexible membranes surrounding a steel tube. The exterior guard cell is inflated with nitrogen gas to reduce end effects on both ends of the interior measuring cell. The interior cell contains water pressurized by gas and is connected to a volume-meter. As pressure is applied in increments to the measuring cell, the changes in volume of the cell as it expands against the circumference of the hole are recorded. Additional details of the pressuremeter equipment and testing procedures are described by Dixon and Jones,[1]* and Menard.[2]

6-Inch Borings

The 6-in. borings were located within 10 to 15 ft of the NX borings to facilitate comparison of the core with the NX core. Depths into rock varied from 22 to 36 1/2 ft, depending on conditions encountered in the NX borings. A 10-in. pipe casing was welded to the desired length and driven, and the hole was cleaned by a tricone roller bit into the shale.

A Christensen Type 61423 5-ft double-tube barrel and face discharge diamond bit with 16 waterways, 4 stones

per carat, 8-in. O.D. and 5 7/8 in.
I.D. was used for coring. Difficulty
was encountered in retaining core in the
barrel with a grit-stripped core catcher
where the core was soft or eroded under-
size. A spring-type catcher was used
fairly successfully in retrieving the
softer core, but would not work in the
harder shale, siltstones, and sand-
stones, making it necessary to change
to the grit-stripped core catcher.

Condition of the core recovered
varied considerably. Weathered shale
was recovered often in pieces 1 to
2 in. long, while shale and siltstone
in good condition were recovered in
lengths occasionally over 3 ft.

Core Logging and Wrapping

The cores were logged and wrapped
as quickly as possible after removal
from the hole to prevent changes in
natural moisture content. The NX core
was wrapped in aluminum foil and dipped
in a wax mixture of paraffin (4 parts),
petroleum jelly (1 part), and a small
amount of beeswax. The 6-in. core was
wrapped in polyethylene film and then
covered with muslin dipped in hot wax.

Core logging included core recovery,
modified core recovery (RQD), rock
hardness, color, lithology, and frac-
ture spacing. For the modified core
recovery (RQD), only pieces 4 in. or
longer were counted in the percentage
recovery per run.

Rock Hardness

Rock hardness was classified on
a relative scale for sedimentary rocks
of the type found at the site:

(a) very soft--weathered, soil-
like, e.g., stiff clay;

(b) soft--some weathering, con-
siderable erosion of core, easily gouged

by knife or screw driver;

(c) medium soft--slight erosion
of core, slightly gouged by knife or
screw driver;

(d) medium hard--no core erosion,
not easily scratched or gouged;

(e) hard--difficult to scratch.

LABORATORY TESTING

The main objective of the testing
program was to correlate, if possible,
the deformation moduli of the shales
tested with basic index properties such
as the water content and Atterberg limits.
These correlations could then be used
to estimate the deformation moduli at
locations on the site where index
properties were available but where
triaxial or consolidation test results
were absent. Estimated settlements
were then calculated using the moduli
determined in this manner. The follow-
ing tests were performed in the
University of Illinois Rock Mechanics
and Soil Mechanics Labs.

(a) Water content was determined
throughout the boring profile and
particularly at all pressuremeter test
locations.

(b) Liquid and plastic limits
were found at selected or representative
locations.

(c) Grain size was analyzed by
mechanical sieving and hydrometer
methods.

(d) Specific gravity determinations
were taken in gray shale and in black.

(e) One-dimensional consolidation
tests, 2.5-in. diameter (6-in. core),
including one remolded sample from a
very soft zone, were made to determine
coefficient of consolidation and drained
modulus.

(f) Anisotropically consolidated, load-controlled triaxial tests were conducted on 1 7/8-in. diameter samples to determine the drained strength and both drained and undrained moduli of the shales.

(g) Unconsolidated-undrained triaxial tests (Q-tests) were conducted on 5 1/2-in. diameter x 8-in. height (6 in. core) samples to determine undrained strengths and undrained moduli.

(h) Two series of direct shear tests were made on 6-in. core under normal pressures ranging from 10 to 100 psi; one series involved medium- to medium-hard gray shale, the other, medium-soft to medium-hard black shale.

Water Contents, Atterberg Limits, and Grain Size Analyses

Field logging and testing indicated the shales at the site could be divided into three main groups:

(a) gray shales and underclays with liquid limits 30 to 43 percent and plasticity indices from 9 to 18 percent (Figure 5); composed of about 2/3 silt and 1/3 clay with a small percent of sand (Figure 4); and with water contents ranging from approximately 6.5 to 10 percent in sound condition to 18 percent when weathered;

(b) dark gray to black shales with liquid limits 38 to 52 percent, and plasticity indices from 13 to 25 percent; composed of about 15 to 20 percent sand with remainder about half silt and half clay; and with water contents from about 10 to 13 percent in sound condition up to 16 percent when weathered.

(c) dark gray to black clay shale with liquid limits 39 to 53 percent and plasticity indices 18 to 30 percent (higher than other black shales); composed of half silt and half clay with only a trace of sand; with water contents 9 to 18 percent.

Although the Atterberg limits and natural water contents of the shales justify categorization into the three groups described above, the plasticity chart shown in Figure 5 indicates that all three of these groups plot in a band parallel to the "A"-line, as do soils of the same geologic origin or mineralogy. Thus the main difference between the soils in the categories described above is probably the percent of clay-sized material. The samples with the lowest clay content plot in the lower left portion of the band shown in Figure 5, and the samples with the highest clay content plot in the upper right portion of the same band.

Comparison of water content values in the NX and 6-in. borings at the same pier indicated in some cases that the NX cores might have taken on water as a result of drilling distrubance.

Drained Moduli

The ultimate settlement of the bridge piers depends upon the stress-strain characteristics of the shales under "drained" conditions. In order to investigate the "drained" stress-strain characteristics of these shales, four consolidation or one-dimensional tests and four "drained" triaxial tests were conducted on shale samples.

The one-dimensional consolidation tests were conducted in a conventional manner on undisturbed samples of shale trimmed in 2 1/2-in. diameter Wykeham

Farrance consolidation rings 3/4 in. high. Two typical void ratio-log pressure (e-log p) curves for the tests are shown in Figure 6. The e-log p curves for the tests showed compression indices (C_c) ranging from 0.06 to 0.07, indicating that the material was very heavily preloaded to pressures much beyond the loads applied in the testing program. The close proximity of the rebound and loading portion of the e-log p curves shows nearly elastic behavior, which indicates that the shales have been preloaded to much higher loads than they were subjected to in the tests.

The logarithm scale of the e-log p curves, however, makes it difficult to visualize the true nature of the stress-strain curves. Figure 7 shows stress-strain curves for the same two test results shown in Figure 6. The one-dimensional stress-strain curve for each test is a curve which increases in stiffness as the stress increases and is thus concave to the stress axis. We chose, for each stress-strain curve, a secant modulus which best represents the stiffness of the shale for the pressures applied by the pier loads.

The "drained" triaxial tests were performed on shale specimens 1 7/8 in. in diameter and about 3 1/3 in. high. The specimens were set up in the triaxial cells and were allowed to come to equilibrium under an all-around confining pressure. The first group of specimens was subjected to a confining pressure equivalent to the present overburden pressure in the field. The shale samples swelled under this confining pressure. The confining pressures of a second group of specimens

were increased until no swelling occurred. After the samples had reached equilibrium, under the confining pressure, the drainage valve was closed and the first axial load was applied by placing weights on a yoke which hung on the piston of the triaxial cell. The deformation under this load was measured and indicates the deformation modulus of the shale under undrained conditions. The drainage valve was then opened until consolidation was completed uner constant stress conditions. After that the total deformation was measured and used in drawing a "drained" stress-strain curve for the shale. Typical "drained" and "undrained" axial stress-strain curves for a shale sample tested are shown in Figure 8.

"Undrained" Moduli

Fifteen unconsolidated-undrained tests were conducted on 5 1/2-in. x 8-in. samples of shale to determine the undrained moduli as well as the undrained shear strength. We tested the samples at a confining pressure of 10 psi and loaded them to failure by applying a stress difference at a deformation rate of .04 in./min. The stress-strain curves obtained for two typical tests are shown in Figure 9.

Three "undrained" triaxial tests on 1 7/8-in. diameter specimens were conducted at confining pressures of 3.75, 5.0, and 5.4 psi.

Direct Shear Tests

Direct shear tests were conducted on 10 samples of gray shale and 11 samples of black shale to assess the peak and residual shear strength of the shale along the bedding planes. The tests were conducted on samples from

the 6 in. core. The samples were 2 in. high with 1/4 in. space between sample holding boxes; they were sheared at a rate of about 1 mm/min.

The results of the tests are summarized in the Mohr diagrams in Figures 10 through 13. The test results indicate that the gray shale has a peak strength envelope with a cohesion intercept of 38 psi and an angle of shearing resistance of 29°. The residual angle of shearing resistance for the gray shale ranged from 15.5° to 22.5°. The black shale had a peak shear strength diagram given by a cohesion of 80 psi and an angle of shearing resistance of 18.5° The residual angle of shearing resistance for the black shale ranged from 9° to 16.5°.

Summary of Test Results

The purpose of this investigation was to determine the deformation moduli of the shales with depth so that the foundation elevations could be selected and the settlement of the piers estimated. The number of tests conducted on this study was not adequate to describe completely the stress-strain characteristics of the shales below each pier. But from the outset of the investigation tests were conducted on both soft and hard specimens of shale in an attempt to get a correlation of the measured moduli and a readily determined index property--such as the initial water content.

Previous studies of the relationship of deformation modulus and strength of soils and rock by Wilson and Dietrich[3] and Deere and Miller[4] have shown that shear strength and deformation moduli are related. A plot of the "undrained" Young's modulus versus the "undrained" compressive strength for the shales tested in the investigation, is shown in Figure 14. The relationship shown there indicates that the ratio of "undrained" Young's modulus to the "undrained" compressive strength is 150:1, 60:1, and 40:1 for the black shale, gray shale, and black "clay" shale, respectively. Previous studies on soils have also shown that the "undrained" shear strength of a saturated soil is related to the water content or void ratio before shearing. Since the relationships shown on Figure 14 substantiate that deformation moduli and strength are related by a constant, it follows that deformation moduli should also be a function of initial water content.

Figure 15 shows the relationship of log $(\sigma_1 - \sigma_3)_f$ versus water content for "undrained" tests on gray shale. It is observed that the relationship is a straight line on the semi-log plot similar to the virgin portion of an e-log p curve for a consolidation test. The plot of log E_i versus water content for "undrained" tests on the gray shale is a straight line parallel to the log strength-water content relationship (see Figure 15). A plot of log "drained" moduli versus water content for two triaxial tests and two consolidation tests on the gray shale also gives a straight line parallel to the other relationships shown in Figure 15. It should be noted that the "drained" modulus is roughly one-half of the "undrained" modulus for a sample at a given initial water content. The "drained" modulus will determine the total settlement of the pier, and the

information contained in Figure 15 enables us to estimate the "drained" modulus at a given location by determining the water content or "undrained" strength. This relationship is used in the computation of settlements at piers where the distribution of water content with depth is known, but where "drained" tests were not conducted.

A similar relationship between "undrained" strength, "undrained" modulus, and "drained" modulus for black shale is given in Figure 16. In general the black shale is stiffer than the gray shale. For the black shale the "drained" modulus is about one-third of the "undrained" modulus.

Deformation Moduli from Pressuremeter Tests

Pressuremeter tests were conducted at 5-ft intervals in six NX holes. A typical pressuremeter test result (shown in Figure 17) gives the volume change of the cell versus pressure applied to the cell. The deformation modulus of the shale on initial loading is related to the initial slope $(\frac{\Delta P}{\Delta V})$ as shown in Figure 17. Equations considering system corrections and similar variables are used to calculate the modulus of deformation from the observed values of $\frac{\Delta P}{\Delta V}$. (2,5) The value of the deformation modulus of interest in this study is the stiffness on initial loading, not the rebound moduli shown in Figure 17. It should be noted that the pressuremeter test is conducted by applying the pressure in increments, and that volume change readings are read at 15, 30, and 60 sec after a constant pressure is reached. Thus the moduli determined from the pressuremeter

test are "undrained" values of the modulus. These values should probably be higher than the "undrained" values determined from the laboratory, because the stress difference on the laboratory samples is applied perpendicular to the laminations in the shale, while the pressure is applied parallel to the laminations in the pressuremeter test.

In Figures 18 and 19 the pressuremeter test results are compared with the laboratory test values. The correlation was made by determining the water content from NX cores taken at locations where the pressuremeter tests were conducted. Figure 18 shows that the moduli from the pressuremeter tests are about three to seven times higher than the "undrained" moduli determined from the laboratory specimens. About 90 percent of the pressuremeter values fall within the dotted lines shown in Figure 18, which are roughly parallel to the relationship determined from the laboratory values. The values of "undrained" moduli from pressuremeter tests on the black shale are shown in Figure 19; they are generally about equal to the "undrained" values from laboratory tests, although there are a good number of points which show very high undrained moduli values from the pressuremeter tests.

The scatter of values beyond reasonable variations indicates the pressuremeter results should be used with caution and preferably with at least a limited amount of other testing. The laboratory values in most cases are too low, compared to field conditions, because of sample disturbance.

CONCLUSIONS BASED UPON LABORATORY AND IN SITU TESTING

Laboratory test results on the shales tested indicate that the "undrained" strength and "undrained" Young's modulus are related. The ratio of the "undrained" moduli to the "undrained" strength is 150:1 and 60:1 for the black shale and gray shale, respectively. It was also found that the "drained" Young's moduli for the same shales were about one-third to one-half of the "undrained" moduli for specimens at the same initial water content.

The "undrained" moduli, "drained" moduli, and "undrained" strength of both shales were closely related to the initial water content. Thus, the water content is an index property which can be used to estimate the modulus of shales at locations where complete test data are not available.

The deformation moduli from the pressuremeter tests showed the same general variation with water content as the laboratory tests. In all cases the moduli from the pressuremeter tests were higher than laboratory tests conducted on samples at comparable water contents. The pressuremeter moduli are essentially "undrained" values, but in general are stiffer than laboratory "undrained" values because of the possible disturbance of laboratory samples and because the loading in the pressuremeter test stresses the shale parallel to the bedding.

The moduli appropriate for settlement estimates should be "drained" moduli, but the laboratory "drained" values are too low because of inevitable sample disturbance. In situ
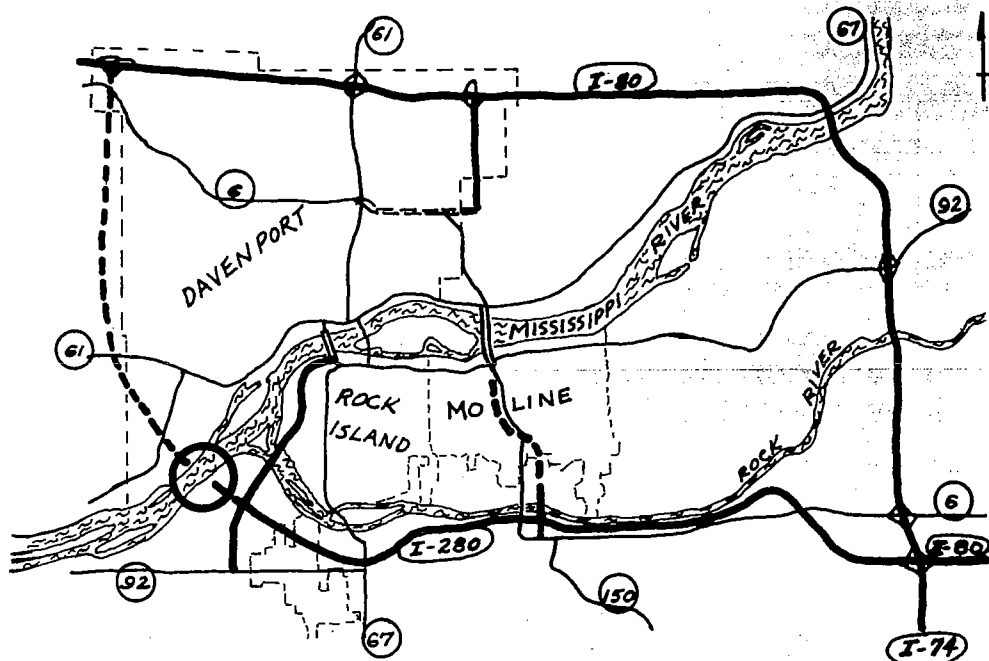
pressuremeter tests give values 5 to 13 times the laboratory drained moduli for the shales tested on this study. For purposes of settlement calculation, it is recommended that the laboratory "drained" moduli be tripled or that one-third the pressuremeter moduli values be used. In the absence of laboratory "drained" tests or in situ pressuremeter tests, we recommend that laboratory "undrained" moduli be used directly for computation of settlements.

The foundation elevation for each pier was selected below the soft upper weathered shales so that the differential settlement between piers would not exceed 1 in. Selecting deformation moduli as recommended above, and noting the variation of moduli and water content as given in Figures 18 and 19, we found the computed differential settlements to be tolerable when the foundation levels were below zones where the water content in the gray and black shales was less than 11 percent and 13 percent respectively. At shallower depths the water contents of both shales increased markedly, core recoveries were low, and the compressibilities were high. When the selection of the foundation elevation on this basis was near an underclay, we usually decided to excavate the underclay. This was because of the potential for some softening after excavation, with subsequent recompression due to construction and loading of the piers.

The preceding engineering studies would not have been possible without careful core drilling and wrapping and preservation of the core samples to maintain natural moisture.
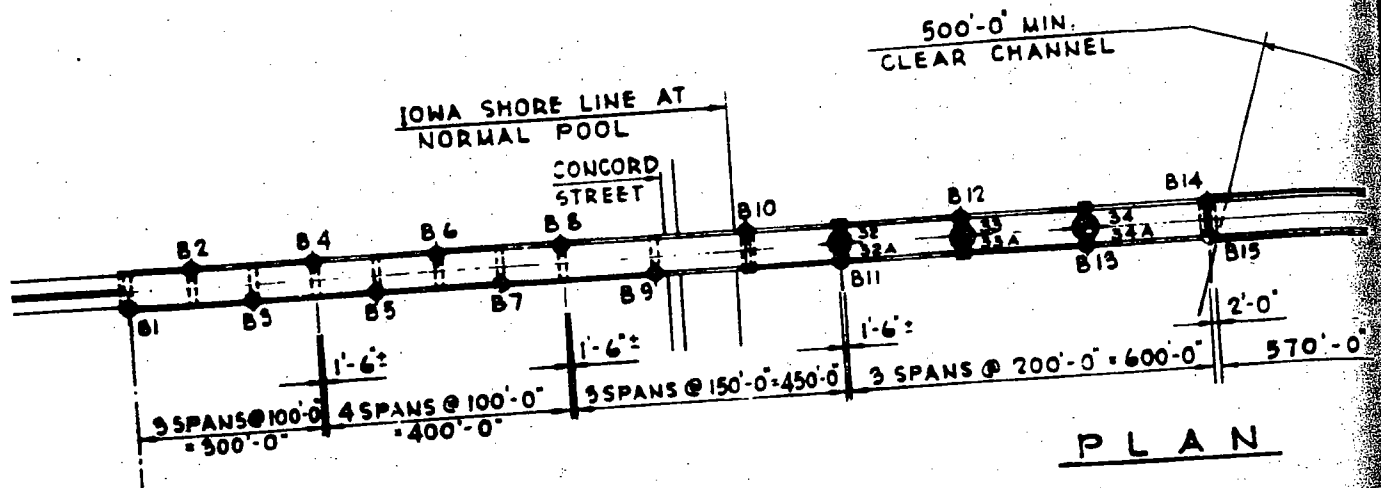
REFERENCES

1. Dixon, S. J., and Jones, W. V.,
    "Soft Rock Exploration with Pres-
    sure Equipment," Civil Engineering,
    October, 1968, pp. 34-36.

2. Menard, L., "Regles pour le calcul
    de la force portante et du tasse-
    ment des fondations on fonction des
    resultats pressiometriques," from
    Proceedings of the Sixth Interna-
    tional Conference on Soil Mechanics
    and Foundation Engineering, Toronto,
    University of Toronto Press, 1965,
    pp. 295-299.

3. Wilson, S. D., and Dietrich, R. J.,
    "Effect of Consolidation Pressure
    on Elastic and Strength Properties
    of Clay," from Research Conference

    on Shear Strength of Cohesive Soils,
    New York, ASCE Soil Mechanics and
    Foundations Division, 1961,
    pp. 419-435.

4. Deere, D. U., and Miller, R. P.,
    "Classification and Index Properties
    of Intact Rock," AFWL-TR-65-116,
    Air Force Special Weapons Center,
    Kirtland AFB, New Mexico, 1966.

5. Hendron, A. J., Jr., Mesri, G.,
    Gamble, J. C., and Way, G.,
    "Compressibility Characteristics of
    Shales Measured by Laboratory and
    In-Situ Tests," in Determination
    of In-Situ Modulus of Deformation
    of Rock, ASTM Special Technical
    Publication No. 477, 1970.

I-280 MISSISSIPPI RIVER BRIDGE

FIGURE 1. LOCATION MAP.

500'-0" MIN.
CLEAR CHANNEL

IOWA SHORE LINE AT
NORMAL POOL

CONCORD
STREET

B10   B12   B14

B2   B4   B6   B8

34
B3   B5   B7   B9   B11   32A   33   33A   34A   B15
B1   B13

2'-0"

1'-6"±   1'-6"±   1'-6"±   570'-0"

5 SPANS @ 100'-0" 4 SPANS @ 100'-0" 3 SPANS @ 150'-0" = 450'-0" 3 SPANS @ 200'-0" = 600'-0"
= 500'-0"   = 400'-0"

PLAN

From DeLeuw, Cather & Company
Boring Location Plan, July 1968

¢ BRG'S
ABUT. "A"

63'-0" MIN. VERT. CL.

CLASSIFICATION LINE
EL. 545.00

¢ CONCORD   HIGH WATER
STREET   EL. 565.00± (1965)

APPROXIMATE EXISTING
GROUND LINE

① ② ③ ④ ⑤ ⑥ ⑦ ⑧ ⑨ ⑩ ⑪ ⑫ ⑬

11+13.38 12+13.38 13+13.38 14+14.38 15+15.38 16+15.38 17+15.38 18+16.38 19+67.38 21+17.38 22+68.38 24+69.38 26+69.38 28+72.30
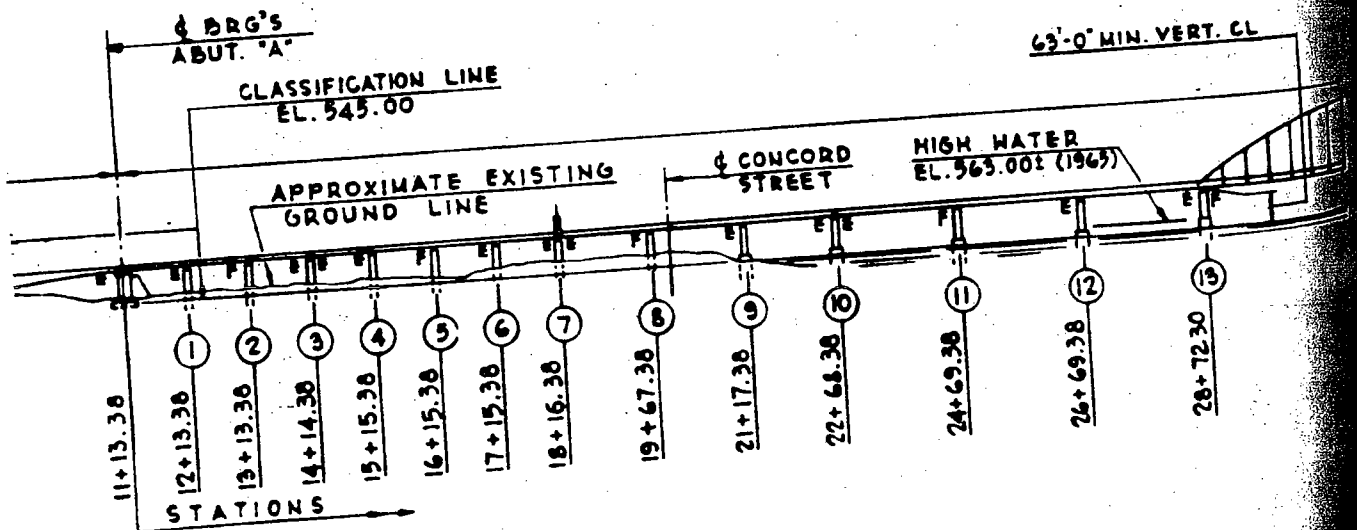
STATIONS ⟶

FIGURE 2. BRIDGE ELEVATION AND BORING LOCATION PLAN.

FLOW

ILLINOIS SHORE LINE
AT NORMAL POOL

TOWNSHIP ROAD

B16   B18   B20   B22   B24   B26   B 28   B 30
B17   B19   B21   B29   B25   B27   B29   B31

2'-0"   1'-6"±   1'-6"±   1'-6"±

3 SPANS @ 200'-0"= 600'-0"   3 SPANS @ 150'-0"= 450'-0"   4 SPANS @ 100'-0"   4 SPANS @ 100'-0"
= 400'-0"   = 400'-0"
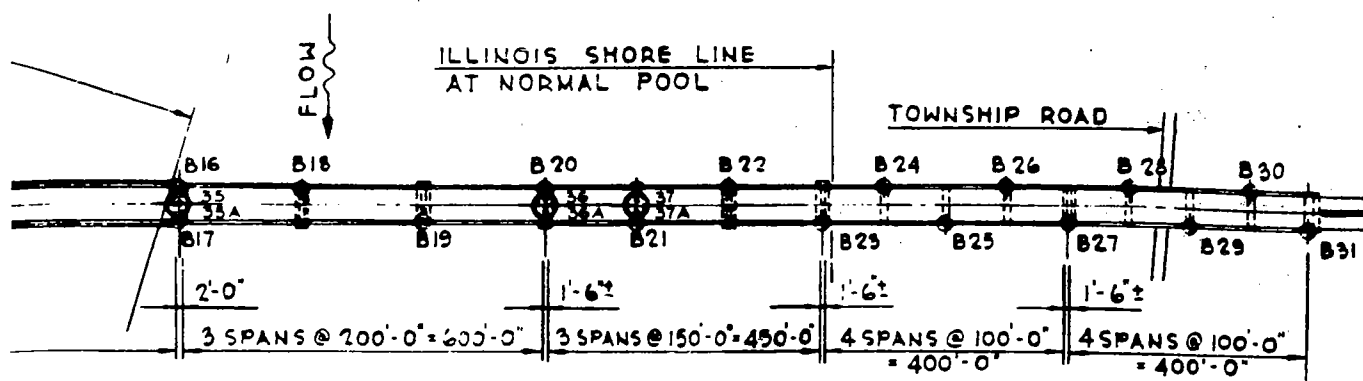
LEGEND

TEST BORING LOCATIONS, NX, 1965
PREVIOUS CONTRACT

TEST BORING LOCATIONS,
THIS CONTRACT
NX & 6-INCH, 1968

℄ BRG'S
ABUT. "B

NORMAL POOL
EL. 544.50

CLASSIFICATION LINE
EL. 545.00

℄ TOWNSHIP
ROAD 58B

(14)   (15)   (16)   (17)   (18)   (19)   (20)   (21)   (22)   (23)   (24)   (25)   (26)   (27)

34+43.46   36+46.38   38+46.38   40+47.38   41+98.38   43+48.38   44+99.38   46+00.38   47+00.38   48+00.38   49+01.38   50+02.38   51+02.38   52+02.38   53+02.38

PIER
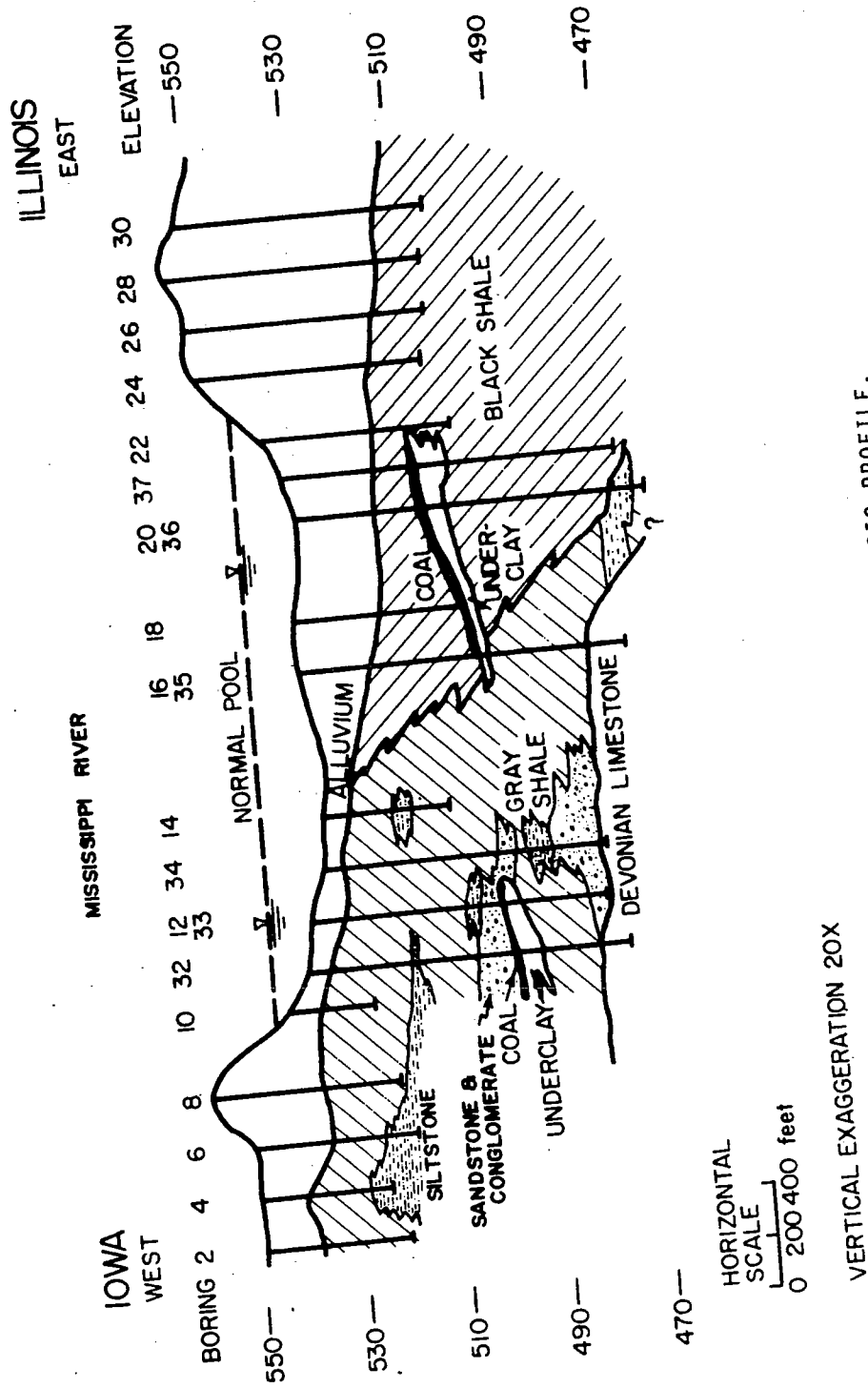NUMBERS

STATIONS
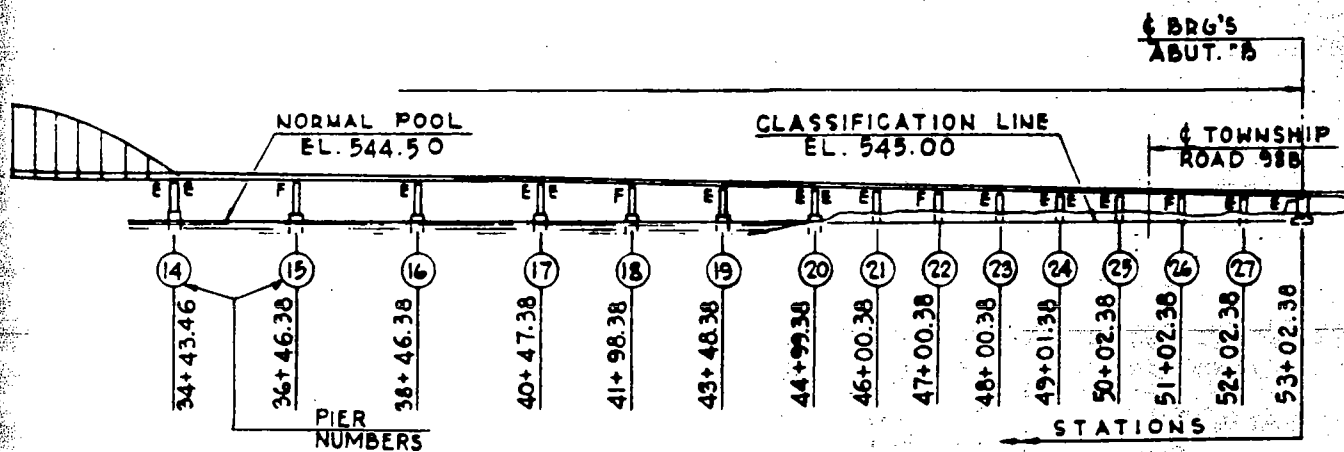
ELEVATION

FIGURE 2 (continued)

82

FIGURE 3. GENERALIZED GEOLOGIC PROFILE.
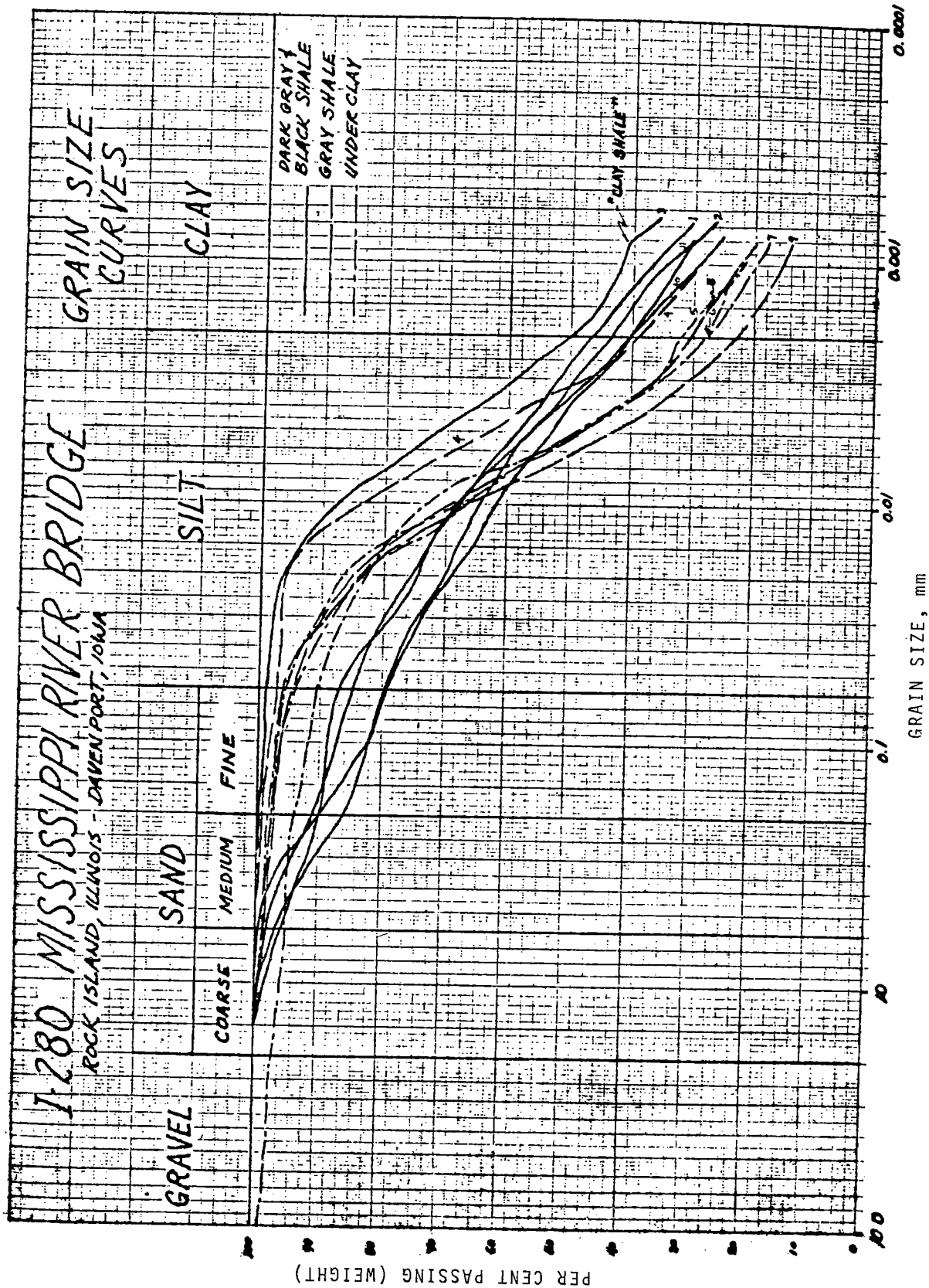
FIGURE 4. GRAIN SIZE CURVES.

84

FIGURE 5. PLASTICITY CHART.

Legend (data series):
- ⊙ DARK GRAY - BLACK SHALE
- ◇ DARK GRAY - BLACK CLAY SHALE
- ☐ GRAY SHALE
- △ UNDERCLAY - CLAYEY SILTSTONE

Axes:
- PLASTICITY INDEX, (Lw - Pw)
- LIQUID LIMIT, w%
- "A-line"

LOG $\bar{p}$, psf
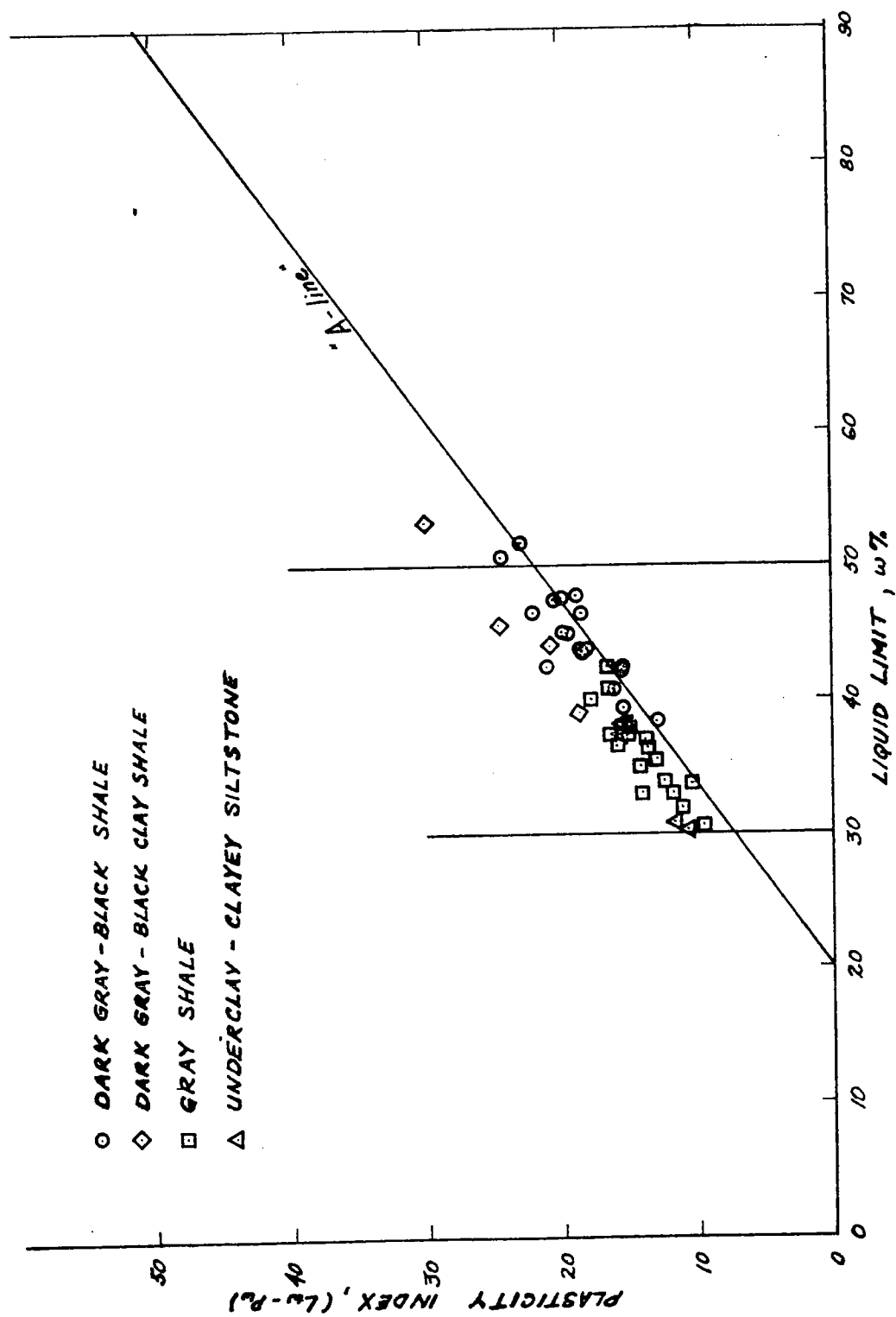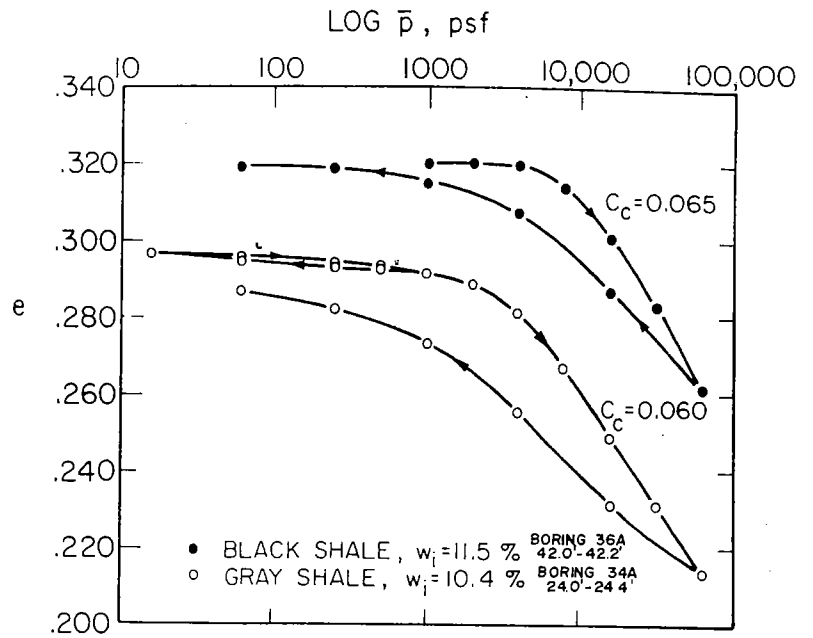
FIGURE 6. VOID RATIO-LOG PRESSURE CURVES
FROM ONE-DIMENSIONAL CONSOLIDATION TESTS.

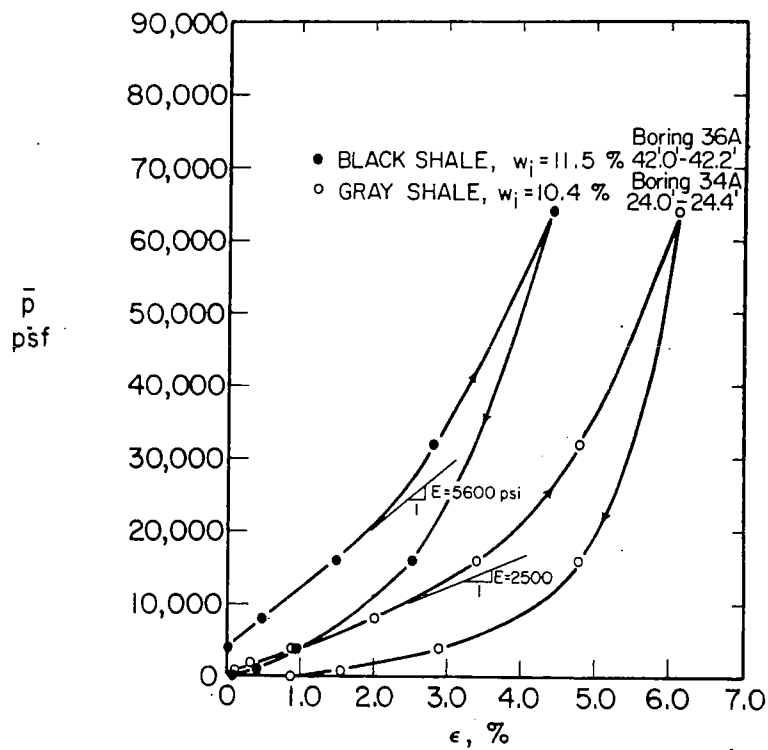FIGURE 7. STRESS-STRAIN CURVES FROM ONE-DIMENSIONAL CONSOLIDATION TESTS.
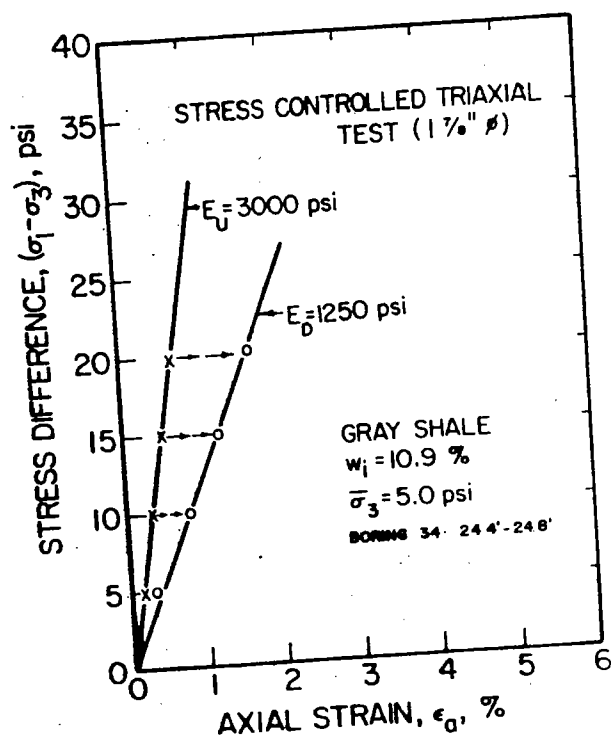
FIGURE 8. STRESS-STRAIN CURVES FROM STRESS-CONTROLLED TRIAXIAL TEST.

FIGURE 9. STRESS-STRAIN CURVES FROM UNCONSOLIDATED-UNDRAINED TRIAXIAL TESTS.
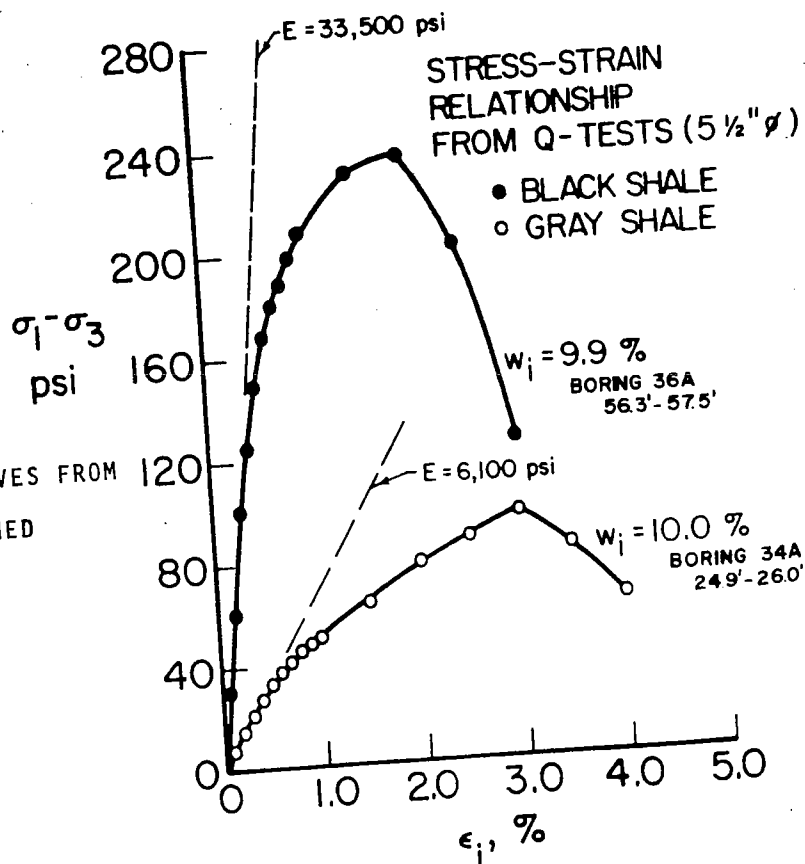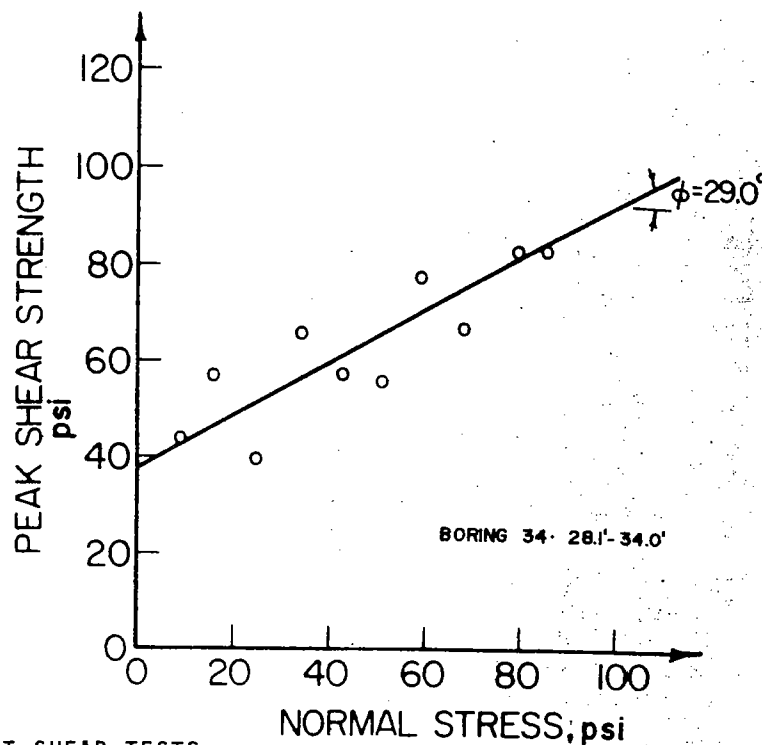
FIGURE 10.   DIRECT SHEAR TESTS -

PEAK SHEAR STRENGTH VS NORMAL STRESS FOR GRAY SHALE.
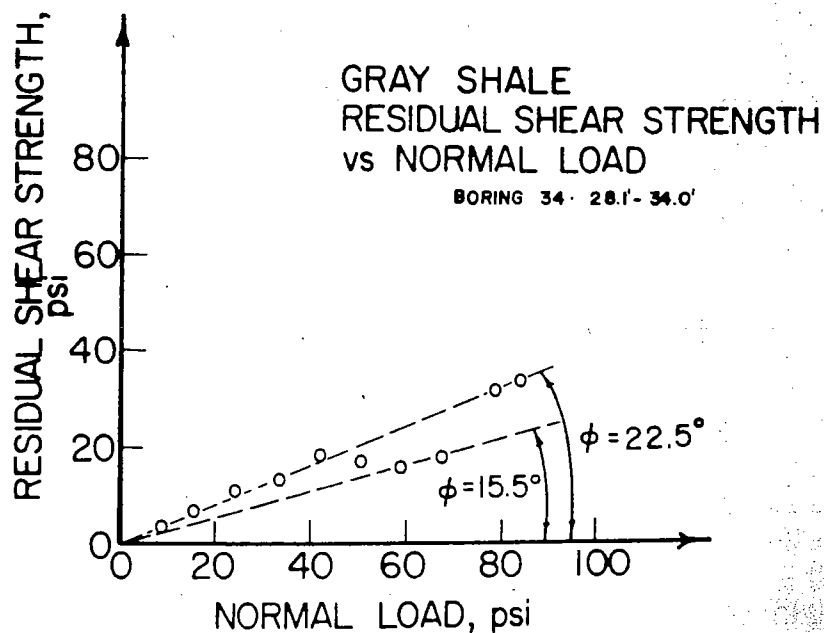
FIGURE 11.   DIRECT SHEAR TESTS -

RESIDUAL SHEAR STRENGTH VS NORMAL STRESS FOR GRAY SHALE.

88
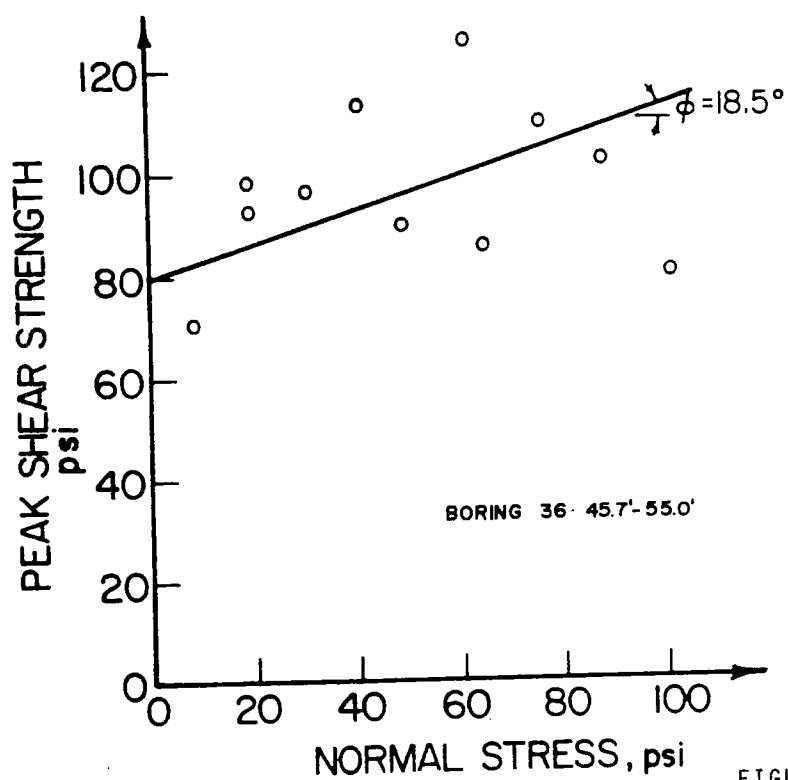
FIGURE 12. DIRECT SHEAR TESTS -
PEAK SHEAR STRENGTH VS NORMAL STRESS FOR BLACK SHALE.
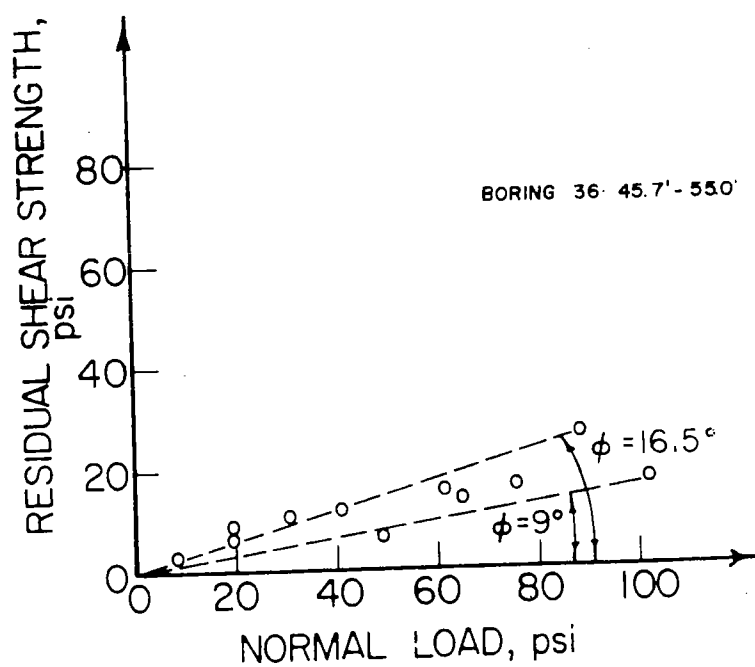
FIGURE 13. DIRECT SHEAR TESTS -
RESIDUAL SHEAR STRENGTH VS NORMAL STRESS FOR BLACK SHALE.
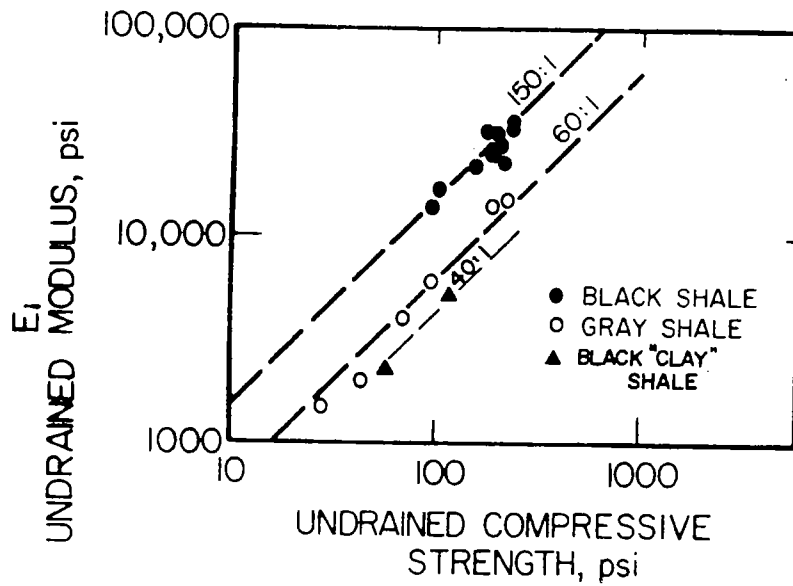
FIGURE 14. UNDRAINED MODULUS VS UNDRAINED COMPRESSIVE STRENGTH.
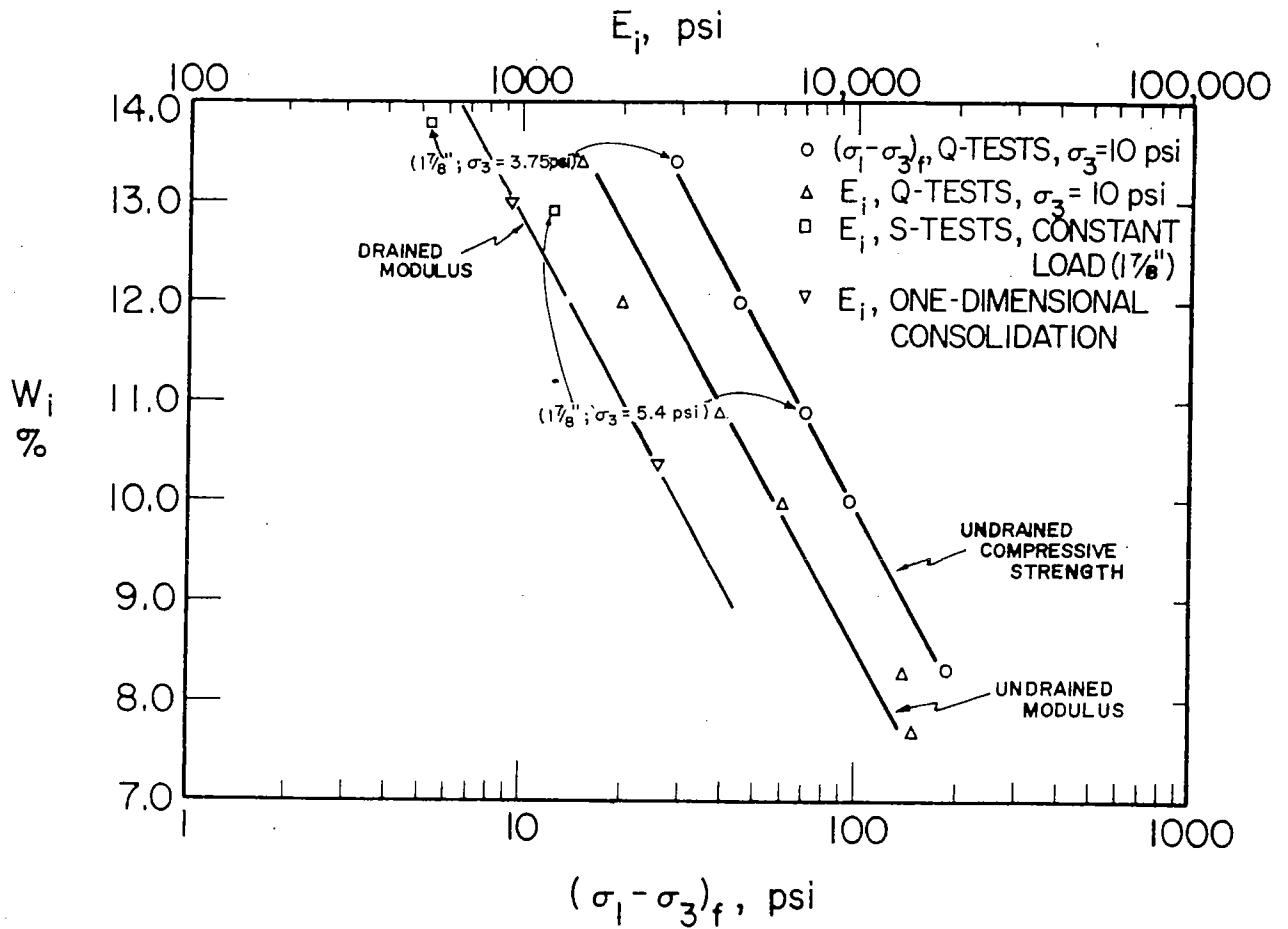
FIGURE 15. MODULUS AND COMPRESSIVE STRENGTH FOR GRAY SHALE.

E_i, psi

- $(\sigma_1 - \sigma_3)_f$, Q-TESTS, $\sigma_3 = 10$ psi
- E_i, Q-TESTS, $\sigma_3 = 10$ psi $(5\frac{1}{2}'')$
- E_i, S-TESTS, CONSTANT LOAD$(1\frac{7}{8}'')$
- E_i, ONE-DIMENSIONAL CONSOLIDATION

$\blacksquare$ ($\sigma_3 = 40$ psi)

UNDRAINED COMPRESSIVE STRENGTH

UNDRAINED MODULUS

DRAINED MODULUS

$(1\frac{7}{8}''; \sigma_3 = 5$ psi$)$

($\sigma_3 = 40$ psi)

W_i %

$(\sigma_1 - \sigma_3)_f$, psi
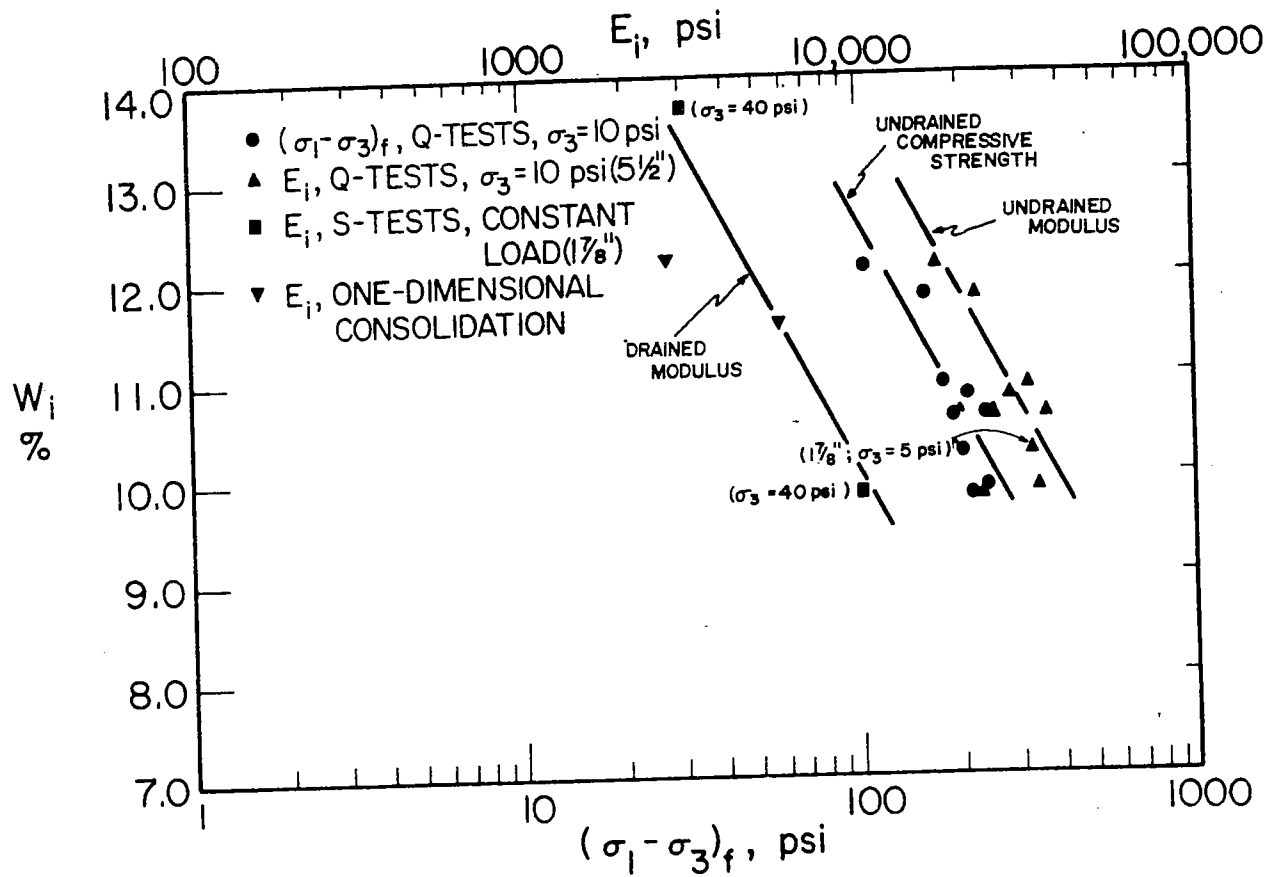
FIGURE 16. MODULUS AND COMPRESSIVE STRENGTH FOR BLACK SHALE.

V_m (cm^3)

Elastic Rebound

$\frac{\Delta V}{\Delta P}$

Elastic Rebound

$\frac{\Delta V}{\Delta P}$

Initial Loading

$\frac{\Delta V}{\Delta P}$

EQ.(1) $E = \dfrac{(1+\nu)(\Delta P)}{\Delta r/r} = 2V(1+\nu)\dfrac{\Delta P}{\Delta V}$

EQ.(2) $E = \dfrac{\Delta P}{(\Delta V - \Delta P \cdot a)d} \cdot K_V$

BORING 34
DEPTH 34.7'

P_m (kg/cm^2)

FIGURE 17. VOLUME CHANGE VS PRESSURE CURVE FROM A TYPICAL PRESSUREMETER TEST.

E_i, psi
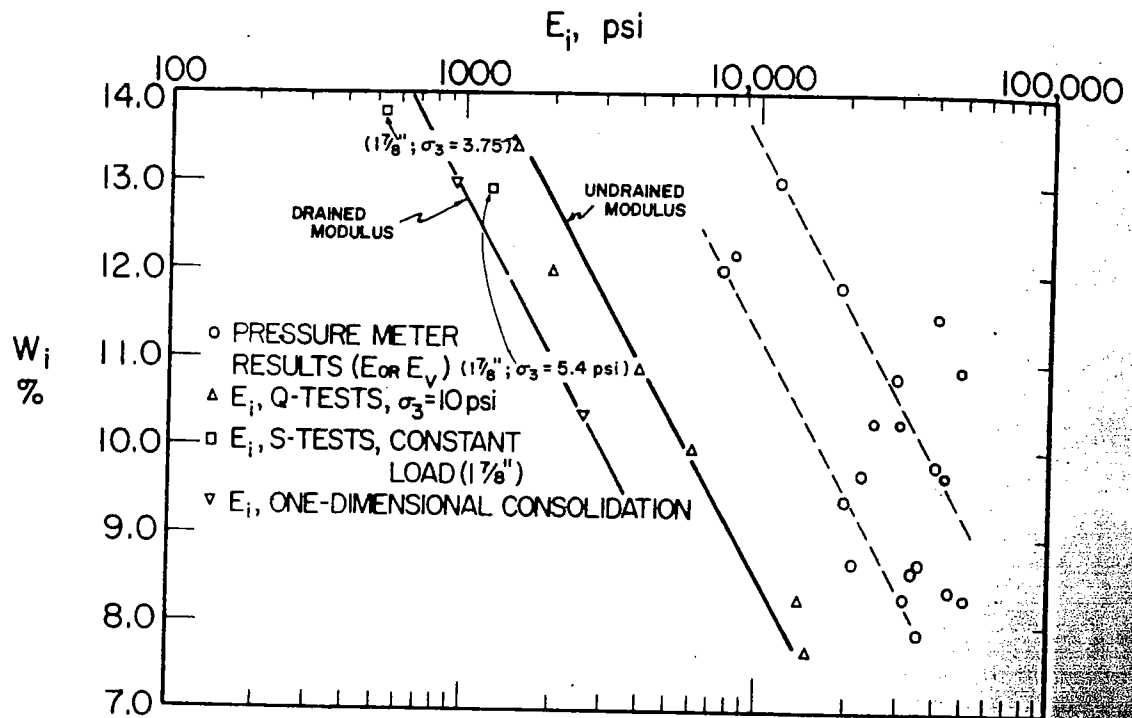
FIGURE 18.   COMPARISON OF LABORATORY AND FIELD MODULUS FOR GRAY SHALE.

E_i, psi
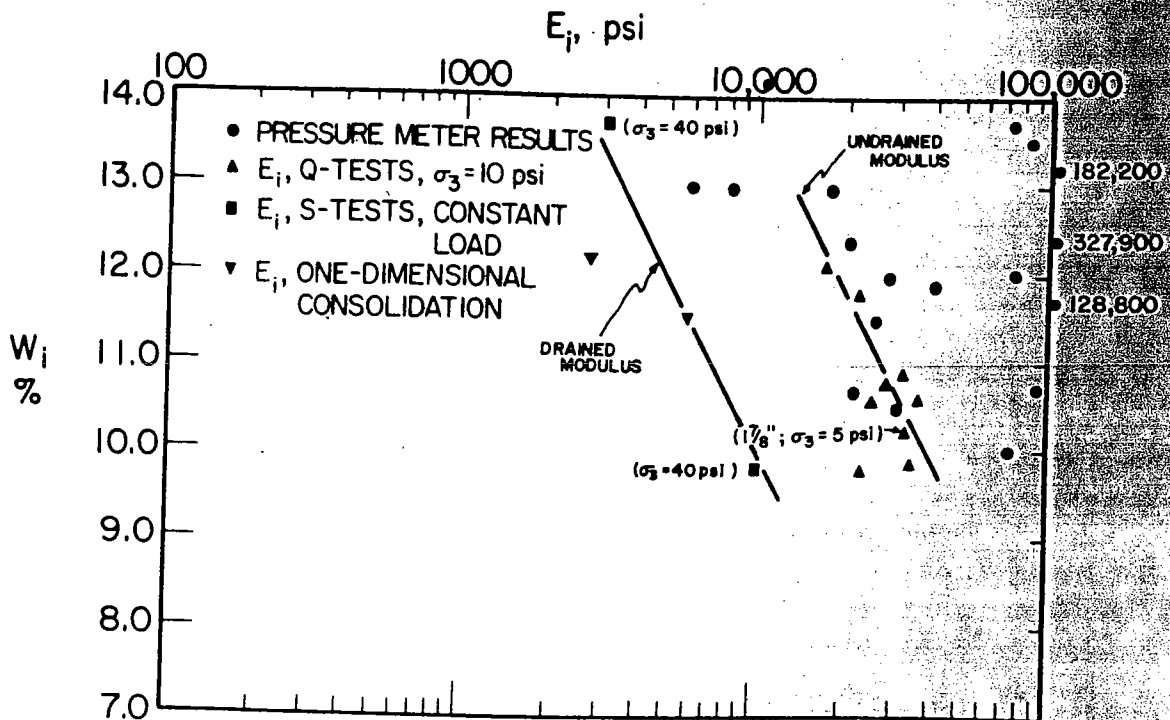
FIGURE 19.   COMPARISON OF LABORATORY AND FIELD MODULUS FOR BLACK SHALE.

VI. SEISMIC MAPPING OF CAVITIES AND VOIDS

Jack A. Ferland*

INTRODUCTION

Shallow refraction exploration techniques usually involve a linear array of detectors with charges fired just above or slightly below land surface at each end of the line. Successively denser strata are indicated by higher velocities, as refraction of seismic waves takes place in both downward and lateral directions.

A "blind" zone exists when materials of low density (including voids) are overlaid by denser material; refraction in only the downward component takes place and the lower speed (lower density) material is not detected.
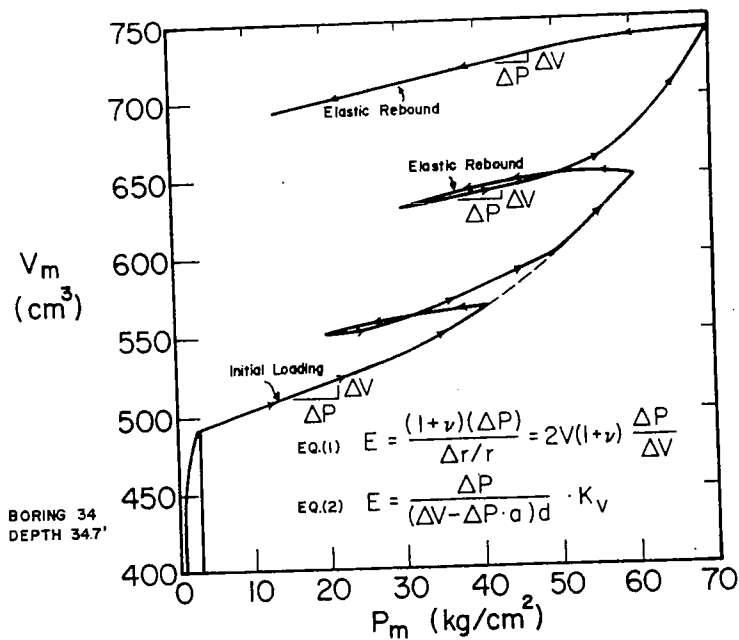
Special shooting techniques were developed between 1926 and 1930 to locate salt domes in Louisiana and Texas. [1]** Detectors were located in arcs with a dynamite charge at the focus. Detector spreads varied in length from 1000 ft to 3 mi. If ray speeds between shot point and detector indicated shorter travel times than previously calculated from known velocities, the rays were assumed to have penetrated the high-speed salt.

*Engineering Geologist, Law Engineering Testing Company.

**Superscript numbers in parentheses refer to the References at the end of this paper.

Once an early wave arrival was detected, the process was repeated with intersecting rays from second, third, and fourth fanspreads until the dome area was defined.

THEORETICAL TRAVEL PATHS

As previously mentioned, conventionally used refraction methods are incapable of determining lower speed material underlying that of higher speeds--if the energy source originates above the high speed layer. Lower velocity material may be seismically detected only when direct (non-refracted) rays are allowed to traverse it.

As shown in Figure 1, travel time in a three-layer system (shot fired below second interface) is determined from aggregate travel paths A through E. [2] Assuming isotropy for each layer, travel times along these paths are:

$$T_{ab} = \frac{X}{V_2} + \frac{2Z_o(V_2^2 - V_o^2)^{1/2}}{V_o V_2}$$

$$+ \frac{2Z_1(V_2^2 - V_1^2)^{1/2}}{V_1 V_2}$$

Low speed material such as cavities or voids within the V_2 layer will cause time delays in traveling from A to E.

DIFFRACTION CONSIDERATIONS

Seismic energy, like light, obeys
laws of optics. Diffraction of waves
traversing cavities is largely a func-
tion of cavity shape, frequency, and
wavelength. If we assume a cavity to
be a geometrical cylinder, then projec-
tions parallel and normal to the long
axis of the cylinder will enscribe a
rectangle and a circle respectively.[3]
Values of wave length and frequency
taken from actual seismic records indi-
cate a lack of significant diffraction
in voids and cavities with width or di-
ameter greater than approximately 1/10
of a wavelength. Thus, in most such
cases, there is no appreciable time loss
or gain.[4]

Diffraction around sharp corners,
such as a pinched-out cavity, is a dif-
ferent proposition. First arrivals of
such waves detected at land surface can
either take the circuitous route through
the high speed material or pass at lower
velocity through the cavity. Rays tak-
ing the longer route may take as little
as or less time than those crossing low
speed material.

FIELD AND OFFICE PROCEDURES

In construction of theoretical trav-
el times for each ray, very accurate
data for velocity and layer thicknesses
of the intact soil or rock are essen-
tial. Velocity control may be obtained
in three ways:

(a) If reflection equipment is a-
vailable, velocities for each layer may
be obtained from a plot of squared shot
to geophone distances against squared
reflection times for each geophone.

(b) True velocities may be obtained
from an arithmetic mean of apparent ve-

locities in conventional refraction pro-
cedures. This method leaves much to be
desired, in that irregularities in the
high speed interface are reflected in
point-scatter on a standard time-dis-
tance curve.

(c) The most satisfactory method
of obtaining good velocity control is
up-hole shooting. This method involves
firing small charges at intervals with-
in a bore hole, from bottom to top.
Travel times from each shot to the sur-
face are recorded on multiple geophones
nested around the top of the hole. Av-
erage travel times for each shot are
plotted against depth of shot and true
velocities are determined from the best
straight-line plot of these points.

Layer thicknesses (Z_o, Z_1, Z_n) may
be obtained by either continuous refrac-
tion or reflection profiles. Depths
may be checked in bore holes used to
fire the fan spreads.

Finally, good surface control is
necessary. Surveys of horizontal and
vertical distances should be to the
nearest 0.1 ft.

Once satisfactory control of veloc-
ities and layer thickness has been ob-
tained, bore holes penetrating the sus-
picious horizon are made. These bore
holes may be made by conventional cor-
ing or plugging, or by blast hole drills.

If routine investigations are con-
ducted, a line of such bore holes is
made with shots fired to adjacent detec-
tor broadsides. With the geophones at
the same stations, a shot in the next
hole is made to cross fans. The process
of overlapping fans is continued until
anomalous arrival times are encountered.
Additional holes are drilled to obtain
the most efficient coverage of overlap-

ping fans, and travel times for these are determined by further shooting (see Figure 2).

Bore hole shots within cavities should be avoided, as losses of seismic energy due to decoupling may result.

The previous discussion has been for cavities in a single depth or elevation range. Vertical cavity delineation may be obtained by firing shots at different depths in the bore holes.

Once satisfactory field data have been obtained, theoretical travel times are calculated. Although the math required is not complicated, the massive computation of travel times along each fan's ray makes computer analysis almost mandatory.

Refraction time losses within the cavity are ignored.

PLOTTING DATA

A plot of shot holes and detector location is made. Rays between respective shot holes and geophones are drawn and both theoretical and actual travel times are plotted on these rays with a scale. Typical scale units of 1 in. = 20 ft. and 1 in = 30 milliseconds have proved satisfactory for this. Shading of time anomalies (the area between theoretical and actual times) is made and cavity thickness along each ray is constructed by multiplying the time anomaly by 1100 ft per sec (air filled cavities) or 5000 ft per sec (water filled cavities).

Interpretations of cavity thickness and orientation are then constructed by piecing individual ray projections together.

FIELD RESULTS

Data from two areas are presented herein. In respect for clients' wishes, locations and names have been kept confidential.

SUBSIDENCE IN AN EARTH FILL

The first case involved subsidence in an earth fill, subjected to internal erosion over cavernous limestone. We were asked to gather data as to the extent of a possible void or soft zone under the subsidence area. An initial velocity survey was taken through the firing of a small charge just below the surface at each end of a linear detector array. The area investigated was 300 ft from the area of known subsidence and was considered, in terms of velocity, characteristic of the whole embankment. Depths calculated for a gravel stratum below the fill and the underlying limestone foundation were in good agreement with construction records.

The entire shooting process was repeated with the detector spread relocated across the subsidence and the charge fired from a position central to the detectors. Calculated travel times were 4 percent earlier than actual first arrivals on high-gain records. By reexamining records used in the initial velocity control, we discovered a slight monotonic increase of velocity with depth and deduced that waves traversing the material were following hyperbolic paths. To compensate for this, theoretical times were increased 4 percent. Figure 3 shows the time anomalies and the conception of a void area as deduced from a single fan. Interestingly, records made with low amplifier

gain settings showed rays traversing the subsidence areas had lower frequencies than rays outside the anomalous areas. Because small time anomalies were observed outside the subsidence area, only those anomalies of 2 milliseconds or greater on two consecutive rays were considered significant.

A series of borings after the initial seismic investigation confirmed the existence of a zone of soft-wet soil in the structure. The general configuration of this zone agreed closely with that indicated by seismic data, but the orientation was more nearly normal to the axis of the embankment. This inconsistency could have been rectified by locating a second fan spread normal to the first.

DOLOMITE CAVERNS

A shooting procedure in the second area was conducted as part of a pre-construction site investigation.

The study area was located in the Copper Ridge member of the Knox Dolomite group. Air photo analysis indicated the presence of many lime sinks in the area of the site. An initial core boring, which revealed only one small cavity, was used to perform the previously described up-hole velocity check. (See Figure 4 for a plot of up-hole times and velocity for this hole.) Layer thicknesses and bedrock irregularities were determined by refraction profiling. Broadsided spreads were laid out with geophones spaced 10 ft apart. Locations and elevations of bore holes and geophones were made directly with an alidade and plane table. Time anomalies were encountered along

each ray except the eastern-most. Because the greatest anomalies trended from east to west, it was concluded that this was the probable orientation of the cavity. A sharp turn or "dog leg" in the system, just east of Boring 4, was deduced from the concave section of the shaded area on B-4's fan. Figure 5 shows the shaded time anomalies and their relationship to a single cavity conceptionalized below.

Rod-drops encountered while drilling in B-1 and B-3 indicated vertical cavity thickness was approximately equal to seismically-projected horizontal thickness.

CONCLUSIONS

Although it cannot differentiate between single and multiple cavities and voids, and though corner diffraction can play a deceptive role in measured travel times, this system does offer a far greater insight into cavity development than may be obtained by conventional boring schemes.

REFERENCES

1. Rosaire, E. E., "Studies In Non-structural Petroleum Prospecting," Geophysics, Vol. 17, No. 2, April, 1952, pp. 244-277.

2. Dobrin, Milton, Introduction to Geophysical Prospecting, 2nd Edition, McGraw-Hill, New York, 1960.

3. Knopoff, L, "Scattering of Compressional Waves by Spherical Obstacles," Geophysics, Vol. 24, No. 1, February, 1959, pp. 30-39.

4. Elliot, Charles, "Some Applications of Seismic Refraction Techniques in Mining Exploration," in Seismic Refraction Prospecting, ed., A. W. Musgrave, Society of Exploration Geophysicists, Tulsa, Oklahoma, 1967, pp. 522-537.

$$T_{AB} = \frac{X}{V_2} + \frac{Z_0(V_2^2 - V_0^2)^{\frac{1}{2}}}{V_0 V_2} + \frac{Z_1(V_2^2 - V_1^2)^{\frac{1}{2}}}{V_1 V_2}$$
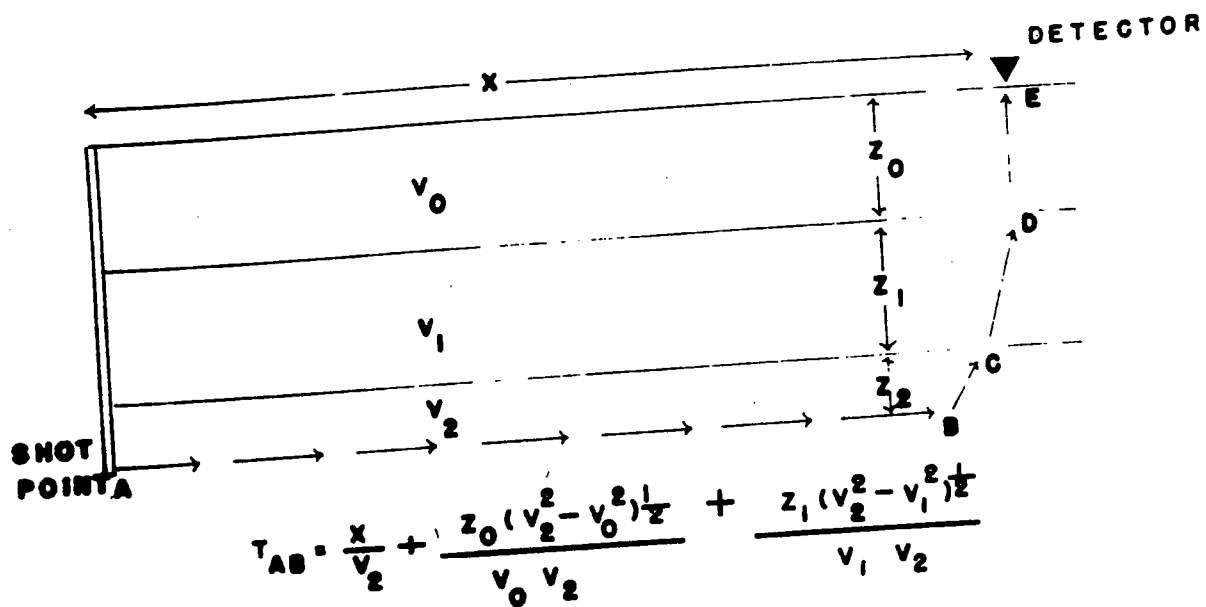
FIGURE 1.   LEAST-TIME RAY PATH, THREE-LAYER SYSTEM.

DETECTOR LOCATIONS

LINE OF
SHOT POINTS

A — MEDIUM RESOLUTION
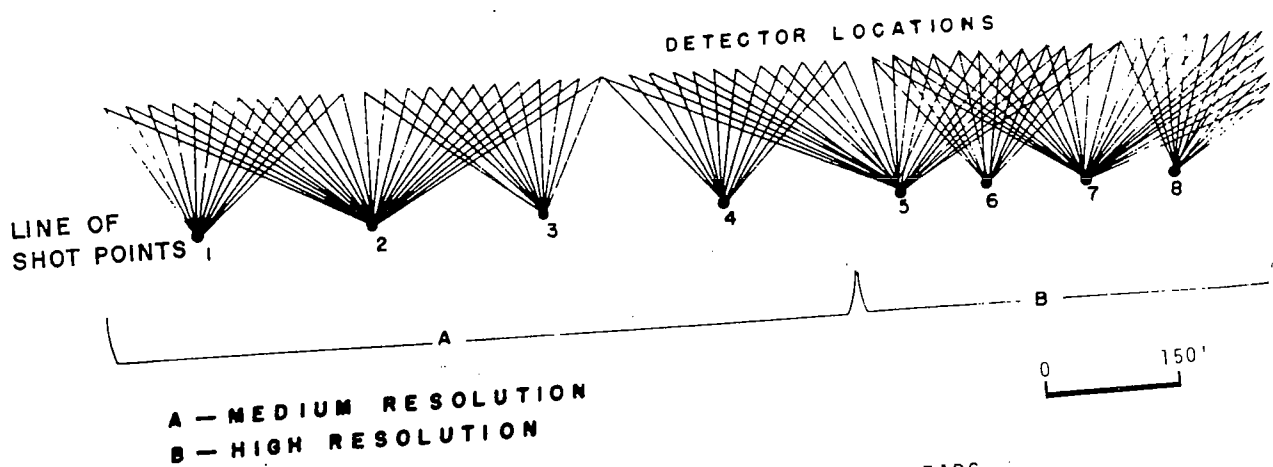B — HIGH RESOLUTION

FIGURE 2.   SUGGESTED SHOT-DETECTOR SPREADS

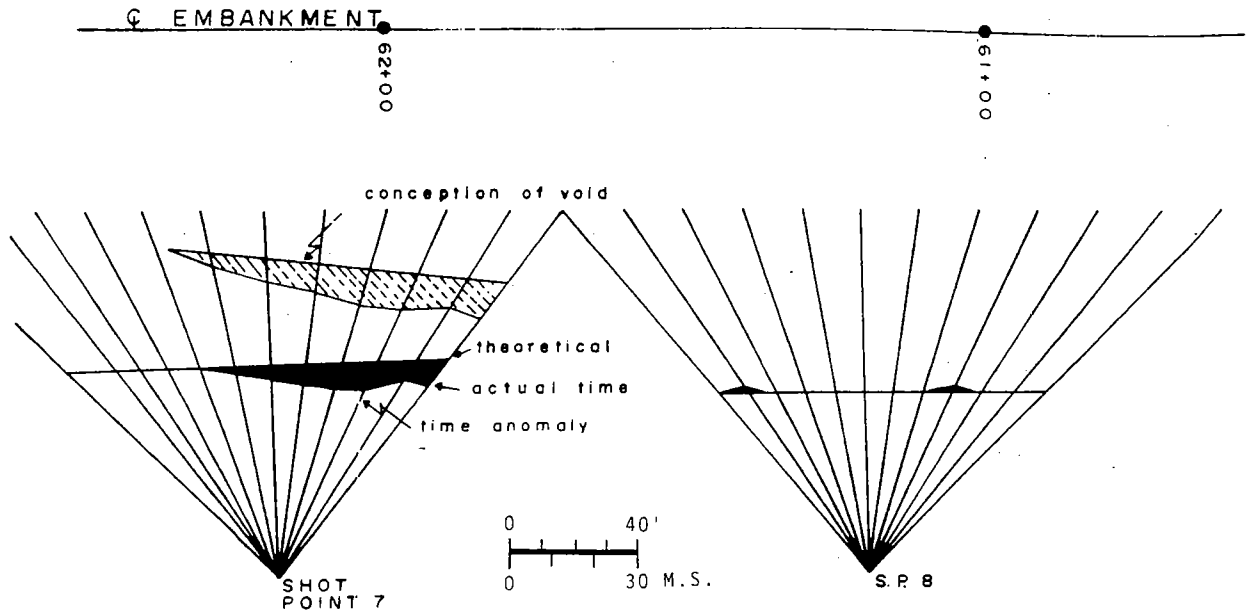FOR ROUTINE CAVITY INVESTIGATION

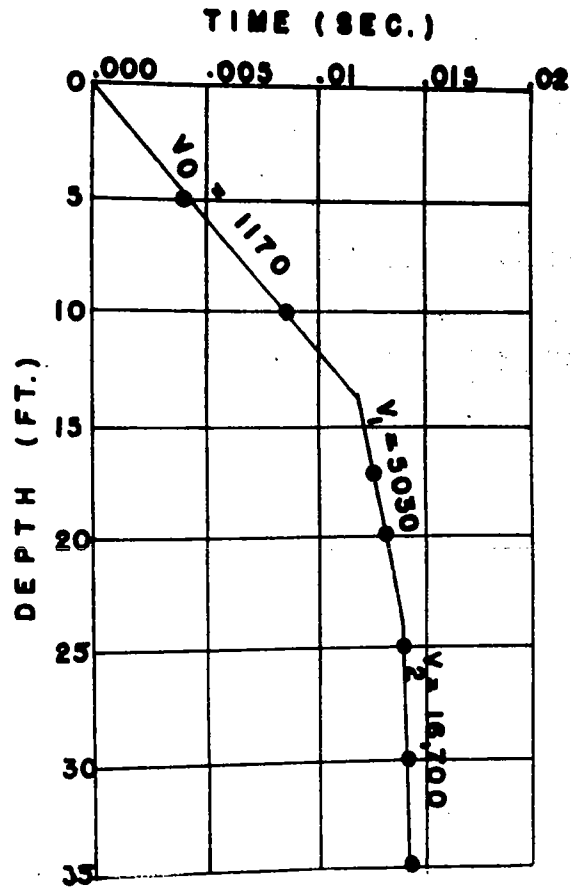FIGURE 3.   SEISMIC SPREADS

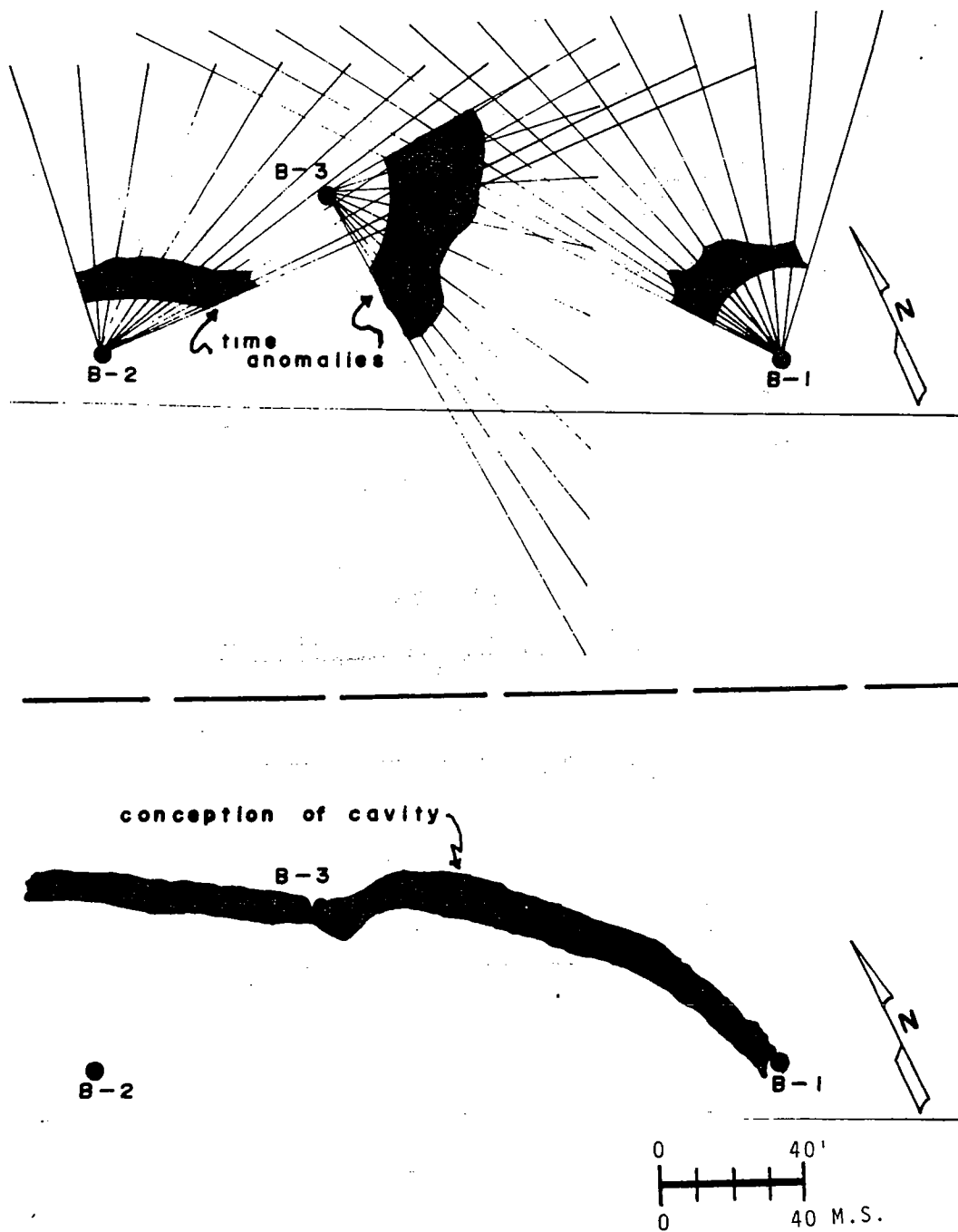FIGURE 4.   UP-HOLE VELOCITIES B-2.

98

FIGURE 5.   SEISMIC SPREAD AND CAVITY PLAN, KNOX DOLOMITE

VII. PROPERTIES OF LIME-TREATED SOILS

M. R. Thompson*

INTRODUCTION

Lime has been widely and success-fully used as a stabilizing agent for fine-grained plastic soils. It is a well-documented fact that the engineering properties of lime-treated soils vary widely, depending on such factors as (a) nature and composition of soil, (b) lime percentage, (c) lime type, (d) curing (time-temperature), and (e) density of compacted mixture. Obviously, the general quality (as evaluated by engineering properties) of a partic-ular lime-soil mixture will govern its use relative to its position (base-sub-base-modified subgrade) in a pavement structure. This paper examines the significant engineering properties of lime-treated soils, grouped for convenience into the following categories:

    (a) strength,
    (b) stress-strain properties,
    (c) freeze-thaw durability, and
    (d) shrinkage characteristics.

The information and data presented in this paper are primarily based on research studies sponsored at the University of Illinois by the Illinois Di-vision of Highways and the Department of Transportation, Federal Highway Administration, Bureau of Public Roads.

MATERIALS AND PROCEDURES

Table 1 is a summary of properties for the various soils included in the different phases of the study, with soil reference numbers assigned to facilitate its use.

Detailed explanations of sample preparation techniques and testing procedures are not included in this paper. For more specific information relating to a particular testing procedure, refer to the appropriate publications in the reference list.

STRENGTH

The strength of lime-soil mixtures can be evaluated in many ways, the most popular of which are unconfined compression and CBR. Only limited data are available concerning the tensile strength properties of lime-soil mixtures.

It should be emphasized that the strength of a lime-soil mixture is dependent on many variables. Soil type, lime type, lime percentage, and curing conditions (time-temperature) are the most important. The strength of a lime-

*Professor of Civil Engineering, University of Illinois, Urbana.

soil mixture is therefore not a "static value," but one that varies in response to changes in the variables listed above.

Unconfined Compression

The unconfined compression test is a simple and effective test procedure. Specimens normally have length/diameter ratios of approximately two in order to minimize end effects. For fine-grained soils normally stabilized with lime, specimens 2 in. in diameter by 4 in. appear to be satisfactory. This specimen size is large enough to allow proper compaction of the mixture and also minimizes the "statistical flaw distribution" effect that contributes to the larger strengths commonly obtained with smaller specimens. Specimens are typically tested in compression using a screw type or hydraulic machine with strain rates of about 0.05 in./min.

The unconfined compressive strength of typical Illinois soils compacted at optimum moisture content and density (ASTM D698-64T) ranges from about 25 psi to approximately 100 psi, depending upon the nature of the soil. The strength of lime-soil mixtures varies substantially.[1,2]* In 2-in. diameter x 4-in. specimens at a 0.05 in./min strain rate, increases in lime-soil mixture strength for Illinois soils cured 28 days at 73°F range up to about 265 psi, with many soils displaying increases greater than 100 psi. Extended curing (56 days at 73°F) of the same

mixtures produces strength increases exceeding 625 psi for some lime-soil combinations. Prolonged curing (75 days at 120°F) of the AASHO Road Test embankment soil (No. 32)** treated with 5 percent lime produced an average compressive strength of 1580 psi. Field data indicated that the strength of some lime-soil mixtures continues to increase with time up to 10 yrs.

The difference between the compressive strengths of natural and lime-treated soil is an indication of the degree to which the lime-soil pozzolanic reaction has proceeded. Substantial strength increase indicates that the soil is reactive with lime and can probably be stabilized to produce a quality paving material.

Shear Strength

The triaxial test was used for evaluating shear strengths.[3] For the fine-grained soils studied (Table 1, Soils 2, 16, 27, 28), specimens cured 1, 2, 4, and 6 days at 120°F were tested in compression at various levels of confining pressure (unconsolidated and undrained type triaxial tests). Lime-soil mixtures are a cemented type material; they do not display the consolidation characteristics exhibited by typical fine-grained soils and are not usually saturated under field service conditions.

The shear strength parameters C and Ø were evaluated from the triaxial test results. The major effect of lime on the shear strength of a reactive fine-grained soil was to produce a substantial increase in cohesion with some minor increase in Ø. At the low confining pressures normally considered to exist in a flexible pavement structure, the cohesion

---

*Superscript numbers in parentheses refer to the References at the end of this paper.

**Soil numbers refer to the table on pp. 109 and 110.

increase is of the greatest signifi-
cance. For such materials as lime-soil
mixtures, which are characterized by
very high cohesion, it is difficult to
evaluate Ø effectively. Specimen-to-
specimen cohesion variation may negate
the effect of the low confining pres-
sures (< 50 psi) normally used in test-
ing highway pavement materials.

For the typical reactive Illinois
soils studied, the angle of shearing
resistance for the lime-soil mixtures
ranged from 25° to 35°, the cohesion of
the mixtures compared to natural soils
was substantially increased, and cohe-
sion continued to increase with curing
time. As indicated by Figure 1, cohe-
sion increased with unconfined compres-
sive strength. Utilizing the highly
significant linear regression equation
shown on Figure 1, we can predict cohe-
sion on the basis of unconfined compres-
sive strength results.

It is apparent that large shear
strengths can easily be developed in a
cured lime-soil mixture. If mixtures
of the quality studied were used in typ-
ical flexible pavement structures, the
strengths would be adequate to prevent
shear failure.[3]

Tensile Strength

Tensile strength properties of
lime-soil mixtures are of concern in
pavement design because of the slab ac-
tion that is afforded by a material pos-
sessing substantial tensile strength.

Two test procedures, split-tensile
and flexure, were used for evaluating
lime-soil mixture tensile strength.

(a) The split-tensile test is es-
sentially a diametral compression test
for brittle materials in which the ma-
terials fail in tension along the load-
ed diameter of the cylindrical test
specimen. Details and an evaluation
of the test procedure for lime-soil mix-
tures are presented in Reference 4.

Eleven selected lime-reactive Ill-
inois soils (Table 1, Soils 2, 6, 8, 9,
17, 18, 24, 25, 26, 27, 32) were stud-
ied. The split-tensile strengths of
2-in. diameter by 4-in. specimens dis-
played large variation depending on the
lime-soil mixture and curing period.
Typical results, shown in Figure 2, in-
dicate that the mixtures do possess
substantial tensile strength. The ra-
tio of split-tensile strength to uncon-
fined compressive strength of the mix-
tures was approximately 0.13 for all
of the mixtures studied.

(b) The flexure test is the most
common method used for evaluating the
tensile strength of highway materials.
Preliminary laboratory studies indicat-
ed that testing 2 x 2 x 7-in. beam
specimens under third-point loading
conditions (0.05 in./min strain rate)
was a satisfactory procedure for evalu-
ating fine-grained lime-soil mixtures.
Typical lime-soil mixture flexural
strengths for various curing conditions
are shown in Table 2; split-tensile
strengths are included for comparison
purposes.[5,6] For any specific mix-
ture, the ratio of the flexural strength
to split-tensile strength decreases as
strength increases, but the ratio is
apparently not the same for all lime-
soil mixtures.

Split-tensile strength is 13 per-
cent of unconfined. Thus, if the ratio
of flexural to split-tensile strength is
taken as approximately 2, a realistic

estimate of flexural strength is 25 percent of the unconfined strength. This ratio is approximately equivalent to those reported for lime-flyash-aggregate and soil-cement mixtures.

California Bearing Ratio (CBR)

CBR tests were conducted with various representative Illinois soils, including soils that reacted well with lime, as well as less reactive, fine-grained soils.[6] The testing procedures recommended by ASTM D1883-61T were used.

Lime-treated soils were cured for 48 hrs at 120°F. Companion specimens which had not been cured were placed in the 96-hr soaking cycle immediately after compaction. The 48-hr curing period is approximately equivalent to 30 days at 70°F and the mixtures that were not cured prior to soaking had little opportunity to develop cementitious products from the lime-soil pozzolanic reaction. The improvements in engineering properties of the non-cured lime-soil mixtures were therefore primarily due to the cation exchange, flocculation, and agglomeration effected by the lime addition. Test results for the natural soils and the lime-soil mixtures are presented in Table 3.

The CBR increases of the non-cured lime-soil mixtures show the benefits that can be obtained from stabilization without prolonged curing. It is apparent that the non-cured specimens have not developed extensive cementing action.

The CBR values for many of the lime-soil mixtures cured for 48 hrs at 120°F are quite large and definitely indicate the extensive development of cementing agents. For those mixtures that display CBR values of 100 or more,

the test result apparently has little practical significance since the cemented nature of these lime-soil mixtures precludes the use of the CBR as a meaningful measure of strength or stability. In general, these materials would also score high in compressive and tensile strength; and the tests for those qualities might provide a better strength evaluation. If extensive cementing action has not developed, whether from lack of curing time or the non-reactivity of the treated soil, CBR values may possess practical significance as a general measure of strength.

Swell values for the non-cured and cured lime-soil mixtures were substantially reduced relative to the natural soils. The maximum swell for the natural soils was 8.8 percent but the largest swell value for the cured lime-soil mixtures was 0.1 percent. Reduced swell characteristics of lime-soil mixtures are generally attributed to decreased water affinity of a calcium-saturated clay and the formation of a cementitious matrix which can resist volumetric expansion.

It is evident that lime treatment of fine-grained soils produces reduced swell and increased CBR, irrespective of the length of curing (essential for developing cementing agents) and lime-reactivity of the soil.

Fatigue Strength

For typical highway pavement loading conditions, the flexural strength, not the shear strength, of reactive lime-soil mixtures will probably be the limiting factor in their application as subbase and base courses.[3] Therefore flexural fatigue is an important consideration in the evaluation of lime-soil

mixtures.

The general flexural fatigue response of four selected lime-soil mixtures (Table 1, Soils 2, 27, 28, 37) was evaluated.[5] The 2 x 2 x 7-in. beam specimens were cured varying periods (24 hrs for Soils 2, 28, and 37, and 48 hrs for Soil 27) at 120°F to produce flexural strengths approximately equivalent to those obtained from 30-day field-curing under normal conditions. The cured beams were subjected to repeated flexural stresses (minimum stress of 10 percent of ultimate, maximum stress varied for different specimens) until failure occurred. Fatigue response curves for the mixtures are shown in Figure 3, where S = stress level expressed as a fraction of ultimate flexural strength and Log N = stress repetitions to failure.

The response curves are typical of fatigue in general and are much like the curves normally obtained for similar materials (with regard to the nature of the cementitious products), such as lime-flyash-aggregate mixtures and concrete. At 5 million stress repetitions, the fatigue strengths of the lime-soil mixtures varied from 41 to 66 percent of the ultimate flexural strength, with an average of 54 percent.

Testing Variability

Testing errors associated with repeat-strength determinations of identical lime-soil mixture specimens were determined. The standard deviations for unconfined compression, split-tensile, and flexural strengths increased with average mixture strength. Average coefficients of variation ($\frac{\text{standard deviation}}{\text{average strength}}$ 100) were

(a) unconfined compressive strength, 10.6 percent,

(b) split-tensile strength, 12.4 percent, and

(c) flexural strength, 10.9 percent. In general, the testing errors were approximately of the same magnitude for the different testing procedures studied.

Factors contributing to testing error include:

(a) heterogenous nature of soils,

(b) non-uniformity of mixtures;

(c) slight deviations in sample preparation and testing techniques,

(d) small variations in curing temperature and time, and

(e) density variations.

The influence of density variations is illustrated in Figure 4 for four separate lime-soil mixtures (Table 1, Soils 2, 27, 28, 37). Density control is obviously an important influence on strength and small density variations will be reflected in a scattering of test results.

STRESS-STRAIN PROPERTIES

A knowledge of stress-strain properties is essential for proper analysis of the behavioral characteristics of a pavement structure containing a lime-soil mixture structural layer. The marked effect of lime on the compressive stress-strain properties of fine-grained soils has already been demonstrated. As shown by Figure 5, the failure stress is increased and the ultimate strain is decreased when lime is mixed with natural soil.

Modulus of Elasticity

As a result of an extensive study of four representative Illinois soils

(Table 1, Soils 2, 16, 27, 28) stabil-
ized with lime, it was possible to de-
velop a generalized compressive stress-
strain relation for cured lime-soil mix-
tures (see Figure 6).[3] The mixtures
studied appeared to be strain-susceptible
and the ultimate strain (for maximum
compressive stress) was approximately
1 percent, regardless of the soil type
or curing period. It was demonstrated
that the compressive modulus of elas-
ticity (for 15 psi confining pressure)
could be estimated from the unconfined
compressive strength of the lime-soil
mixture according to the following re-
lation:

E(ksi) = 9.98 + .124 unconfined
compressive strength (psi).

It is important to note that the
study in question utilized the average
compressive strains, based on the total
deformation of the specimen, for evalu-
ating E.

As suggested in Reference 3, for
lime-soil pavement layers possessing
high shear strength, the flexural stres-
ses in the lime-soil mixture may be the
controlling design factor. In view of
this, it seemed desirable to evaluate
flexural moduli of elasticity for typi-
cal cured lime-soil mixtures.[6]

Four highly reactive Illinois soils
(Table 1, Soils 2, 16, 27, 37) were sta-
bilized with lime and the beam specimens
were cured for 48 and 96 hrs at 120°F.
After curing, Baldwin SR-4 Type A-1
strain gauges were attached to the mid-
portion of the beams. The 2 x 2 x 2-in.
beams were tested under third-point
loading conditions, providing a constant
moment region in the 2-in. mid-span seg-
ment containing the strain gauges. As
the beams were statically loaded in in-

crements, top and bottom beam strains
were measured with a strain indicator.
Based on the strain measurements, beam
curvature, $\emptyset$, was determined as follows:

$$\emptyset = \frac{\varepsilon_{top} + \varepsilon_{bottom}}{d}, \text{ where}$$

ε_{top}, ε_{bottom} = measured strains
on top and bottom of the beam, and

d = depth of beam (2 in. for spec-
imens tested).

Moment-curvature plots for the beams
were prepared (Figure 7) and the slope
of the secant at 50 percent of ultimate
moment was evaluated. Utilizing the
relation

$$E = \frac{M}{I\emptyset}, \text{ where}$$

E = modulus of elasticity,

M = moment,

I = moment of inertia of beam
cross section,
the modulus of elasticity in flexure
was calculated.

Test results (average of two spec-
imens) are shown in Figure 8. The trend
of increasing flexural modulus with in-
creased curing and flexural strength
is apparent. For the range of data
considered, the highly significant (α
= 0.01) regression equation shown in
Figure 8 can be used to estimate the
flexural modulus of elasticity. The
flexural moduli appear to be substan-
tially larger than compressive moduli
for the same mixture. Similar static-
loading behavior has been noted in soil
cement studies.

Poisson's Ratio $\left(\dfrac{\text{lateral strain}}{\text{axial strain}}\right)$

Poisson's ratio was determined as
follows for four lime-soil mixtures
(Table 1, Soils 2, 16, 27, 3).[6]

The 2-in. diameter by 4-in. speci-

mens were cured 48 and 96 hrs at 120°F. After curing, four SR-4 Type A-1 strain gauges were mounted at mid-height on the specimens (two vertical, two lateral). The specimens were loaded statically in increments and corresponding vertical and lateral strains were measured with a strain indicator. Poisson's ratio ($\frac{\text{lateral strain}}{\text{axial strain}}$) was then calculated for various stress levels.

Values at low stress levels (less than 25 percent of ultimate compressive strength) ranged from 0.08 to 0.12, with an average of 0.11. These values are in agreement with those previously reported for rock, lime-flyash-aggregate mixtures, and soil cement. At higher stress levels (greater than 50-75 percent of ultimate compressive strength), Poisson's ratio increased, ranging from 0.27 to 0.37, with an average of 0.31. Similar behavior has been noted for lime-flyash-aggregate mixtures. In Figure 9, a typical plot shows the influence of stress level, expressed as a percent of ultimate compressive strength, on Poisson's ratio for lime-soil mixtures.

FREEZE-THAW DURABILITY

The resistance of four typical lime-soil mixtures (Table 1, Soils 2, 27, 28, 37) to cyclic freeze-thaw was evaluated in an extensive study.[7] Specimens cured for 48 or 96 hrs at 120°F were subjected to 12 freeze-thaw cycles (modified British test). Length change and compressive strength were determined at 0, 3, 6, 9, and 12 cycles.

Typical linear regression relations displaying the influence of freeze-thaw cycles on length change and compressive

strength are shown in Figures 10 and 11. The interrelation between length changes and compressive strength decreases is illustrated in Figure 12. The validity of using initial unconfined compressive strength (0 cycles) as a measure of freeze-thaw resistance is demonstrated in Figure 13.

Average rates of strength decrease for the mixtures studied were 9 psi/cycle and 18 psi/cycle for 48- and 96-hr curing respectively.

A recent study has shown that some lime-soil mixtures display autogenous healing properties.[8] If the stabilized soil has the ability to regain strength or "heal" with time, the distress produced during winter freeze-thaw cycles will not be cumulative, since autogenous healing during favorable curing conditions would serve to restore the stability of the material. This phenomenon is illustrated in Figure 14.

Durable lime-soil mixtures can be obtained when reactive soils are stabilized with quality lime. Testing systems developed in another study display substantial merit for evaluating lime-soil mixture freeze-thaw durability.[7]

SHRINKAGE CHARACTERISTICS

Past experience with stabilized materials, such as soil cement and lime-flyash mixtures, has indicated that moisture-induced shrinkage cracking problems may develop.

Moisture-related shrinkage and swell properties were evaluated for four typical lime-soil mixtures.[9] Beam type specimens (2 x 2 x 4-in.) for length change measurements and 2-in.

diameter x 4-in. strength specimens were used in the study. Shrinkage was induced by drying at 120°F and swelling was effected by subjecting the materials to a high humidity environment, then completely immersing them in water. Periodic measurements of shrink and swell were made and initial and final split-tensile strengths were determined.

Average shrink and swell values and strengths are presented in Table 4. First-cycle shrinkage curves for the natural soils are given in Figure 15 and a typical continuous shrinkage and swell curve is shown in Figure 16. A maximum linear shrinkage and swell curve for a typical mixture is presented in Figure 17.

The addition of lime to the soils studied improved shrinkage and swell resistance. First-cycle shrinkage was substantially reduced and strength properties were improved. In general, cyclic shrinkage and swell remained within tolerable limits (less than 0.3 percent except for Sable B mixture). The magnitude of shrinkage and swell and the strength loss associated with shrink-swell cycles appeared to be related to natural soil properties. Mixtures with higher clay content and higher plasticity soils generally displayed greater shrinkage and swell (Figure 18). Longer curing seemed to decrease the first-cycle shrinkage and subsequent shrinkage and swell for all the mixtures.

Theoretical calculations, based on the shrinkage data obtained, strength data, and assumed values for modulus of elasticity, indicated that for typical field service conditions cracking would not be extensive. Theoretical transverse crack spacings generally were in excess of 40 ft, even for low strength mixtures.

The findings from this study appear to confirm those of other investigators. In general, shrinkage cracking does not seem to be a significant problem with lime-soil mixtures. Periodic investigations of the lime-stabilized test road in Randolph County, Illinois, during the last seven years have shown no evidence of shrinkage cracks in the treated base.[10] Similar results have been noted in many areas where lime-soil mixtures are extensively utilized.

Problems concerning cracking in lime-soil mixtures are complicated by the fact that cracking may be caused by reasons other than shrinkage. Therefore, it is important when evaluating these materials in the field to differentiate between shrinkage cracks and cracks caused by subgrade volume changes, inadequate depth design, and overloading before the mixture has attained its design strength.

SERVICE CONDITIONS

Utilizing data concerning the engineering properties of typical lime-soil mixtures, it was possible to analyze, on a theoretical basis, the probable field performance of pavements containing lime-soil layers. Such factors as vertical subgrade stress, flexural stresses in the stabilized layer, total pavement deflection, load-deflection behavior, and ultimate load-carrying capacity were evaluated for typical lime-soil mixtures and variable subgrade support conditions. The limited data in the literature concerning the field performance of the lime-soil mixtures were also included in the analysis.

The comprehensive analysis of field service conditions definitely showed that lime-soil mixtures can be utilized as component layers of the pavement structure.[11] The position of the lime-treated soil layer in the pavement structure (modified subgrade-subbase-base) depends on its quality, which can be approximated by compressive strength.

Based on the theoretical analysis, available field performance records, and criteria currently being used by other agencies, minimum compressive strength criteria were established for various lime-soil mixture usages. The concept of "residual strength" of the lime-soil mixture--strength after the first winter of cyclic freezing and the thawing and/or extended soaking period-- was utilized. The minimum strength requirements developed are presented in Table 5. It is emphasized that the requirements are minimum quality requirements and are not to be used as design strengths. The design strength must be determined from an evaluation of the specific lime-soil mixture being considered.

MIXTURE DESIGN PROCESS

The main objectives of the lime-soil mixture design are (a) to establish an appropriate lime content for construction and (b) to evaluate the properties of the design mixture.

Utilizing data and techniques previously developed for the mixture, we established design procedure.[12] The design process recognizes the distinction between those soils that react with lime to produce a substantial strength increase and those soils that do not re-

act to produce high strength material. Mixture design procedures and details of the test methods are presented in Reference 11.

SUMMARY

The treatment of fine-grained soils with lime, approximately three to seven percent by dry weight of soil basis, effects many significant engineering property changes. Typically:

(a) strength and modulus of elasticity are increased,

(b) plasticity, shrinkage, and swell are reduced,

(c) workability is improved and,

(d) durable mixtures are obtained.

Typical engineering properties for lime-treated soils have been presented in this report.

In many instances, when reactive soils are stabilized with quality lime, the cured lime-soil mixtures are adequate for use as subbase or base course material for certain types of pavement construction. In other situations, the lime treatment may be used primarily for subgrade modification or to expedite construction operations.

REFERENCES

1. Thompson, Marshall R., "Lime-Reactivity of Illinois Soils," Journal of the Soil Mechanics and Foundations Division, American Society of Civil Engineers, Vol. 92, No. SM5, September, 1966.

2. Thompson, M. R., Factors Influencing the Plasticity and Strength of Lime-Soil Mixtures, Engineering Experiment Station Bulletin No. 492, University of Illinois, Urbana, 1967.

3. Thompson, Marshall R., "Shear Strength and Elastic Properties of Lime-Soil Mixtures," Highway Research Board Record No. 139, 1966.

108

4. Thompson, Marshall R., "The Split-Tensile Strength of Lime-Stabilized Soils," Highway Research Board Record No. 92, 1965.

5. Swanson, T. E., and Thompson, M. R., "Flexural Fatigue Strength of Lime-Soil Mixtures," Highway Research Board Record No. 198, 1967.

6. Thompson, M. R., "Engineering Properties of Lime-Soil Mixtures," ASTM, publication pending, 1967.

7. Dempsey, B. J. and Thompson, M. R., "Durability Properties of Lime-Soil Mixtures," Highway Research Board Record No. 235, 1968.

8. Thompson, M. R. and Dempsey, B. J., "Autogenous Healing of Lime-Soil Mixtures," Highway Research Board Record No. 263, 1969.

9. Dempsey, B. J. and Thompson, M. R., "Shrinkage and Swell Properties of Lime-Soil Mixtures," Civil Engineering Studies, Highway Engineering Series No. 29, Illinois Cooperative Highway Research Program, Series No. 94, University of Illinois, Urbana, April, 1969.

10. Thompson, M. R. and Hollon, G. W., "A Lime Stabilized Test Road in Randolph County, Illinois," Civil Engineering Studies, Highway Engineering Series No. 10, Illinois Cooperative Highway Research Program, Series No. 10, August, 1962.

11. Thompson, M. R., "Lime Treated Soils for Pavement Construction," Journal of the Highway Division, American Society of Civil Engineers, Vol. 94, No. HW2, November, 1968.

12. Thompson, M. R., "Mixture Design for Lime-Treated Soils," Civil Engineering Studies, Highway Engineering Series No. 26, Illinois Cooperative Highway Research Program, Series No. 94, University of Illinois, Urbana, January, 1969.

Pg. 109 IS BLANK

TABLE 1.

NATURAL SOIL PROPERTIES.

Soil Reference Number	Soil Type	Horizon	Class Drainage	AASHO Class	< 2μ Clay, %	Liquid Limit, %	Plasticity Index, %	pH	Organic Carbon, %	Base Saturation, %	Ca/Mg Ratio	Carbonates	Cation-Exchange Capacity, meq/100 gms	Exchangeable Cations (meq/100 gms) Ca	Mg	Mn	K	Quartz, %	Illite, %	Chlorite, %	Kaolinite, %	Montmorillonite, %	Mixed Layer, %
1	Bryce Silty Clay	A	Poor	A-7-5 (17)	40	57.9	24.2	6.9	3.69	100	2.9	R*	35.1	26.18	9.13	0.94	0.49	20	40	20	Trace	Trace	20
2	Bryce Silty Clay	B	Poor	A-7-6 (18)	52	53.1	28.8	7.4	0.86	98	1.8	NC	29.15	18.06	10.23	0.44	0.37	5	45	25	Trace	0	25
3	Clare Silt Loam	B	Poor	A-7-6 (20)	39	58.6	38.8	5.5	0.38	82	1.3	NC	21.43	3.63	2.70	0.85	0.30	35	15	0	15	0	35
4	Wisconsinan Clay Till	-	--	A-7-6 (17)	65	49.3	26.9	8.2	0.74	100	3.1	C**(8.6%)	16.88	41.37	13.48	0.66	0.43	8	60	32	0	0	0
5	Cowden Silt Loam	A	Poor	A-4 (8)	19	33.4	7.7	6.3	1.42	83	1.1	NC	15.3	11.25	1.01	0.27	0.19	30	10	Trace	10	65	50
6	Cowden Silt Loam	B	Poor	A-7-6 (19)	38	54.0	32.5	6.0	0.43	92	1.6	NC	24.3	12.7	7.7	1.99	0.31	5	20	10	5	0	Trace
7	Cowden Silt Loam	C₁	Poor	A-6 (10)	30	34.2	15.2	7.9	0.19	100	1.7	NC	15.8	8.05	4.8	3.33	0.24	20	20	10	0	96	45
8	Cowden Silt Loam	B	Poor	A-7-6 (19)	34	53.4	31.4	5.5	0.43	94	1.1	NC	25.08	11.91	11.32	1.03	0.38	13	0	31	0	71	0
9	Cowden Silt Loam	C	Poor	A-6 (9)	20	32.4	12.6	7.0	0.13	100	1.3	NC	14.78	8.57	6.82	1.19	0.29	16	13	0	0	0	0
10	Drummer Silty Clay Loam	A	Poor	A-7-6 (14)	30	49.6	20.6	7.0	3.93	100	2.9	NC	34.0	26.18	9.0	0.23	0.48	15	25	10	0	Trace	50
11	Drummer Silty Clay Loam	B	Poor	A-7-6 (19)	34	54.4	30.8	7.4	0.57	100	1.9	NC	21.6	17.77	9.44	0.44	0.35	15	20	10	0	55	Trace
12	Elliott Silt Loam	A	Poor	A-7-5 (12)	29	45.6	17.5	6.3	3.43	91	3.7	NC	23.25	15.9	4.25	0.28	0.67	25	30	10	5	Trace	30
13	Elliott Silt Loam	B	Moderately well to imperfect	A-7-6 (18)	52	52.6	28.4	6.2	0.82	85	1.3	NC	22.15	10.61	8.29	0.32	0.50	10	40	Trace	15	35	Trace
14	Fayette Silt Loam	A	Moderately well to imperfect	A-7-5 (9)	19	41.4	11.2	6.7	2.40	100	3.4	NC	18.45	14.2	4.23	0.14	0.36	5	25	10	Trace	60	Trace
15	Fayette Silt Loam	B	Well	A-7-5 (17)	32	49.9	28.6	6.0	0.49	89	1.2	NC	19.28	9.33	7.98	0.23	0.24	5	10	5	Trace	80	Trace
16	Fayette Silt Loam	C	Well	A-6 (8)	21	31.9	10.1	7.8	0.14	100	5.3	C (20%)	11.53	22.2	4.2	0.33	0.24	Trace	30	10	Trace	60	Trace
17	Accretion Clay fl	-	--	A-6 (12)	26	35.9	21.9	7.4	0.15	100	.9	NC	14.01	6.64	7.65	0.56	0.33	Trace	0	5	Trace	0	95
18	Accretion Clay fe	-	--	A-6 (10)	25	32.5	14.2	6.9	0.86	100	1.0	NC	15.11	7.59	7.47	0.54	0.23	5	0	10	Trace	0	85
19	Homer Silt Loam	A	Well to Moderately Well	A-4 (8)	16	26.1	1.9	5.2	0.80	90	3.5	NC	8.20	2.76	0.78	0.33	0.80	30	15	15	Trace	0	90

*Carbonaceous
**Calcareous

TABLE 1.

NATURAL SOIL PROPERTIES. (Continued)

Soil Reference Number	Soil Type	Horizon	Drainage Class	AASHO Class	< 2μ Clay, %	Liquid Limit, %	Plasticity Index, %	pH	Organic Carbon, %	Base Saturation, %	Ca/Mg Ratio	Carbonates	Cation-Exchange Capacity, meq/100 gms	Exchangeable Cations (meq/100 gms) Ca	Mg	Na	K	Clay Mineralogy (< 2μ) Quartz, %	Illite, %	Chlorite, %	Kaolinite, %	Montmorillonite, %	Mixed Layer, %
20	Homer Silt Loam	B₂	Well to Moderately Well	A-7-6 (11)	25	41.4	17.4	4.7	0.17	62	1.2	NC	17.65	5.93	4.87	0.23	0.37	Trace	25	10	Trace	0	65
21	Homer Silt Loam	B₂	Well to Moderately Well	A-7-6 (13)	29	44.5	20.4	4.4	0.12	98	1.0	NC	21 15	5.98	5.87	0.55	0.47	Trace	25	10	Trace	65	Trace
22	Huey Silt Loam	B	Imperfect	A-7-6 (17)	31	46.3	28.9	9.0	0.17	100	2.3	NC	16.40	10.55	4.62	4.63	0.32	35	0	0	10	55	0
23	Huey Silt Loam	D	Imperfect	A-6 (15)	27	38.6	26.4	8.5	0.10	100	2.1	NC	13.84	8.92	4.32	3.45	0.28	35	0	0	10	55	0
24	Accretion Gley #3	-	--	A-6 (7)	18	33.7	18.4	7.6	0.11	100	1.6	NC	15.23	9.66	5.89	0.78	0.16	5	0	10	Trace	85	Trace
25	Illinoian Till	-	--	A-6 (6)	17	24.6	11.7	8.2	0.46	100	12.7	C (13.5%)	5.56	37.96	2.98	0.20	0.28	Trace	45	15	10	0	30
26	Illinoian B Horizon	-	--	A-6 (11)	29	37.2	19.2	6.8	0.11	100	1.4	NC	16.17	9.78	7.25	0.27	0.28	5	20	5	5	0	70
27	Illinoian Till	-	--	A-6 (6)	14	25.5	11.0	8.2	0.10	100	5.4	C (18.6%)	6.21	17.54	3.22	0.14	0.20	Trace	80	10	Trace	0	10
28	Wisconsian Loam Till	-	--	A-4	18	24.5	7.8	8.3	0.21	100	6.0	C (13.8%)	5.90	26.69	4.43	0.33	0.19	19	59	22	0	Trace	20
29	Miami Silt Loam	A	Well	A-4 (8)	11	26.0	NP*	6.8	1.77	100	3.2	NC	11.5	9.22	2.92	0.18	0.26	30	25	15	10	Trace	55
30	Miami Silt Loam	B	Well	A-6 (9)	26	27.7	11.3	4.6	0.56	46	1.2	NC	12.58	3.19	2.74	0.17	0.23	30	30	0	5	Trace	20
31	Miami Silt Loam	C	Well	A-6 (9)	23	28.7	14.3	7.9	0.38	100	10.2	C (14.1%)	11.35	25.25	2.48	0.40	0.30	10	90	15	5	0	0
32	Ottawa A-6	-	--	.6 (8)	25	25.2	10.8	8.3	0.53	100	1.2	C (27.4%)	13.10	7.77	6.38	0.40	0.22	5	80	15	0	0	0
33	Calcareous Peorian Loess	-	--	A-4 (8)	7	28.5	3.0	8.0	0.25	100	2.0	C (15.0%)	6.48	11.99	5.88	0.60	0.22	Trace	15	10	Trace	0	Trace
34	Leached Peorian Loess	-	--	A-4 (8)	11	29.5	3.9	6.7	0.17	100	1.6	NC	9.34	5.87	3.76	0.24	0.18	Trace	15	10	5	75	Trace
35	Plano Silt Loam	A	Poor	A-6 (10)	29	36.1	14.8	7.4	1.57	100	8.3	NC	19.03	21.45	2.6	0.66	0.25	15	25	10	5	75	45
36	Plano Silt Loam	B	Poor	A-7-6 (19)	40	54.5	35.7	8.2	0.36	100	2.0	NC	25.73	16.4	8.85	3.85	0.38	10	20	10	5	55	Trace
37	Sable Silty Clay Loam	B	Poor	A-7-6 (16)	36	50.7	23.5	7.8	0.47	100	1.8	NC	28.19	16.88	9.24	0.33	0.36	35	10	0	10	0	45
38	Tama Silt Loam	A	Well to Moderately Well	A-7-5 (20)	31	62.6	33.7	5.9	3.60	79	4.5	NC	32.7	20.2	4.53	0.29	0.67	15	25	5	5	75	90
39	Tama Silt Loam	B	Well to Moderately Well	A-7-6 (20)	39	62.6	33.7	5.7	0.90	88	2.1	NC	27.18	14.98	7.1	0.18	0.46	5	10	10	Trace	75	Trace

*Non-plastic

TABLE 2.

TENSILE STRENGTH PROPERTIES OF LIME-SOIL MIXTURES.

Soil No.	Soil	% Lime	Curing Hours @ 120F	Flexural Strength psi (σ_F)	Split Tensile Strength, psi (σ_T)	Ratio
2	Bryce B	5	24	92	42	2
			48	105	53	2
			96	122	88	1
	Champaign County Till	3	48	69	(a)	-
			96	93	(a)	-
16	Fayette C	5	24	66	46	1
			96	166	126	1
27	Illinoian Till, Sangamon County	3	24	86	35	2
			48	164	92	1
			96	202	106	1
37	Sable B	3	48	63	(a)	-
			96	77	(a)	-
28	Wisconsinan Loam Till	3	24	83	35	2
			48	140	63	2
			96	157	78	2

a - Test not conducted.

TABLE 3.

CBR VALUES FOR SELECTED SOILS AND LIME-SOIL MIXTURES.

| | | Natural Soil | | | Lime-Soil Mixtures | | | |
| | | | | | No Curing[b] | | 48 Hrs. Curing @ 120F | |
Soil No.[a]	Soil	CBR,%	Swell,%	% Lime	CBR,%	Swell,%	CBR,%	Swell,%
	Good Reacting Soils							
18	Accretion Gley 2	2.6	2.1	5	15.1	0.1	351.0	0.0
24	Accretion Gley 3	3.1	1.4	5	88.1	0.0	370.0	0.1
2	Bryce B	1.4	5.6	3	20.3	0.2	197.0	0.0
5	Champaign Co. Till	6.8	0.2	3	10.4	0.5	85.0	0.1
3	Cisne B	2.1	0.1	5	14.5	0.1	150.0	0.1
6	Cowden B	7.2	1.4	3	--	---	98.5	0.0
8	Cowden B	4.0	2.9	5	13.9	0.1	116.0	0.1
9	Cowden C	4.5	0.8	3	27.4	0.0	243.0	0.0
	Darwin B	1.1	8.8	5	7.7	1.9	13.6	0.1
	East St. Louis Clay	1.3	7.4	5	5.6	2.0	17.3	0.1
16	Fayette C	1.3	0.0	5	32.4	0.0	295.0	0.1
26	Illinoian B	1.5	1.8	3	29.0	0.0	274.0	0.0
27	Illinoian Till	11.8	0.3	3	24.2	0.1	193.0	0.0
25	Illinoian Till	5.9	0.3	3	18.0	0.9	213.0	0.1
37	Sable B	1.8	4.2	3	15.9	0.2	127.0	0.0
Non-Reactive Soils								
15	Fayette B	4.3	1.1	3	10.5	0.0	39.0	0.0
30	Miami B	2.9	0.8	3	12.7	0.0	14.5	0.0
39	Tama B	2.6	2.0	3	4.5	0.2	9.9	0.1

a) See Table 1.

b) Specimens were placed in 96 hour soak immediately after compaction.

TABLE 4.

SHRINKAGE AND SWELL DATA.

Soil Type	First Cycle Shrinkage of Natural Soil (%)	Curing Time (hours)[a]	Shrink-Swell Cycle	Lime-Soil Mixtures		Split Tensile Strength (psi)[c]		Split Tensile Strength Loss Per Shrink-Swell Cycle (psi/cycle)
				Per Cent Length Change (%)[b]				
				Shrinkage	Swell	Initial[d]	Final	
Illinoian Till (Sangamon County)	-0.28	48	1 2 3 4	-0.26 -0.28 -0.24 -0.24	-0.15 -0.17 -0.16 -0.18	68.2	56.4	3.0
		96	1 2 3 4	-0.20 -0.20 -0.19 -0.20	-0.12 -0.13 -0.13 -0.13	69.8	59.2	2.6
Champaign County Till	-0.44	48	1 2 3 4	-0.12 -0.10 -0.08 -0.06	+0.22 +0.12 +0.11 +0.08	21.6	5.7	4.0
		96	1 2 3 4	-0.08 -0.08 -0.05 -0.03	+0.19 +0.10 +0.10 +0.12	26.2	7.6	4.6
Bryce B	-2.37	48	1 2 3 4	-1.12 -0.97 ---- ----	-0.29 -0.48 ---- ----	59.4	22.4	18.5
		96	1 2 3 4	-0.57 -0.45 ---- ----	+0.18 +0.28 ---- ----	53.7	17.0	18.4
Sable B	-1.61	48	1 2 3 4	-1.12 ---- ---- ----	+0.46 ---- ---- ----	42.6	Disintegrated	42.6
		96	1 2 3 4	-0.70 ---- ---- ----	+0.79 ---- ---- ----	33.8	Disintegrated	33.8

a: Cured at 120F.

b: Per cent length change is computed as the measured length change times 100 divided by the initial specimen height at the end of the curing period (average of 4 specimens).

c: Specimens tested at a constant deformation rate of 0.05 in./min. (average of 4 specimens).

d: Initial split tensile strength specimens were soaked for 24 hours in demineralized water at $72 \pm 4F$ before testing.

TABLE 5.

TENTATIVE LIME-SOIL MIXTURE COMPRESSIVE STRENGTH REQUIREMENTS.

Anticipated Use	Residual Strength Requirement, psi (a)	Strength Requirements for Various Anticipated Service Conditions (b)			
		Extended (8 day) Soaking (psi)	Cyclic Freeze-Thaw (e)		
			3 Cycles (psi)	7 Cycles (psi)	10 Cycles (psi)
Modified Subgrade	20	50	50	90 50*	120
Subbase					
Rigid Pavement	20	50	50	90 50*	120
Flexible Pavement					
Thickness of Cover (c)					
10 inches	30	60	60	100 60*	130
8 inches	40	70	70	110 75*	140
5 inches	60	90	90	130 100*	160
Base	100(d)	130	130	170 150*	200

a) Minimum anticipated strength following first winter exposure.

b) Strength required at termination of field curing (following construction) to provide adequate residual strength.

c) Total pavement thickness overlying the subbase. The requirements are based on the Boussinesq stress distribution. Rigid pavement requirements apply if cemented materials are used as base courses.

d) Flexural strength should be considered in thickness design.

e) Number of freeze-thaw cycles expected in the lime-soil layer during the first winter of service.

*Note: Freeze-thaw strength losses based on 10 psi/cycle except for 7 cycle values indicated by an * which were based on a previously established regression equation.
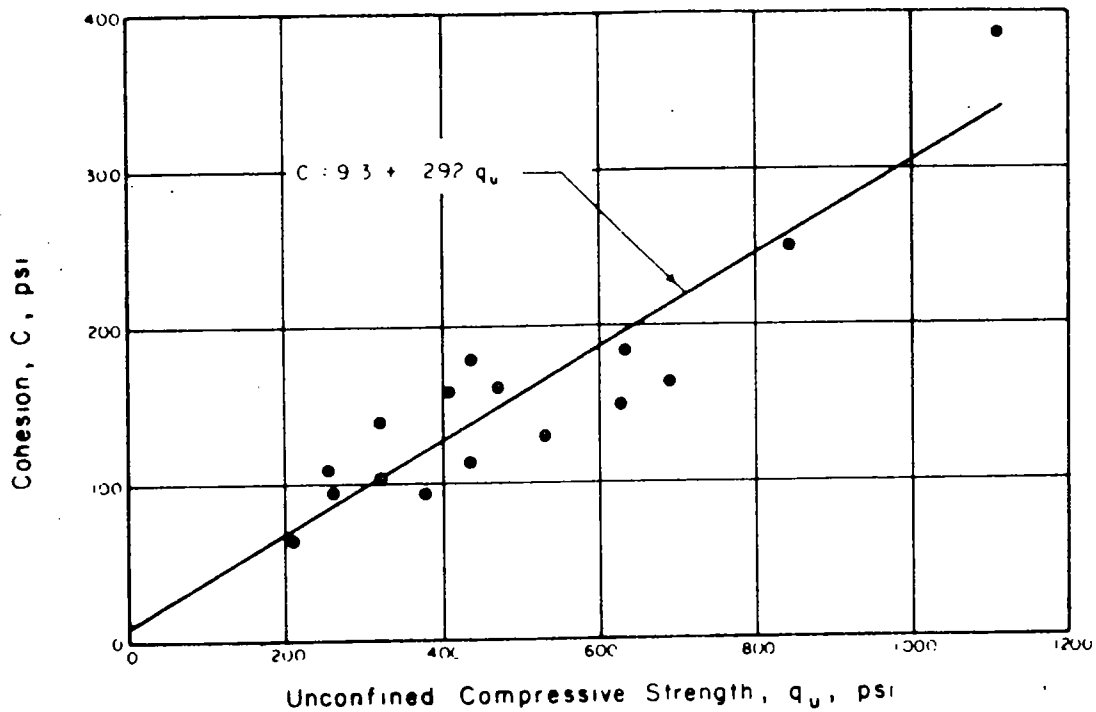
FIGURE 1. COHESION VS UNCONFINED COMPRESSIVE STRENGTH OF LIME-SOIL MIXTURES.
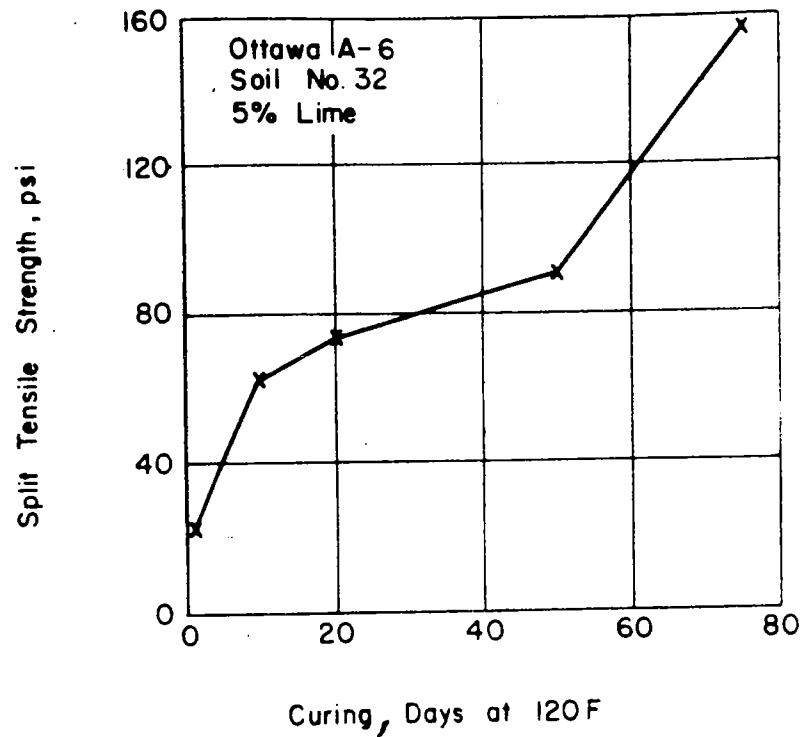
FIGURE 2. SPLIT-TENSILE STRENGTH OF A CURED LIME-SOIL MIXTURE.
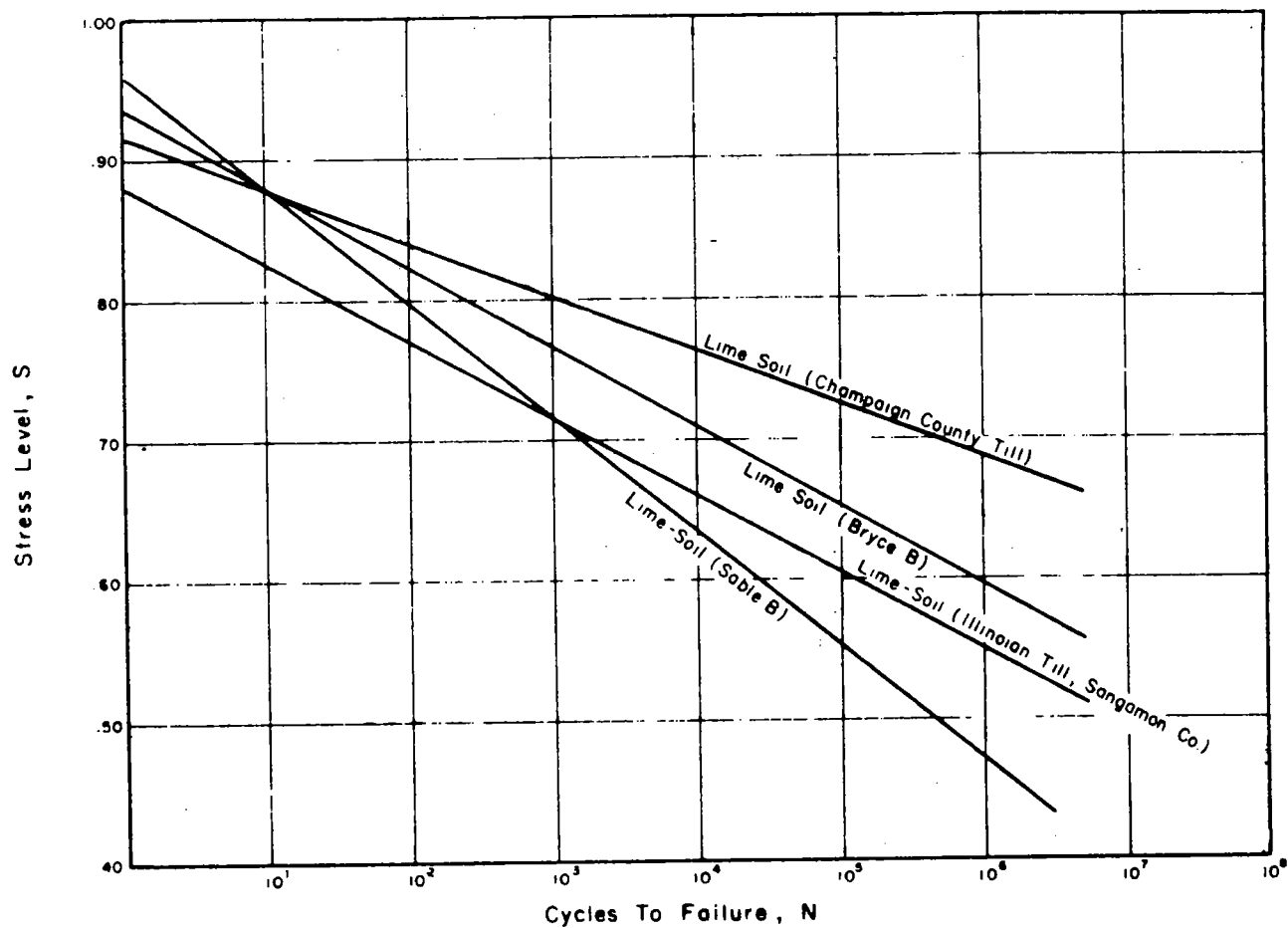
FIGURE 3.   FLEXURAL FATIGUE RESPONSE CURVES.
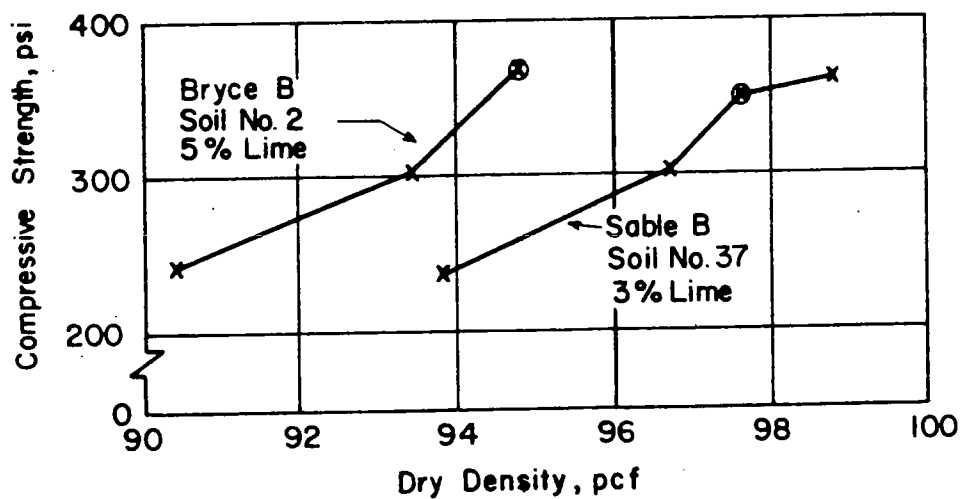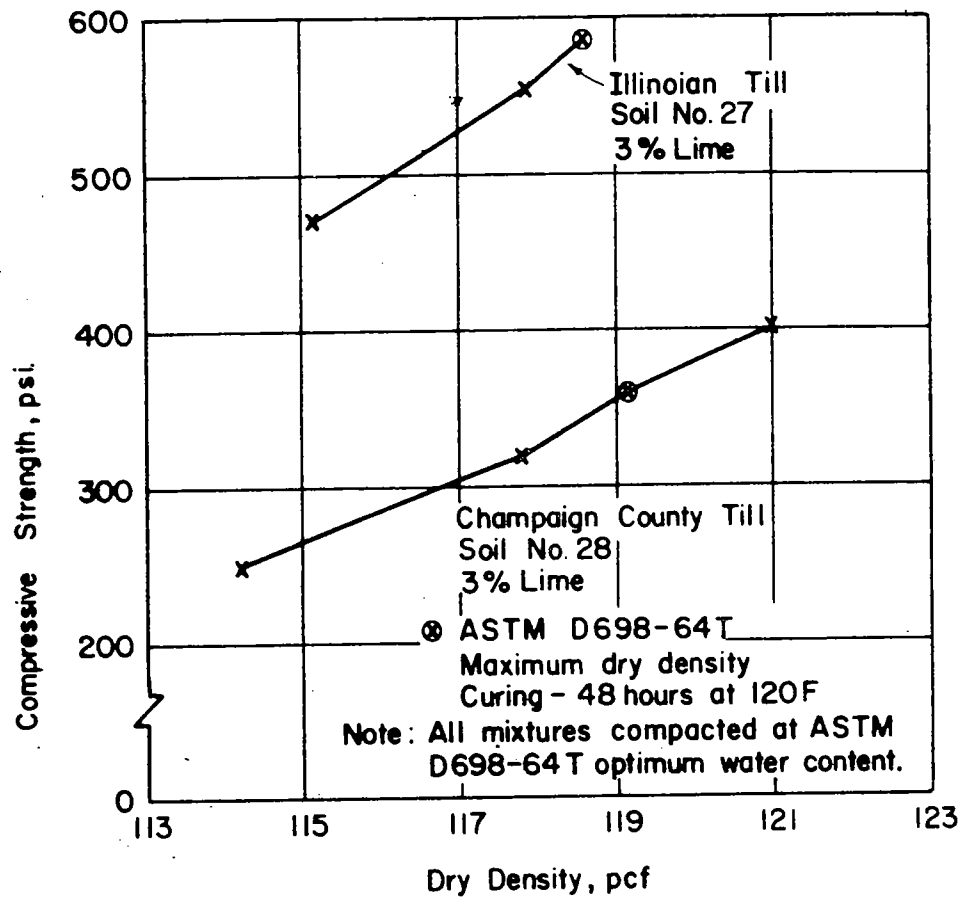
FIGURE 4. INFLUENCE OF DENSITY ON THE
STRENGTH OF CURED LIME-SOIL MIXTURES.
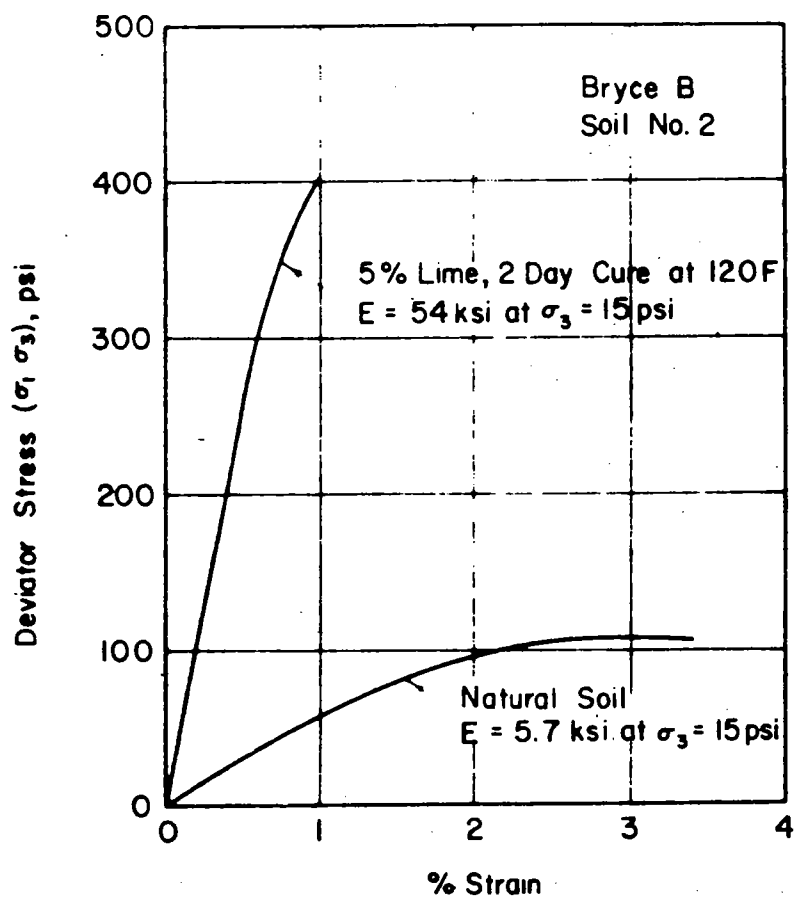
FIGURE 5.   TYPICAL STRESS-STRAIN CURVES FOR NATURAL AND LIME-TREATED SOIL.
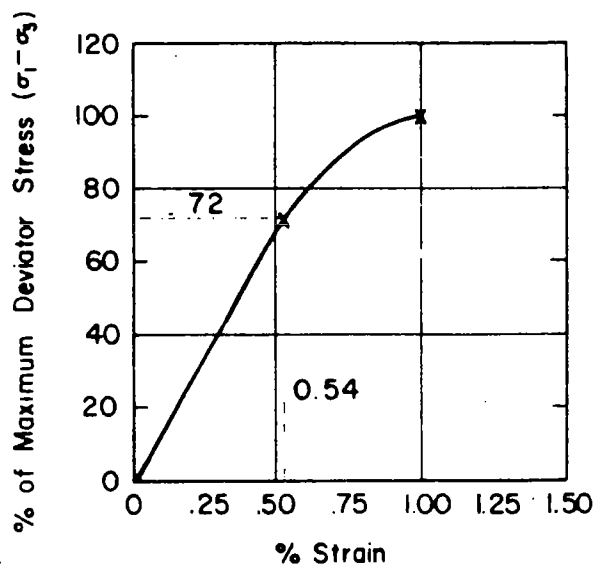
FIGURE 6.   GENERALIZED STRESS-STRAIN CURVE FOR CURED LIME-SOIL MIXTURES.
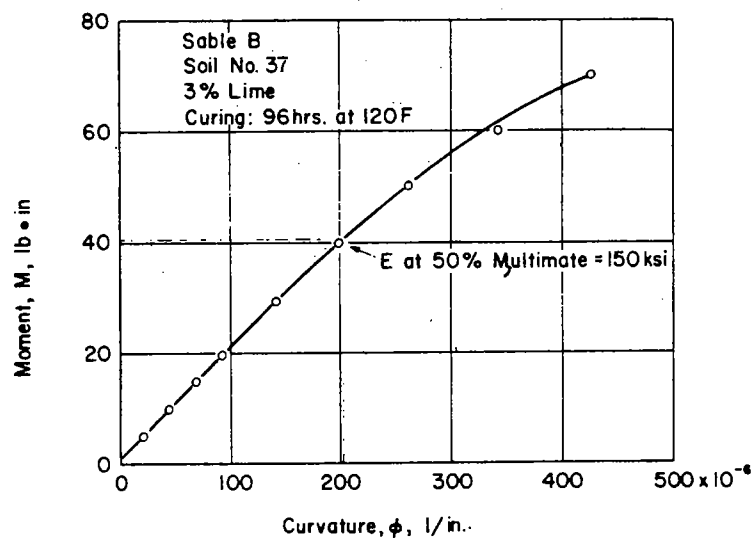
FIGURE 7. TYPICAL M-Ø PLOT FOR A
LIME-SOIL FLEXURAL SPECIMEN.

FIGURE 8. FLEXURAL STRENGTH-
FLEXURAL MODULUS RELATION
FOR LIME-SOIL MIXTURES.

$$E_{flex} \, (ksi) = 4.6 \, \sigma_{flex} \, (psi) - 139.0$$
$$R = .93$$
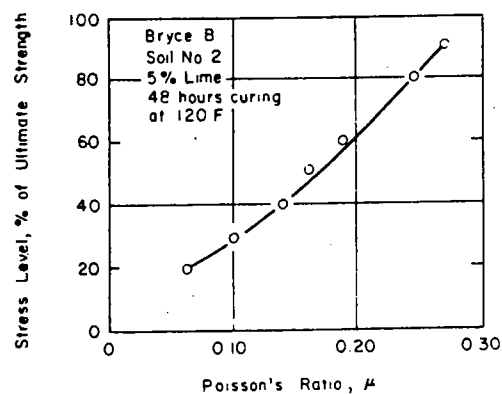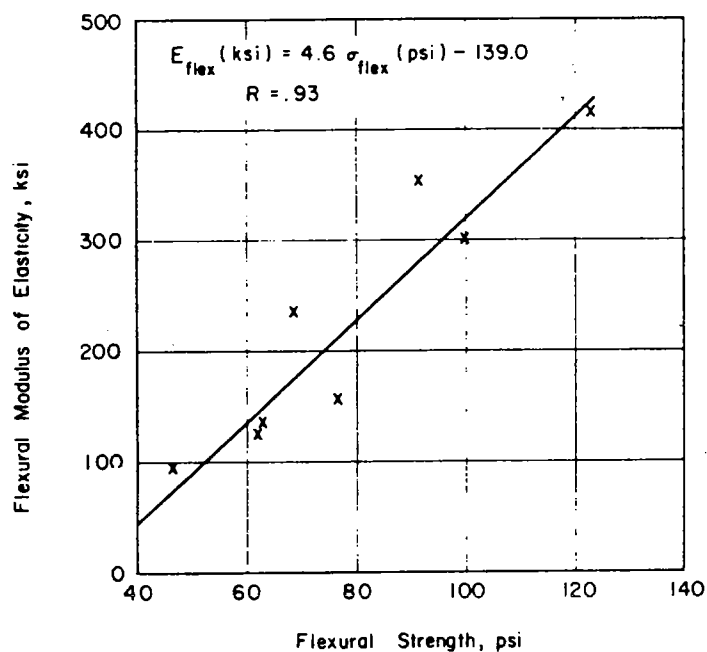
FIGURE 9. INFLUENCE OF STRESS
LEVEL ON POISSON'S RATIO.
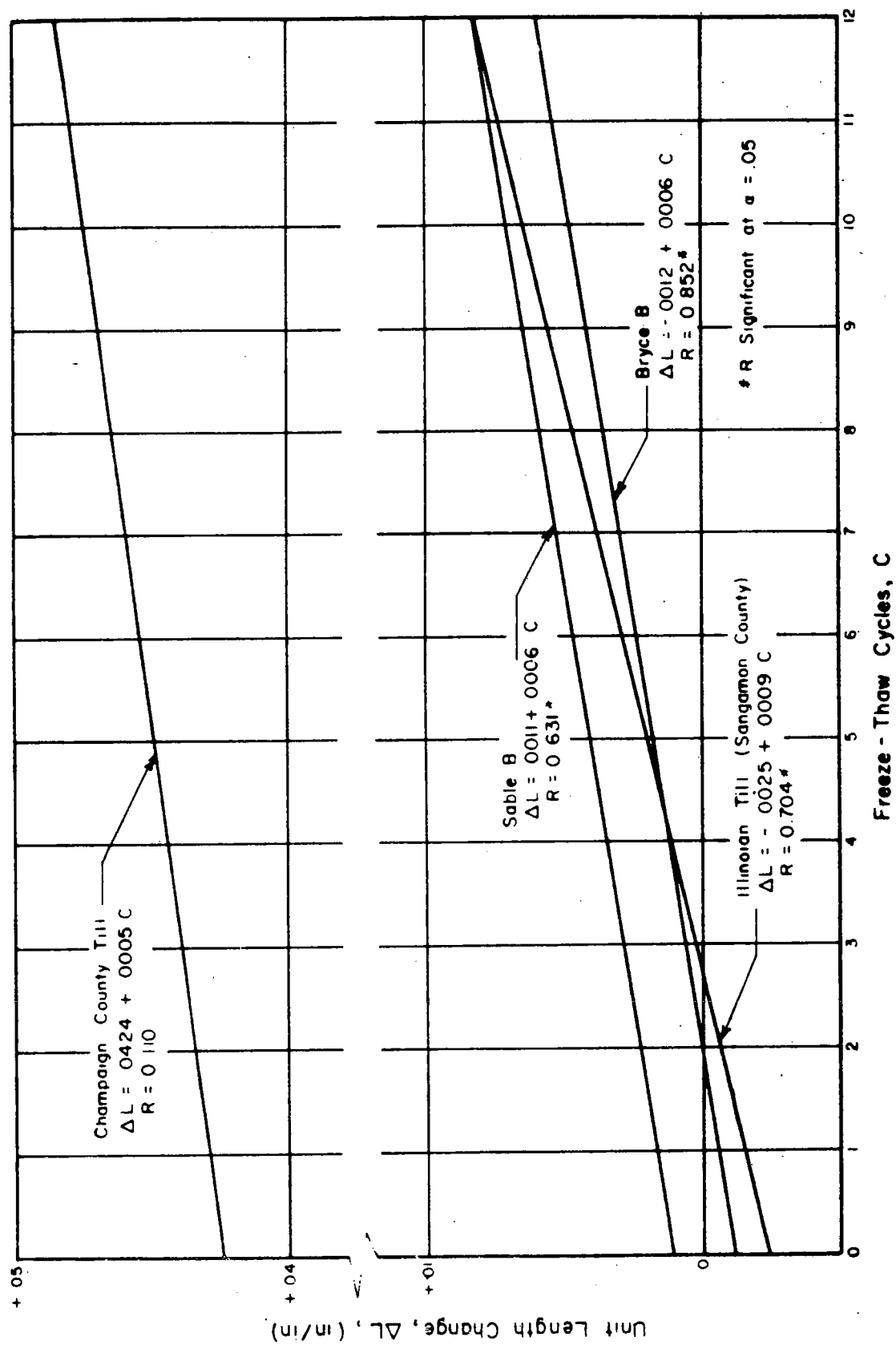
FIGURE 10. INFLUENCE OF FREEZE-THAW CYCLES ON UNIT LENGTH CHANGE (48-HR CURING)
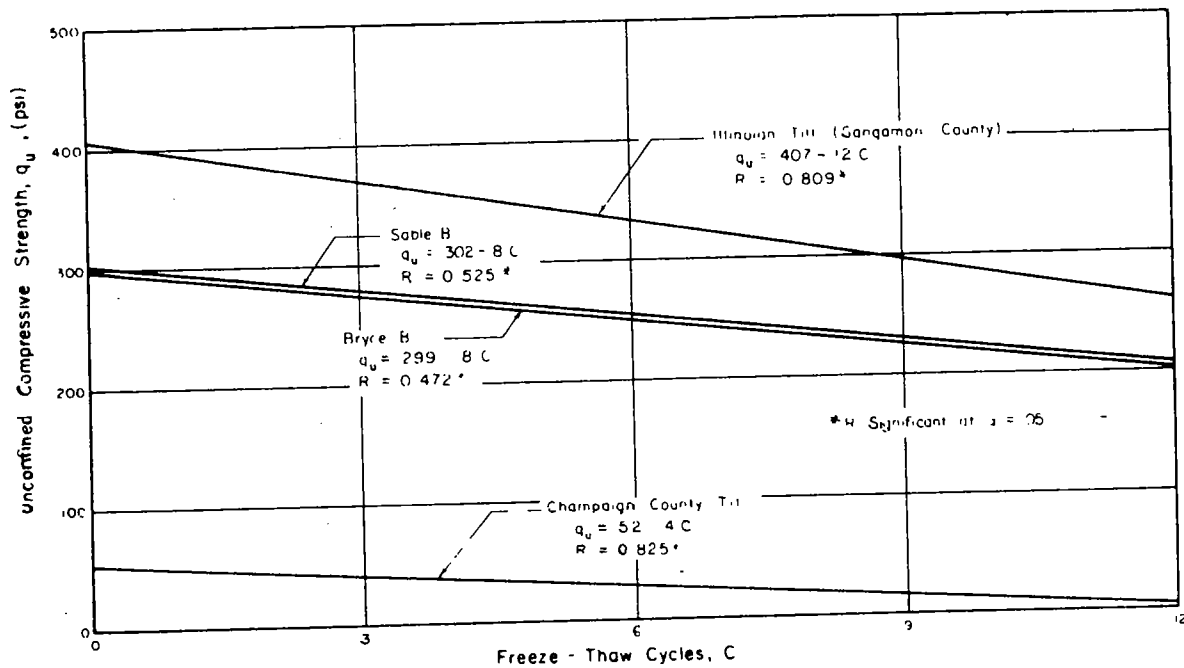
FIGURE 11. INFLUENCE OF FREEZE-THAW CYCLES ON
UNCONFINED COMPRESSIVE STRENGTH (48-HR CURING).
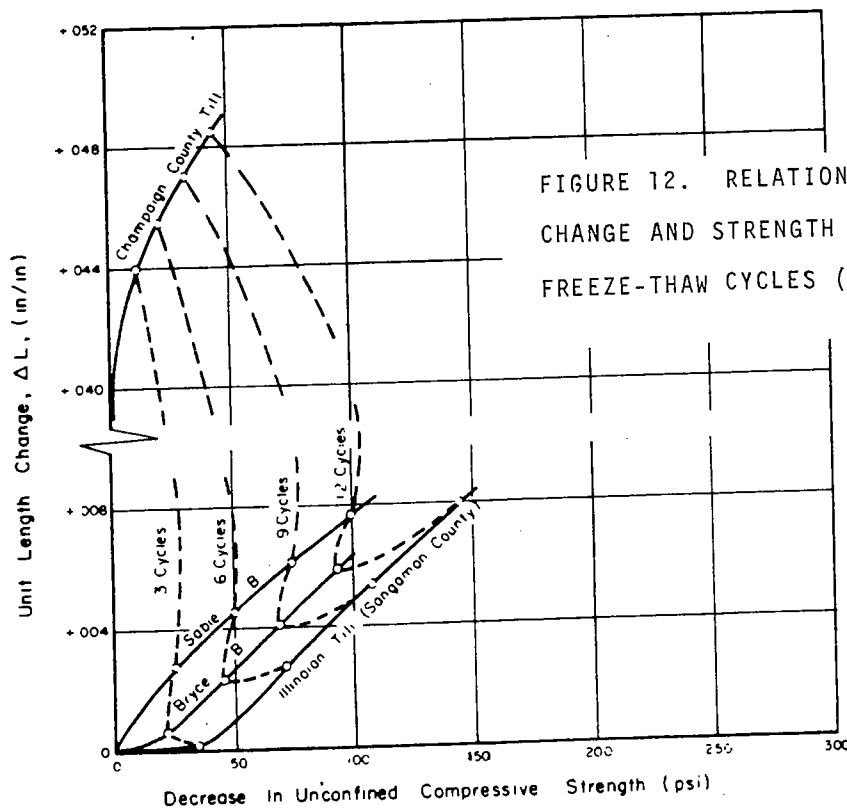
FIGURE 12. RELATIONSHIP BETWEEN UNIT LENGTH
CHANGE AND STRENGTH DECREASE WITH
FREEZE-THAW CYCLES (48-HR CURING).
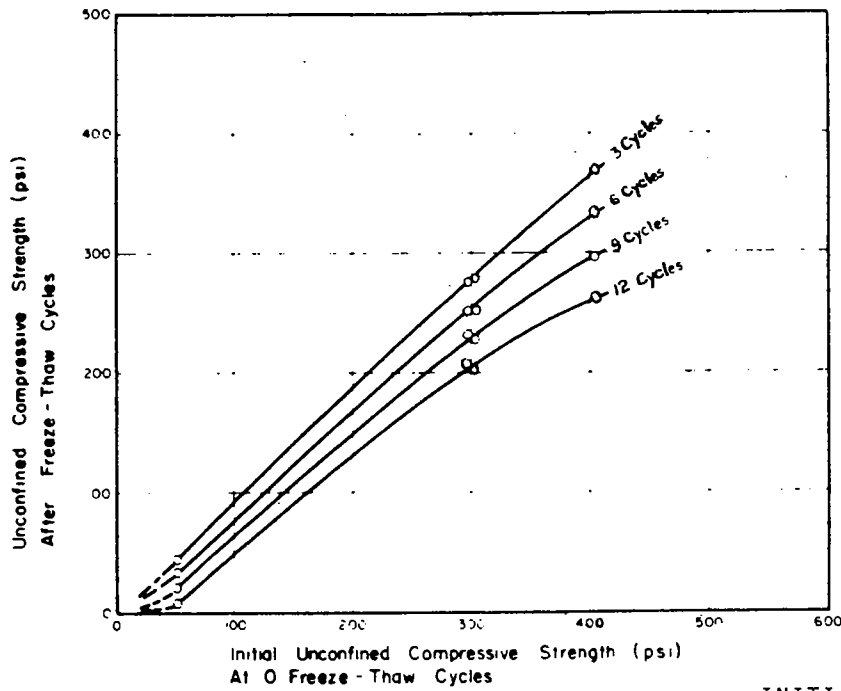
FIGURE 13. INFLUENCE OF INITIAL UNCONFINED COMPRESSIVE STRENGTH ON THE RESIDUAL STRENGTH AFTER FREEZE-THAW CYCLES (48-HR CURING).
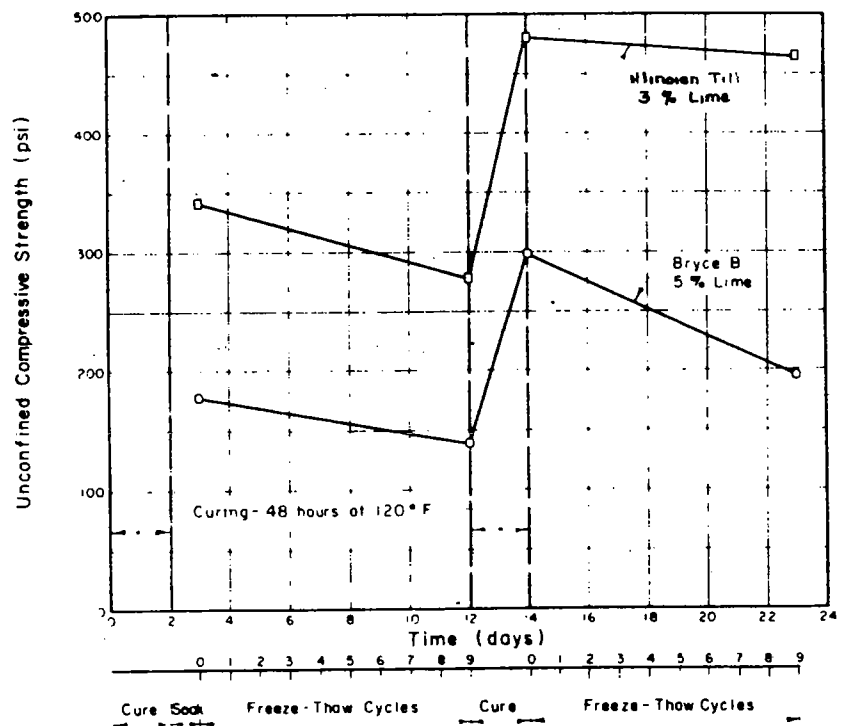
FIGURE 14. INFLUENCE OF CYCLIC FREEZE-THAW AND INTERMEDIATE CURING ON UNCONFINED COMPRESSIVE STRENGTH.
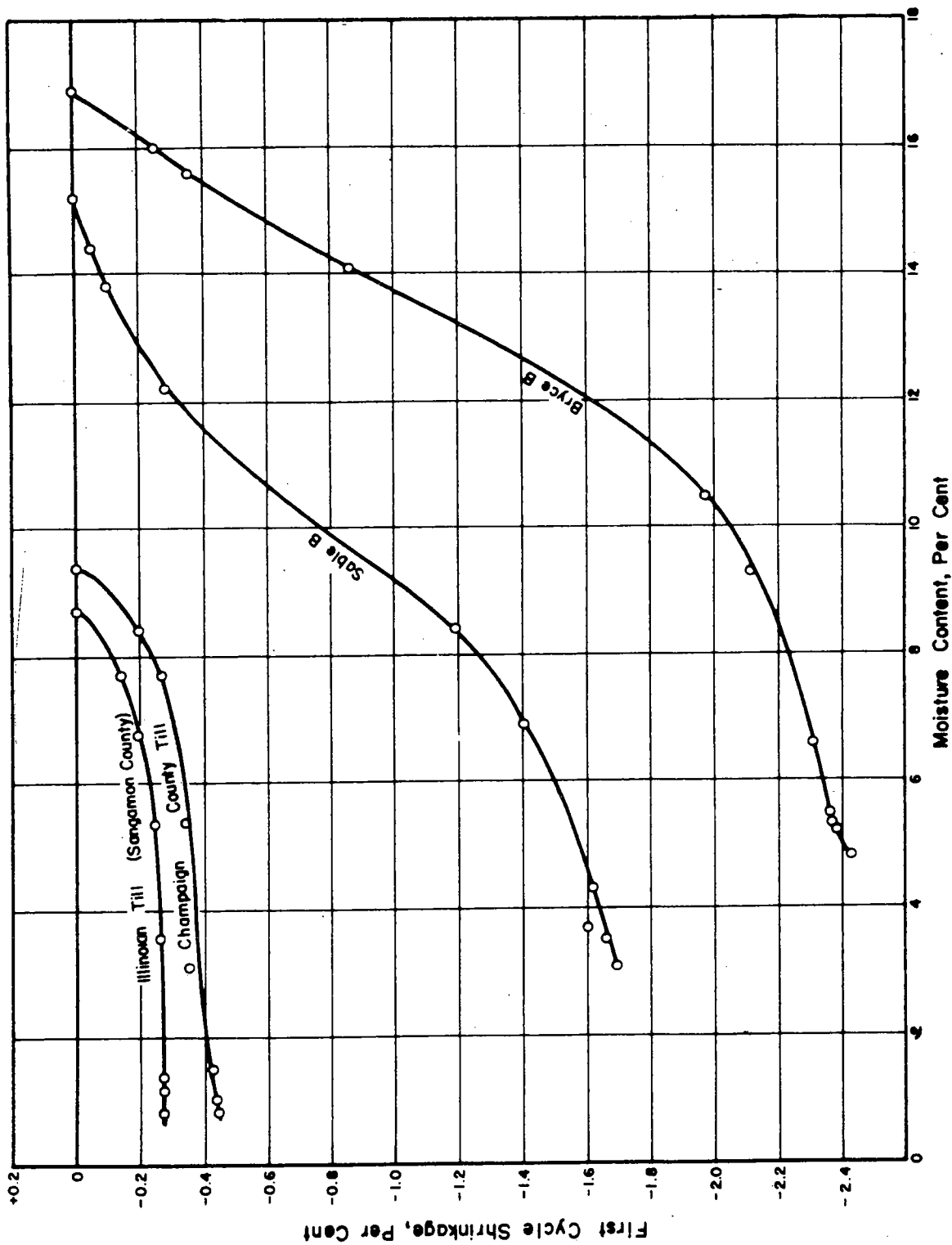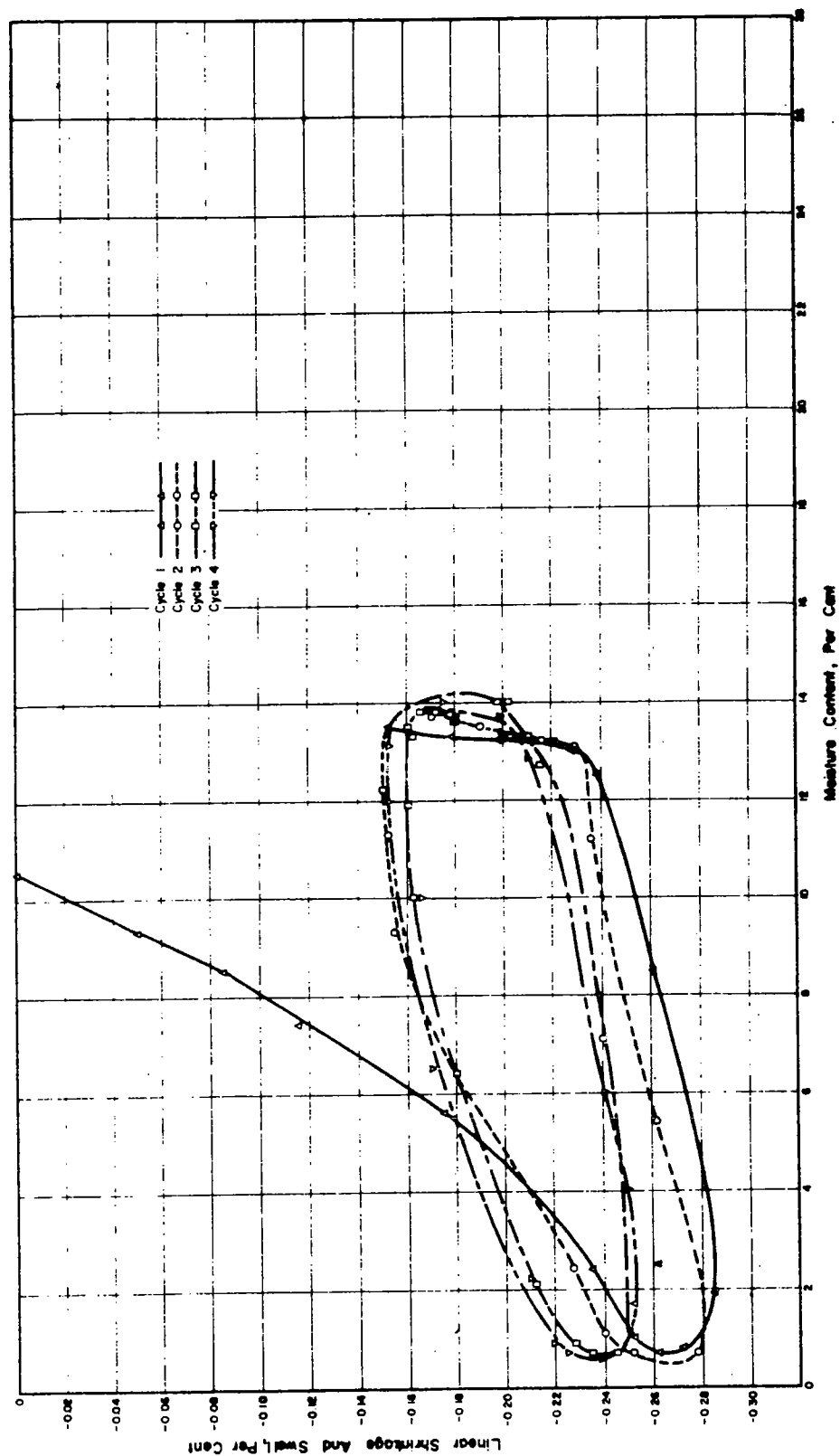
FIGURE 15.   FIRST-CYCLE SHRINKAGE OF-NATURAL SOILS.

FIGURE 16. CONTINUOUS SHRINKAGE AND SWELL CURVES FOR ILLINOIAN TILL (SANGAMON COUNTY) MIXTURE (48-HR CURING).
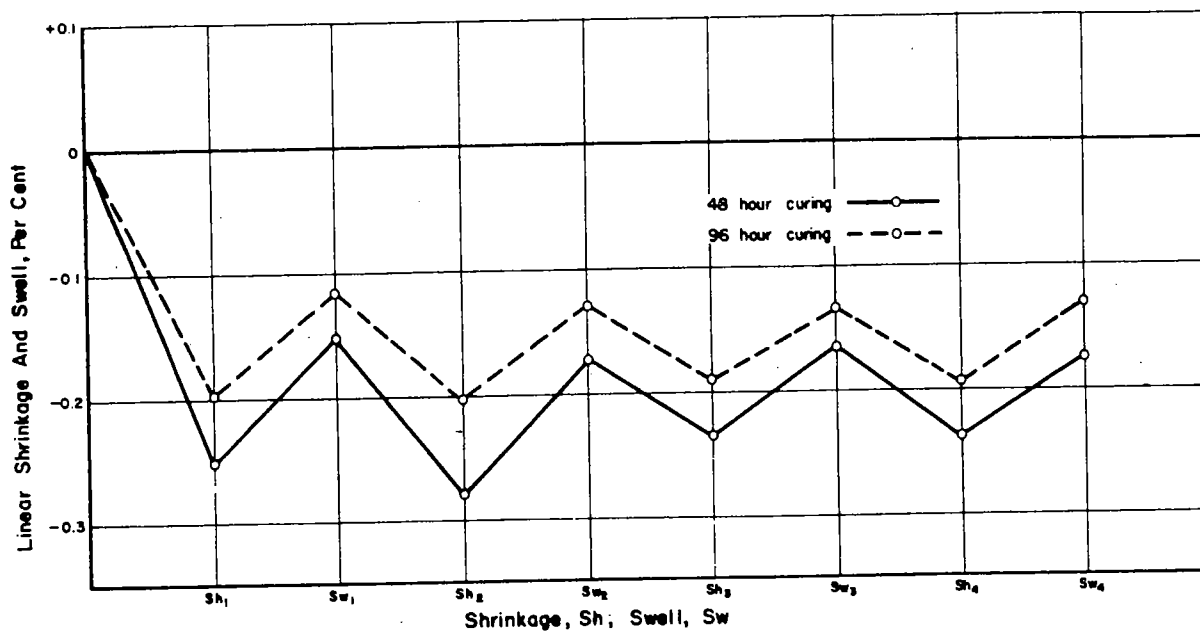
FIGURE 17. MAXIMUM LINEAR SHRINKAGE AND SWELL
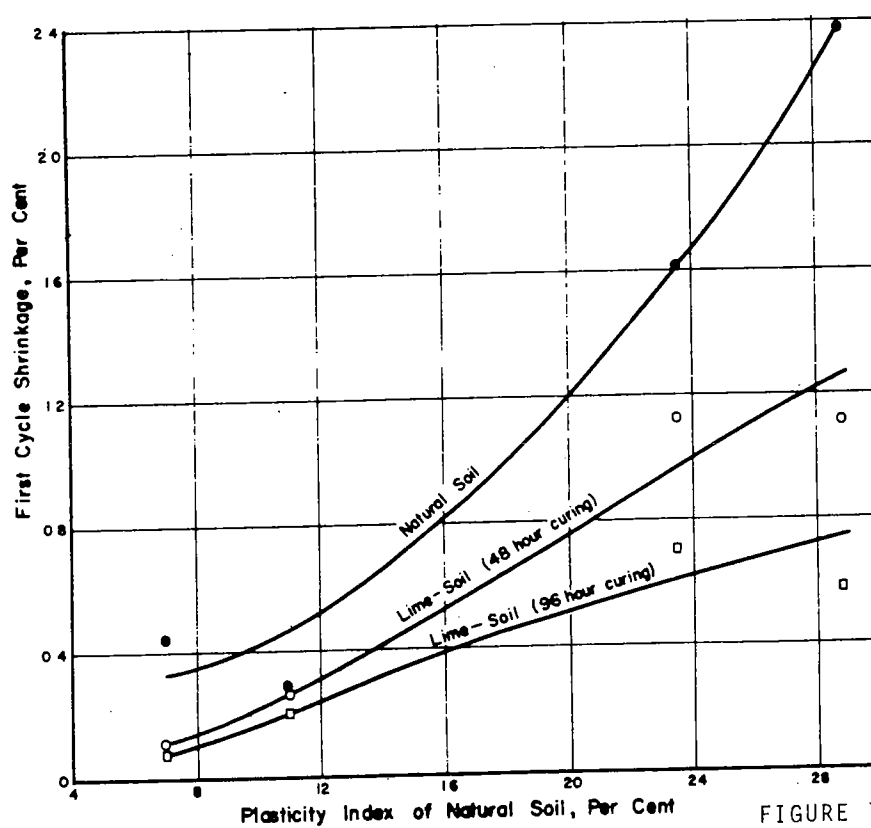OF ILLINOIAN TILL (SANGAMON COUNTY) MIXTURE.

FIGURE 18. INFLUENCE OF
PLASTICITY INDEX OF NATURAL SOIL ON FIRST-CYCLE SHRINKAGE.